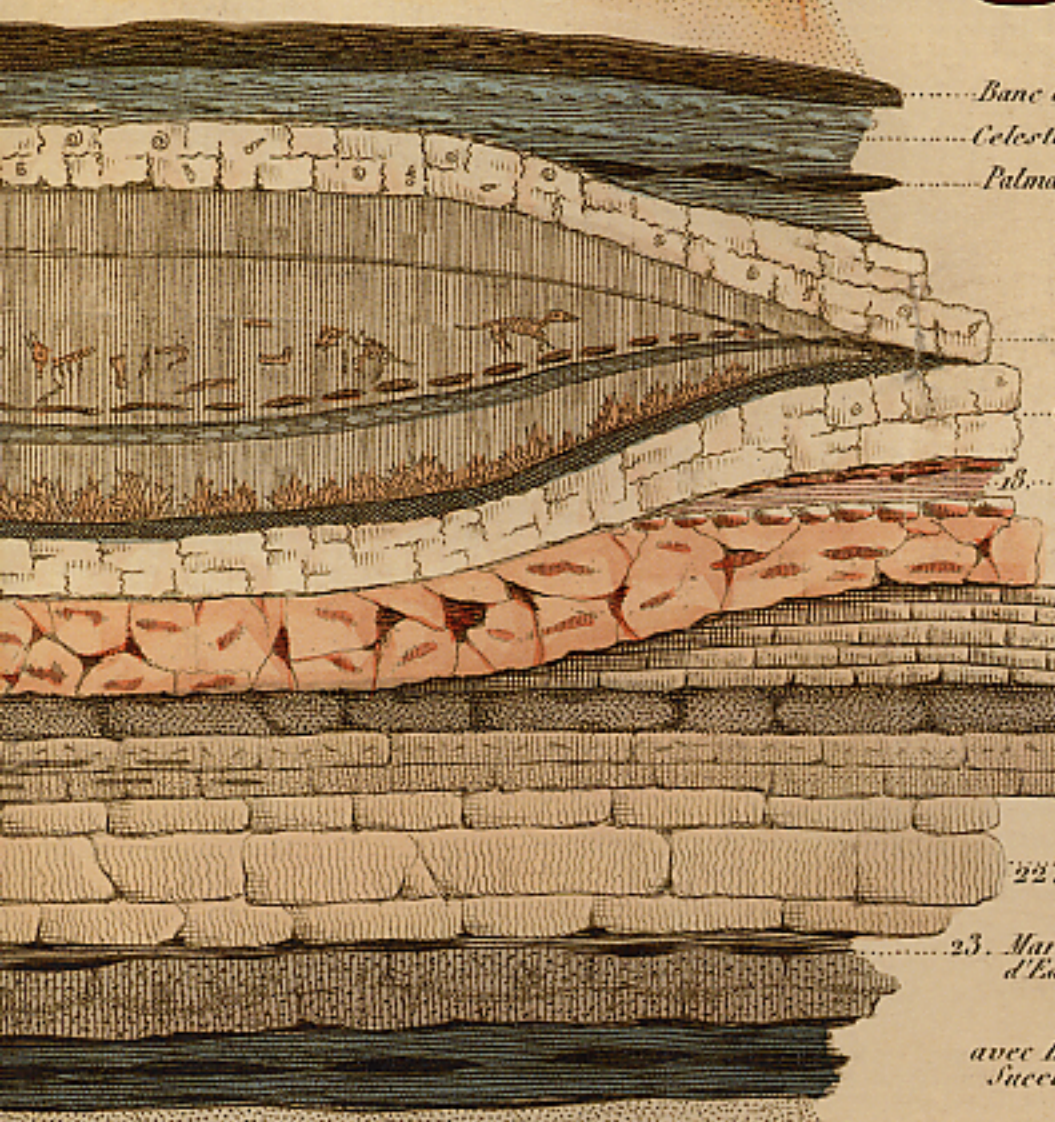




*Lamantin*  
*Fer Hydroxidé Sablonneux*

# Stratigraphy



*Banc d'Huitres*  
*Celestine en Nodules*  
*Palmarcité ou Lignite Suisse ou Paléotherien*

*Calcaire Lacustre*  
*et*  
*Calcaire Siliceux*

18. *Magnésite*  
*et*  
*Silex résinite*

*Calcaire dit Clignart*  
19. *à Potamides des Pierres &c.*

21. *Calcaire dit Roche*  
*à Cérîtee*

22. *Calcaire dit Lambourde*  
*à Coquilles variées, Miliolides &c.*

23. *Marne argileuse avec quelques Coquilles*  
*d'Eau douce et Lignite en plicquettes*

*avec Huitres, Potamides, Mélanopsides,*  
*Succin &c.*

*Niveau de la Seine à o du pont de la Tournelle*



*Celestine, Pyrites*

**CONTENTS**      **Volume 4**      **Number 1**      **2007**

**MAGNETOBIOSTRATIGRAPHY**

- 1**      **Martin P. Crundwell and Campbell S. Nelson**  
A magnetostratigraphically-constrained chronology for late Miocene  
bolboformids and planktic foraminifers in the temperate Southwest Pacific

**TECTONOSTRATIGRAPHY**

- 35**      **Robert E. Weems and Lucy E. Edwards**  
Post-middle Miocene origin of modern landforms in the eastern Piedmont of  
Virginia

**CLIMATOSTRATIGRAPHY**

- 49**      **David F. Ufnar**  
Early-Cenomanian Terrestrial Facies and Paleoclimate Records of the Lower  
Tuscaloosa Formation, Southwestern Mississippi

**CHRONOSTRATIGRAPHY**

- 67**      **Gilbert Klapper**  
Conodont taxonomy and the recognition of the Frasnian/Famennian (Upper  
Devonian) Stage Boundary

**CYCLOSTRATIGRAPHY**

- 77**      **Walther Schwarzacher**  
Sedimentary cycles and stratigraphy

**ANNOUNCEMENT**

- 66**      **“Catbox” — Ellis and Messina Catalogues on one DVD**

# A magnetostratigraphically-constrained chronology for late Miocene bolboformids and planktic foraminifers in the temperate Southwest Pacific

Martin P. Crundwell<sup>1</sup> and Campbell S. Nelson<sup>2</sup>

<sup>1</sup>GNS Science, P.O. Box 30368, Lower Hutt, New Zealand

<sup>2</sup>Department of Earth Sciences, University of Waikato, PB 3105, Hamilton, New Zealand  
email: m.crundwell@gns.cri.nz

**ABSTRACT:** High-resolution bolboformid and planktic foraminiferal distribution data from the upper Miocene section of ODP Site 1123, Chatham Rise, New Zealand, have been integrated with the magnetostratigraphic record from the same site to establish a magnetobiochronology based on the geomagnetic polarity time scale (GPTS-95). Although the upper Miocene sequence is adversely affected by dissolution, 33 bioevents are identified based on dissolution resistant taxa that are also found at DSDP Site 593 – an important biostratigraphic reference section for the Neogene in the Tasman Sea. A scatter plot based on the stratigraphic positions of shared bioevents at these oceanic sites approximates a linear line of correlation. The tight grouping of the biostratigraphic data around the line of correlation and the consistency of their stratigraphic order suggest most events are synchronous or nearly so, even though the sites are more than 1400km apart and associated with different water masses. This implies that even though the biostratigraphic construct is based on only two oceanic sites, it provides a robust late Miocene biochronostratigraphic framework for the temperate Southwest Pacific.

Shared bolboformid events include the appearances and disappearances of *Bolboforma subfragoris* s.l. (11.56-10.61 Ma), *B. gruetzmacheri* (10.46-10.31 Ma), *B. capsula* (10.20-10.13 Ma), *B. pentaspinosa* (10.15-10.08 Ma), *B. gracilireticulata* s.l. (9.75-9.61 Ma), *B. metzmacheri* s.s. (lower occurrence interval 9.54-9.34 Ma, upper occurrence interval 9.01-8.78 Ma), *B. metzmacheri ornata* (8.45-8.28 Ma), *B. praeintermedia* (8.25-8.21 Ma), and abundance spikes associated with the uppermost *B. subfragoris* s.l. occurrence interval BBs-1123/D (10.61 Ma) and the lower *B. metzmacheri* s.s. occurrence interval BBm-1123/A (9.54 Ma). Shared planktic foraminiferal events include dextral coiling excursions in *Globoconella miotumida* (10.92-10.82 Ma and 9.62-9.42 Ma), the regional disappearance of *Globoquadrina dehiscens* (8.88 Ma), and the evolutionary appearances of *Globoconella conomiozea* (ca. 6.87 Ma), *Globoconella mons* (ca. 5.72 Ma), *Globoconella sphericomiozea* (ca. 5.53 Ma), *Globoconella pliozea* (ca. 5.39 Ma), *Truncorotalia crassaformis* (ca. 5.15 Ma), and *Globoconella puncticulata* (ca. 5.11 Ma).

## INTRODUCTION

High quality age models for deep-sea sections are a key component in the correlation and synthesis of global data sets for the study of paleoceanographic processes. The establishment of a robust biochronostratigraphic framework for marine microfossils is complex and often involves several correlation steps, the most important being the correlation between biostratigraphic events and the global polarity time scale (GPTS). Although microfossil events have been calibrated to the GPTS in different parts of the world (e.g. Hodell and Kennett 1986; Chaisson and Leckie 1993; Sprovieri et al. 1996), no reliable late Miocene biochronostratigraphic framework exists for the temperate Southwest Pacific. Presently, chronologies in this region are based on a small number of tenuous paleontological, magnetostratigraphic, and stable isotope correlations with dated horizons or interpolated horizons from uplifted marine sections on land in New Zealand (e.g. Kennett and Vella 1975; Wright et al. 1985; Edwards 1987; Roberts et al. 1994), and from outside of the region (e.g. Lazarus et al. 1995; Spencer-Cervato 1999). Because these paleontological data often lack internal consistency, and biostratigraphic events are often diachronous across major water mass boundaries (Jenkins 1992; Spencer-Cervato 1994), there is a need to establish a more reliable regional biochronostratigraphic framework in order to gain a better perspective of oceanographic and climatic changes in southern mid-latitudes. This is particularly important in the late Miocene

where there is a paucity of events suitable for biostratigraphic correlation.

Ocean Drilling Program (ODP) Site 1123, Chatham Rise, New Zealand, allows for the first time the development of a high quality late Miocene magnetobiochronology in the temperate Southwest Pacific (text-fig. 1). Late Miocene calcareous microfossil assemblages at the site have been variably affected by differential dissolution, but dissolution-resistant bolboformids and planktic foraminifers are sufficiently well represented to establish a sequence of bioevents that can be correlated with Deep Sea Drilling Project (DSDP) Site 593 (text-fig. 1), an important biostratigraphic reference section for the Neogene in the Tasman Sea (Jenkins and Srinivasan 1986; Lohmann 1986; Hoskins 1990; Scott 1992; Grützmacher 1993; Crundwell 2004). The primary aim of this paper is to establish a regional magnetobiochronology for these data based on bioevents at Site 1123 and the geomagnetic polarity time scale GPTS-95 (Cande and Kent 1995).

## MATERIAL AND METHODS

ODP Site 1123 was reported in the Initial Reports for Leg 181 to have a virtually complete Neogene magnetostratigraphic record that extends back to Chron C6r – ca. 20 Ma (Shipboard Scientific Party 1999a). However, a subsequent review of the magnetostratigraphy (Crundwell et al. 2004) has identified an interval in the latest Miocene between Chron C3Br.2n to

C3n.1n (7.34–4.29 Ma) where the polarity record is ambiguous – it encompasses the upper part of the studied section (text-fig. 2). The magnetostratigraphy of the lower part of the section, between Chron C5An.1r and C3Br.2n (12.18–7.34 Ma), has a virtually complete polarity record, but there is a suspected break in the sequence of less than 100kyr within Chron C4Ar.2r (Shipboard Scientific Party 1999a).

While the resolution of shipboard biostratigraphic sampling was adequate for the interpretation of the paleomagnetic record, the sample interval (ca. 190–320kyr) was too coarse to identify or define short-lived bioevents and to allow a reliable magnetobiochronology to be established. To improve biostratigraphic resolution through the late Miocene, a suite of 353 micropaleontological samples has been examined from the base of core 1123B-44X (427.40 r-mcd; revised-metres composite depth) to the top of core 1123B-18X (170.20 r-mcd). All samples are fossiliferous, but preservation is highly variable. The adopted sample spacing (ca. 22kyr) is about three times coarser than the biostratigraphic resolution of Site 593 (Crundwell 2004), but is sufficient to identify most short-lived bolboformid and planktic foraminiferal events should they be present.

The interval reported in this study was cored continuously with the extended core barrel, but there are potential gaps in the record between some cores where there was less than 100% recovery (Table 1). This places a cautionary caveat on the location of some bioevents in the cored succession, although physical properties measurements of the core and downhole logging (Shipboard Scientific Party 1999a) suggest much of the variability in core recovery was caused by core deformation during coring and retrieval operations.

All paleontological data from the site relate to ODP Hole 1123B and depths are reported in revised-metres composite depth (r-mcd). Depth translations from metres below seafloor (mbsf) to r-mcd are based on core splice data and linear transforms given in Table 1. Biostratigraphic events are reported in the text in terms of the sample in which they are found, but magnetostratigraphic and chronostratigraphic assignments are based on horizons between the sample with the named event and the closest constraining sample (i.e. interpolated depth).

Distribution (presence/absence) data were initially compiled for all planktic foraminifers from systematic scans of the >150µm fractions. No foraminifera were removed from samples, but all bolboformids were picked and mounted onto two-hole slides to allow identifications to be checked before bolboformid census data were compiled. The bolboformid data were then supplemented with picks of all bolboformids from the >125µm fraction to provide more detailed census information. Planktic-benthic foraminiferal ratios, and coiling data for *Globoconella miotumida* and *Gc. conomiozea*, were also compiled, based wherever possible on counts of at least 100 specimens in the >150µm fraction. All fossil materials from this study – washed residues, mounted slides, and figured specimens – are lodged in the DSDP/ODP collections at GNS Science, Lower Hutt, New Zealand.

The adopted bolboformid taxonomy is based on Spiegler and Daniels (1991), Grützmacher (1993), and Spiegler (1999), and employs population concepts of Crundwell et al. (2005). To a large extent, the higher taxonomy of planktic foraminifers follows Kennett and Srinivasan (1983), except the genus/subgenus ranking of each phylogenetic group is raised to that of a genus (e.g. *Globorotalia* (*Globoconella*) = *Globoconella*; *Globo-*

*rotalia* (*Truncorotalia*) = *Truncorotalia*). Adopted species concepts are largely based on Hornibrook (1982), Hornibrook et al. (1989), and Scott et al. (1990). The type references of bolboformid and planktic foraminiferal species identified at Site 1123 are listed in Appendix 1 and an explanation of bioevents and bolboformid zones is given in Appendix 2.

## OCEANOGRAPHIC SETTING

ODP Site 1123 is located at 42°47.147'S, 171°29.941'W on the northeastern slope of the Chatham Rise, about 1000km east of central New Zealand (text-fig. 1). The site lies at a depth of 3290m, and it is near the northern limit of the modern Subtropical Front (STF).

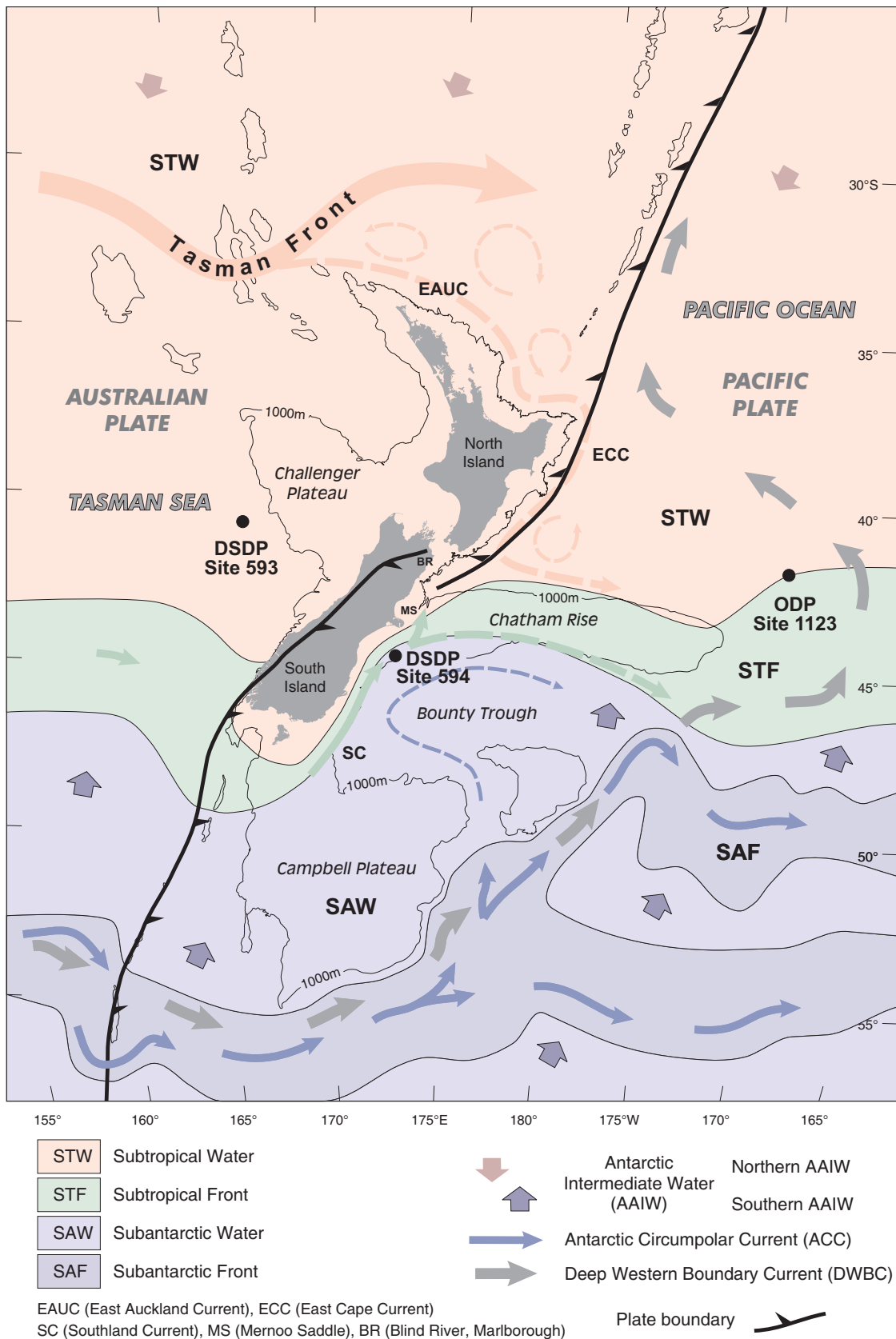
Presently, Site 1123 is dominated by warm Subtropical Surface Water, associated with the East Cape Current (ECC) – a series of semi-permanent, deep-seated eddies that pass south along the eastern North Island margin, before turning east along the northern flank of Chatham Rise (Heath 1985; Chiswell and Roemmich 1988). The STF is displaced by the New Zealand subcontinent and linked around the south-eastern margin of the South Island margin by the Southland Current (SC). At Mernoo Saddle, a branch of the SC continues north and the remainder of the SC flows east along the southern flank of Chatham Rise (Chiswell 1994). The strongest temperature gradients occur along the shallow crest of Chatham Rise (Uddstrom and Oien 1999), where the STF occupies a band ca. 150km wide, between the ECC and SC (Carter et al. 1998). Off eastern Chatham Rise, where the currents bounding the STF are less constrained by bathymetry, the front is up to 400km wide. Satellite SST data ([www7320.nrlssc.navy.mil/global\\_ncom](http://www7320.nrlssc.navy.mil/global_ncom)) show summer–winter amplitude variations of 4–6°C at Site 1123 and across the STF.

In the deeper ocean, off eastern New Zealand, oxygen-rich Antarctic Intermediate Water flows northwards across Site 1123 at depths of 600–1450m (Wyrski 1962; Shipboard Scientific Party 1999a). Circumpolar Deep Water (CDW) associated with the Antarctic Circumpolar Current passes northwards along the eastern margin of the New Zealand subcontinent, below a depth of 1450m (Shipboard Scientific Party 1999a), and Antarctic Bottom Water (AABW) flows northwards, to the east of the site. During winter months, a northwards-directed flow of Subantarctic Mode Water moves across the site at depths of 150–450m.

Although seafloor spreading between Australia and Antarctica has shifted the New Zealand subcontinent northwards by as much as 5° of latitude since the beginning of the late Miocene (Weissel et al. 1977) the present-day pattern of oceanic circulation in the region appears to have remained substantially unchanged over the last 10 myr (Edwards 1975; Nelson and Cooke 2001). However, significant glacial–interglacial climatic variability has been recorded at Site 593 during the Miocene (Cooke et al. in review) and at Site 1123 during the Pleistocene (Crundwell et al. in review). Glacial–interglacial variability is also evident in proxy carbonate data from the Pliocene and Miocene section of Site 1123 (Shipboard Scientific Party 1999b).

## BOLBOFORMIDS

Bolboformids are an enigmatic group of calcareous microfossils that have generally been interpreted as phytoplanktic organisms (Rogl and Hochuli 1976; Tappan 1980; Spiegler and Daniels 1991), although comparative oxygen isotope data from the analysis of bolboformid shells (Poag and Karowe 1986; Spiegler



TEXT-FIGURE 1

Bathymetric map of the New Zealand subcontinental region (1000m contour), Tasman Sea, and Southwest Pacific Ocean, showing the location of ODP and DSDP sites referred to in this study, the positions of major fronts at the ocean surface (summer situation), and the flow of Antarctic Intermediate Water, Antarctic Circumpolar, and Pacific Deep Western Boundary currents (Shipboard Scientific Party 1999b).

and Erlenkeuser 2001) suggest they spent at least part of their lifecycle below the photic zone, in mid to lower levels of the water column. They are important index fossils that supplement calcareous nannofossil and planktic foraminiferal zonations in mid- to high-latitude regions of Europe and the Atlantic and southern Indian oceans (Spiegler and Daniels 1991; Spiegler and Müller 1992). Their high resistance to dissolution makes them particularly important for the correlation of oceanic sequences affected by calcite dissolution (Müller et al. 1985). The discovery of bolboformids in late Miocene oceanic sequences of the Southwest Pacific and Tasman Sea regions (Poag and Karowe 1986; Grützmacher 1993) and in uplifted marine sequences in New Zealand (Crundwell et al. 1997a) offers considerable scope for improving biostratigraphic resolution and global correlations in this region. The most studied bolboformid sequence in this region is at DSDP Site 593, where there is a well-defined succession of short-lived appearances and disappearances of monospecific bolboformid populations, with peak abundances sometimes reaching several thousand specimens per gram of sediment (Grützmacher 1993; Crundwell et al. 1997a). Bolboformids have also been noted at other oceanic sites in the Southwest Pacific and Tasman Sea regions – ODP Site 1120 (50°S), DSDP Sites 594 (46° S), 592 (36° S), and 590B (31° S) – but their abundance and diversity generally decreases at lower latitudes (Grützmacher 1993).

Bolboformids are reported to be rare in the Initial Reports for ODP Site 1123 (Shipboard Scientific Party 1999a), but the present study identifies a well-defined sequence of short-lived appearances and disappearance of monospecific bolboformid populations between cores 1123B-41X and 32X. The bolboformids are moderately well preserved, even in samples where planktic foraminifers are severely affected by dissolution. The predominantly early late Miocene bolboformid succession spans about 3.4 million years and it is similar to the succession at DSDP Site 593 (Crundwell 2004). It includes at least 18 well-defined events – lowest and highest occurrences, and distinctive abundance spikes (text-fig. 3). The persistence of monospecific populations is relatively high (60-100%) and the disappearance of each species is usually followed by a barren interval of 30-330kyr where there are no bolboformids. Although the occurrence intervals of most species are well defined, additional higher-resolution sampling may extend the ranges of some species, particularly where specimen numbers are low. Abundance spikes may also be better resolved with higher-resolution sampling.

### **Bolboformid biostratigraphy and biochronology**

Bolboformid events at Site 1123 are described in ascending stratigraphic order. The distribution and abundance of bolboformids are shown in text-fig. 3, and species are illustrated in text-figure 4.

***Bolboforma subfragoris* s.l. taxon-range zone (11.56-10.50 Ma):** In the context of this study, *B. subfragoris* s.l. encompasses several morphologically similar spirospinose species, subspecies, and morphotypes. The range zone of *B. subfragoris* s.l. at Site 1123 includes four occurrence intervals that are separated by barren intervals without bolboformids. For descriptive purposes, the occurrence intervals are referred to in ascending order as the BBs-1123/A to BBs-1123/D intervals. The lowest and highest intervals, BBs-1123/A and BBs-1123/D, include highly serrated spiral-flanged specimens (text-fig. 4/12 and 4/10) that closely resemble spirospinose forms of *B.*

*subfragoris* from Site 593 (Grützmacher 1993), and intervals BBs-1123/B and BBs-1123/C near the middle of the taxon range zone, include small smooth-walled forms with weak nodular surface ornament (text-fig. 4/11).

The lowest occurrence of *B. subfragoris* s.l. is at the base of the BBs-1123/A interval in sample 1123B-41X-6, 0-5cm. This is close to the base of core 1123B-41X, which has only 86.3% of core recovery, although downhole logs and shipboard measurements of physical core properties suggest the core is relatively complete and that the datum is reliably located. The lowest occurrence datum is 14m below the base of the *Gc*-1123/A coiling zone – a distinctive interval of dextrally-coiled *Globoconella miotumida* (text-fig. 5), which is correlated with the base of the Tongaporutuan Stage (Crundwell et al. 2004). It occurs in Chron C5r.2r(0.55) and has an interpolated magnetostratigraphic age of 11.56 Ma.

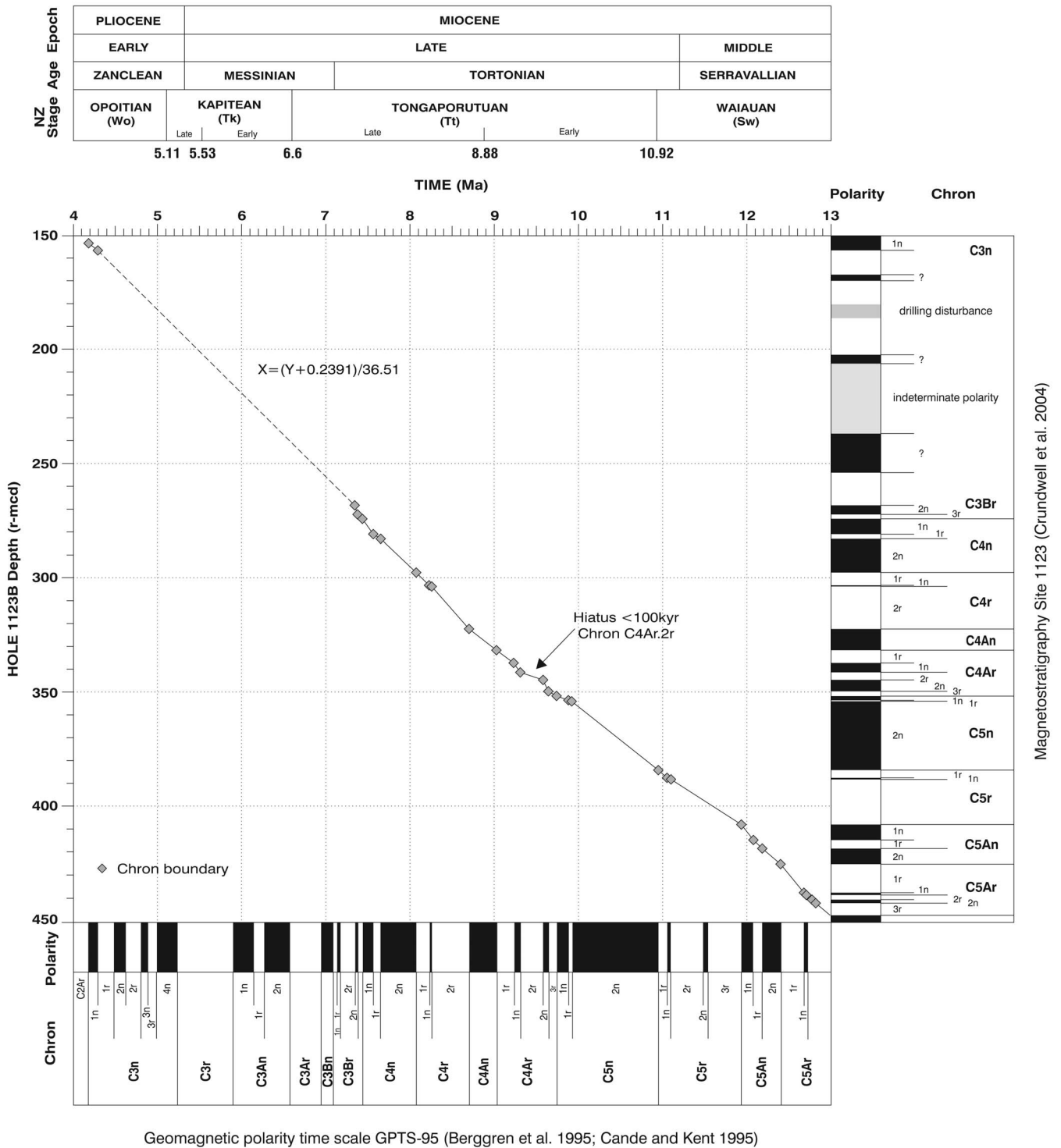
The highest occurrence of *B. subfragoris* s.l. occurs at the top of the BBs-1123/D interval. Immediately prior to its disappearance in sample 1123B-39X-1, 100-104cm, it occurs in nine consecutive samples. Following a barren interval without bolboformids, monospecific populations of the succeeding species *Bolboforma gruetzmacheri*, first appear 1.6m (ca. 60kyr) higher in the core. The highest occurrence of *B. subfragoris* s.l., which marks the top of the *B. subfragoris* s.l. taxon-range zone at Site 1123, occurs in Chron C5n.2n(0.56) and it has an interpolated magnetostratigraphic age of 10.50 Ma.

The base of the BBs-1123/D interval, the uppermost occurrence interval of the *B. subfragoris* s.l. taxon-range zone, is marked by a prominent abundance spike in sample 1123B-39X-4, 50-53cm where abundances in the >125µm sediment size fraction peak at about 3800 specimens per gram (text-fig. 3). The abundance spike occurs above the *Gc*-1123/A coiling zone in Chron C5n.2n(0.71) and it has an interpolated magnetostratigraphic age of 10.61 Ma.

***Bolboforma gruetzmacheri* occurrence interval (10.46-10.31 Ma):** *Bolboforma gruetzmacheri* is a very distinctive bolboformid ornamented with irregular, widely spaced blind and interconnected blade-like ridges (text-fig. 4/9). It has previously been identified by Grützmacher (1993) at oceanic sites in the Southwest Pacific as *Bolboforma* sp. H. At Site 1123 it has a very short occurrence interval that extends from 1123B-38X-7, 0-4cm to 1123B-38X-4, 50-54cm. It is a persistent species that occurs in eight out of nine samples. It is most common near the base of its range, where abundances in the >125µm sediment size fraction peak at 1385 specimens per gram (text-fig. 3). Very low abundances in the upper part of the species stratigraphic range diminish the reliability of its highest occurrence, although following a barren interval without bolboformids, monospecific populations of the succeeding species, *B. capsula*, first appear 3.5m (ca. 120kyr) higher in the core. The *B. gruetzmacheri* occurrence interval extends from Chron C5n.2n(0.53) to C5n.2n(0.38) and it has an interpolated magnetostratigraphic age of 10.46-10.31 Ma.

***Bolboforma capsula* occurrence interval (10.20-10.13 Ma):** *Bolboforma capsula* is another very distinctive species with a moderately smooth, bell-like, axially corrugate and tuberculate, encapsulated test (text-fig. 4/8). It is confined to four consecutive samples inclusive of 1123B-38X-2, 0-4cm and 1123B-38X-1, 10-14cm. Specimen numbers, however, are very low and there is uncertainty regarding the reliability of its lowest and highest occurrences. The occurrence interval of *B.*

New Zealand stage correlation (Crundwell et al. 2004)

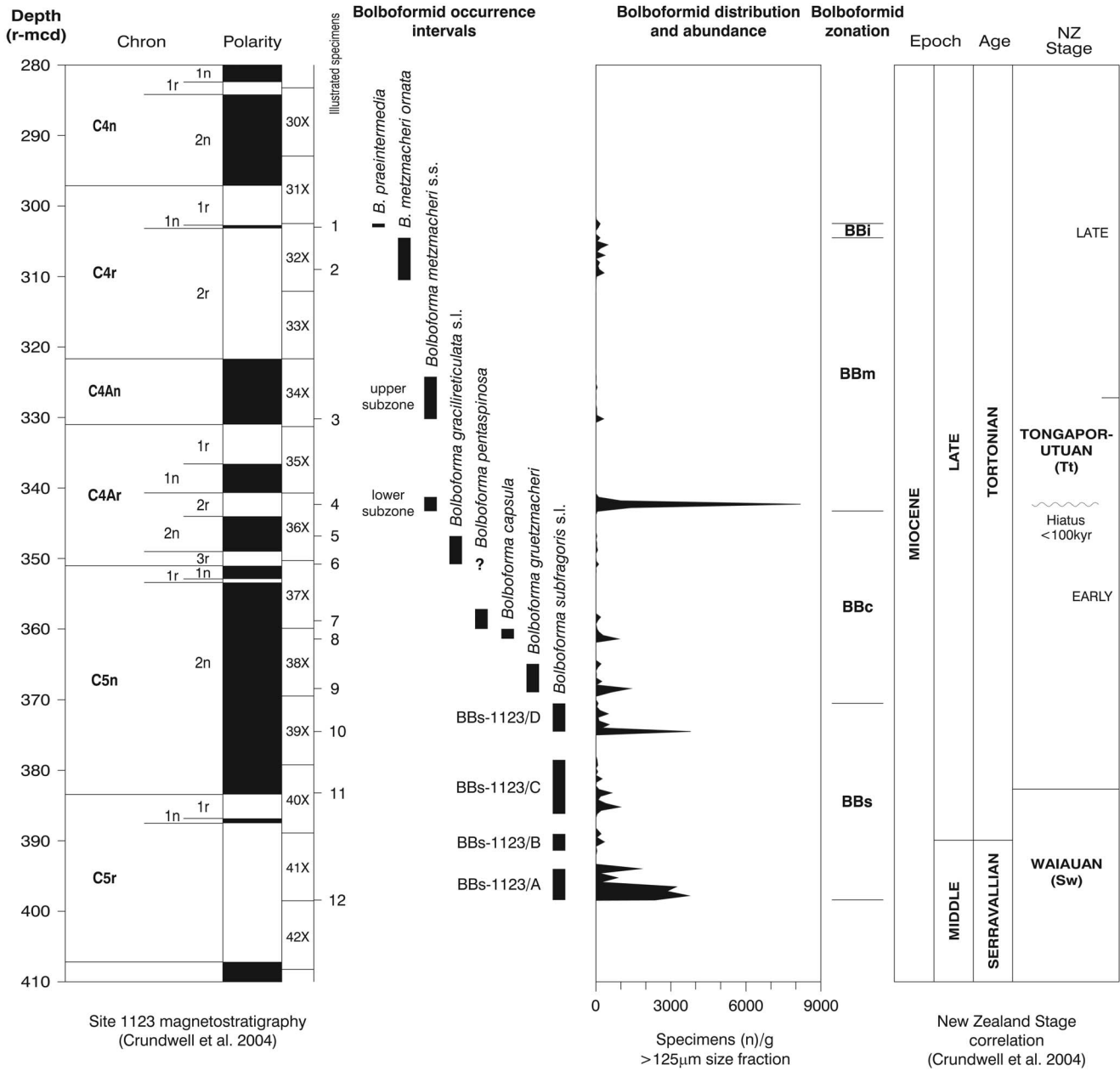


Magnetostatigraphy Site 1123 (Crundwell et al. 2004)

Geomagnetic polarity time scale GPTS-95 (Berggren et al. 1995; Cande and Kent 1995)

TEXT-FIGURE 2

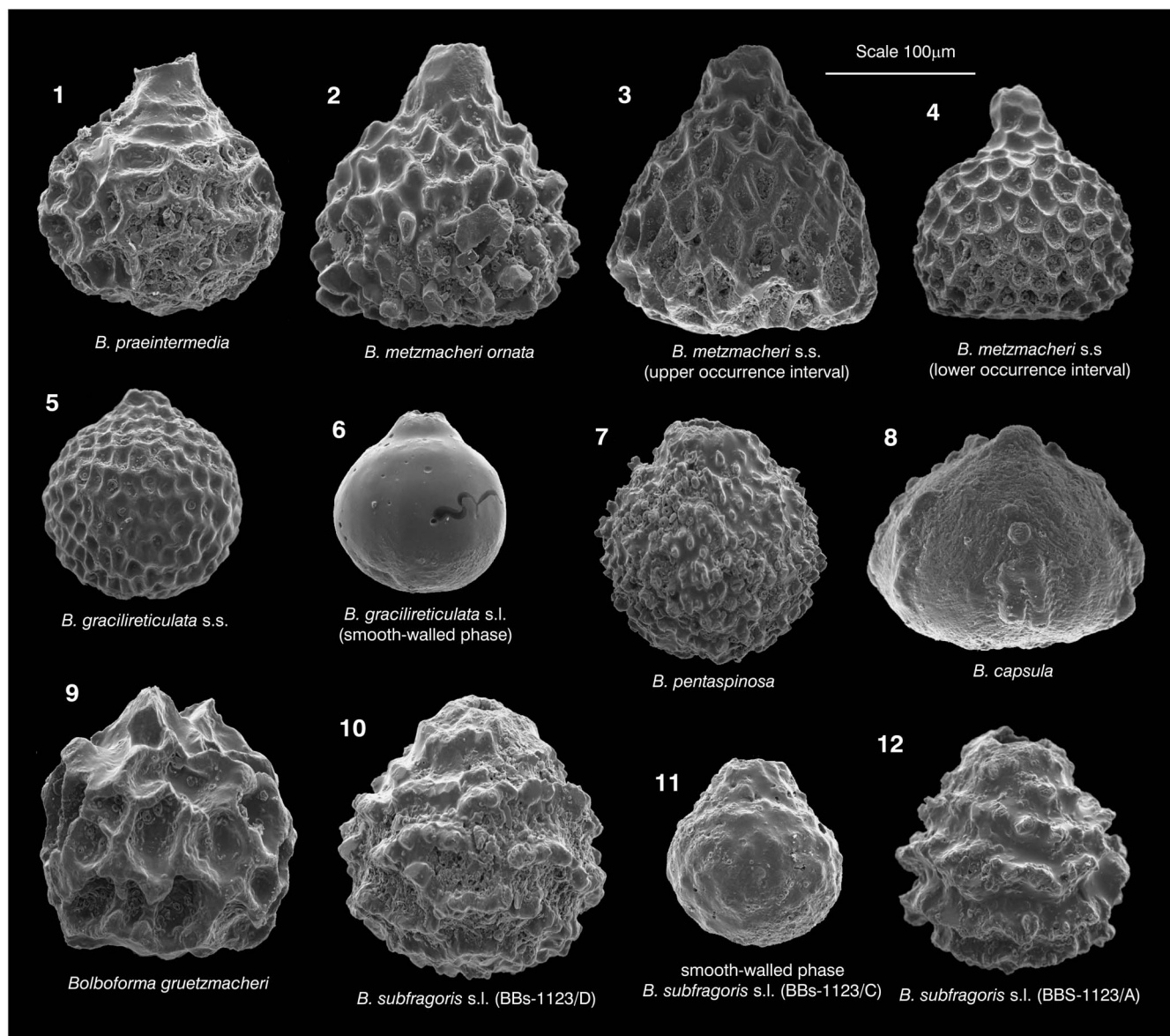
Cross-plot of magnetostratigraphic data from Site 1123 and the geomagnetic polarity time scale (GPTS-95) – the basis of the site’s chronology. The lower part of the magnetostratigraphic sequence is virtually complete, except for a short hiatus within Chron C4Ar.2r and a possible short hiatus in the uppermost part of Chron C5n. The upper part of the magnetostratigraphic sequence from the top of Chron C3Br.2r to the base of C3n.1n is poorly constrained. All ages for this interval are interpolated (dashed line).



Species	Depth (r-mcd)	Max abundance	Species	Depth (r-mcd)	Max abundance
<i>Bolboforma praeintermedia</i>	302.50 - 303.00	171	<i>Bolboforma capsula</i>	360.00 - 361.40	918
<i>Bolboforma metzmacheri ornata</i>	304.50 - 310.50	480	<i>Bolboforma gruetzmacheri</i>	364.90 - 368.90	1385
<i>Bolboforma metzmacheri</i> s.s.			<i>Bolboforma subfragoris</i> s.l.		
– upper occurrence interval	324.20 - 330.20	310	– 1123/D occurrence interval	370.50 - 374.50	3791
– lower occurrence interval	341.30 - 343.30	8189	– 1123/C occurrence interval	378.50 - 386.20	978
<i>Bolboforma gracilireticulata</i> s.l.	346.80 - 350.80	109	– 1123/B occurrence interval	389.02 - 391.43	341
<i>Bolboforma pentaspinosa</i>	358.30 - 360.00	188	– 1123/A occurrence interval	393.97 - 398.42	2836

TEXT-FIGURE 3

Bolboformid distribution and abundance data (see Appendix 3). The numbered horizons of illustrated specimens (1-12) correspond to Figure 4. Max abundance = specimens (n) /g in the >125µm sediment size fraction. Bolboformid zonation based on Spiegel and Daniels (1991) and Grützmacher (1993). BBi = *Bolboforma intermedia* Interval Zone, BBm = *B. metzmacheri* Taxon-range Zone, BBc = *B. capsula* Interval Zone, BBs = *B. subfragoris* s.l. Taxon-range Zone. Definitions of biozones are given in Appendix 2.



TEXT-FIGURE 4

SEM photomicrographs of bolboformids from Hole 1123B. All images are shown to the same scale.

- |  |  |
|--|--|
| 1 <i>Bolboforma praeintermedia</i> Spiegler; 32X-1, 50-55cm                                | 7 <i>Bolboforma pentaspinosa</i> Spiegler; 37X-6, 100-104cm  |
| 2 <i>Bolboforma metzmacheri ornata</i> Spiegler; 32X-5, 50-55cm                            | 8 <i>Bolboforma capsula</i> Spiegler; 38X-2, 0-4cm   |
| 3 <i>Bolboforma metzmacheri</i> s.s. (Clodius) upper occurrence interval; 34X-6, 100-105cm | 9 <i>Bolboforma gruetzmacheri</i> Crundwell; 38X-6, 100-104cm  |
| 4 <i>Bolboforma metzmacheri</i> s.s. (Clodius) lower occurrence interval; 36X-2, 10-14cm   | 10 <i>Bolboforma subfragoris</i> s.l. Spiegler (BBs-1123/D occurrence interval); 39X-4, 50-53cm                            |
| 5 <i>Bolboforma gracilireticulata</i> s.s. Spiegler; 36X-5, 10-14cm                        | 11 Small smooth-walled form <i>Bolboforma subfragoris</i> s.l. Spiegler (BBs-1123/C occurrence interval); 40X-3, 100-103cm |
| 6 <i>Bolboforma gracilireticulata</i> s.l. Spiegler; 37X-1, 50-54cm                        | 12 <i>Bolboforma subfragoris</i> s.l. Spiegler (BBs-1123/A occurrence interval); 41X-6, 0-5cm                              |

*capsula* extends from Chron C5n.2n(0.27) to C5n.2n(0.21) and it has an interpolated magnetochronologic age of 10.20-10.13 Ma.

The top of the *B. capsula* occurrence interval overlaps with the base of the *B. pentaspinosa* occurrence interval (Appendix 3). Although this suggests there may have been contemporary bolboformid populations in the vicinity of Site 1123, for a short period at least, the overlap is an unusual feature of the bolboformid distribution and other sedimentary factors, such as bioturbation and reworking, may have been involved.

***Bolboforma pentaspinosa* occurrence interval (10.15-10.08 Ma):** *Bolboforma pentaspinosa* is distinguished from other highly spinose bolboformid species by its small subspherical shell and low collar-like apertural neck (text-fig. 4/7). It is confined to a short interval between samples 1123B-38X-1, 10-14cm and 1123B-37X-6, 50-54cm. The base of the *B. pentaspinosa* occurrence interval overlaps with the top of the *B. capsula* occurrence interval. It extends from Chron C5n.2n (0.22) to C5n.2n (0.16) and has an interpolated magnetochronologic age of 10.15-10.08 Ma.

A specimen of *B. pentaspinosa* has also been noted higher in the section, in sample 1123B-37X-2, 0-4cm, but it is an isolated occurrence and it is thought to be either reworked or a contaminant. Rare specimens of *B. pentaspinosa* were also noted in the Initial Reports for Site 1123, in samples 1123B-27X CC, 30X CC and 32X CC (Shipboard Scientific Party 1999a), but a re-examination of shipboard samples failed to confirm the occurrences.

***Bolboforma gracilireticulata* s.l. occurrence interval (9.75-9.61 Ma):** In the context of this study, *B. gracilireticulata* s.l. encompasses an intergrade of small finely sculptured cancellate forms (*B. gracilireticulata* s.s.) and smooth-walled forms that have previously been identified as bolboformid cysts (e.g. Grützmacher 1993) or *B. laevis* (text-figs. 4/5 and 4/6). Although this small species is relatively uncommon at Site 1123, peak abundances of >20,000 specimens per gram have been noted at Site 593 in the 125-150 $\mu$ m sediment size fraction (Crundwell 2004). At Site 1123, *B. gracilireticulata* s.l. occurs in six out of nine samples between 1123B-37X-1, 50-54cm and 1123B-36X-5, 10-14cm. The lower part of the species stratigraphic range consists almost entirely of smooth-walled forms, and the upper part includes subequal numbers of *B. gracilireticulata* s.s. and small smooth-walled forms. The *B. gracilireticulata* s.l. occurrence interval extends from the base of Chron C4Ar.3r to Chron C4Ar.2n(0.51) and has an interpolated magnetochronologic age of 9.75-9.61 Ma.

***Bolboforma metzmacheri* s.s. taxon-range zone (9.54-8.78 Ma):** *Bolboforma metzmacheri* s.s. is ornamented with a coarsely cancellate-ridged sculpture. It superficially resembles the benthic foraminifer *Oolina hexagona*, but is distinguished by its flattened aboral surface and the more irregular pattern of its surface ornament (text-fig. 4/4). The taxon-range zone range of *B. metzmacheri* s.s. includes occurrence intervals in its lower and upper parts that are separated by an extended barren interval where there are no bolboformids. The lower occurrence interval extends from 1123-36X-2, 110-114cm to 1123-36X-1, 60-64cm, and the upper occurrence interval extends from 1123-34X-6, 100-105cm to 1123-34X-2, 100-105cm.

The base of the lower *B. metzmacheri* s.s. occurrence interval occurs 2.5m above the top of the Gc-1123/B coiling zone

(text-fig. 5; see later discussion). This well-defined interval extends from C4Ar.2r(0.86) to C4Ar.2r(0.11) and has an interpolated magnetochronologic age of 9.54-9.34 Ma. It includes a prominent abundance spike in sample 1123-36X-2, 10-14cm where abundances in the >125 $\mu$ m sediment size fraction peak at about 8200 specimens per gram (text-fig. 3). The spike in abundance, which is the largest such spike noted at Site 1123, coincides with a possible hiatus of <100kyr within Chron C4Ar.2r (text-fig. 2; Shipboard Scientific Party 1999a). It has an interpolated magnetochronologic age of 9.44 Ma, but the hiatus places a cautionary caveat on the reliability of the age.

The base of the upper *B. metzmacheri* s.s. occurrence interval coincides with the entry of moderate numbers of bolboformids and is well defined, but bolboformid numbers decrease in the upper part of the interval and occurrences are intermittent (Appendix 3). The upper *B. metzmacheri* s.s. occurrence interval extends from C4An(0.94) to C4An(0.25) and has an interpolated magnetochronologic age of 9.01-8.78 Ma. The regional disappearance of the planktic foraminifer *Globoquadrina dehiscens* occurs near the middle of the upper *B. metzmacheri* s.s. occurrence interval.

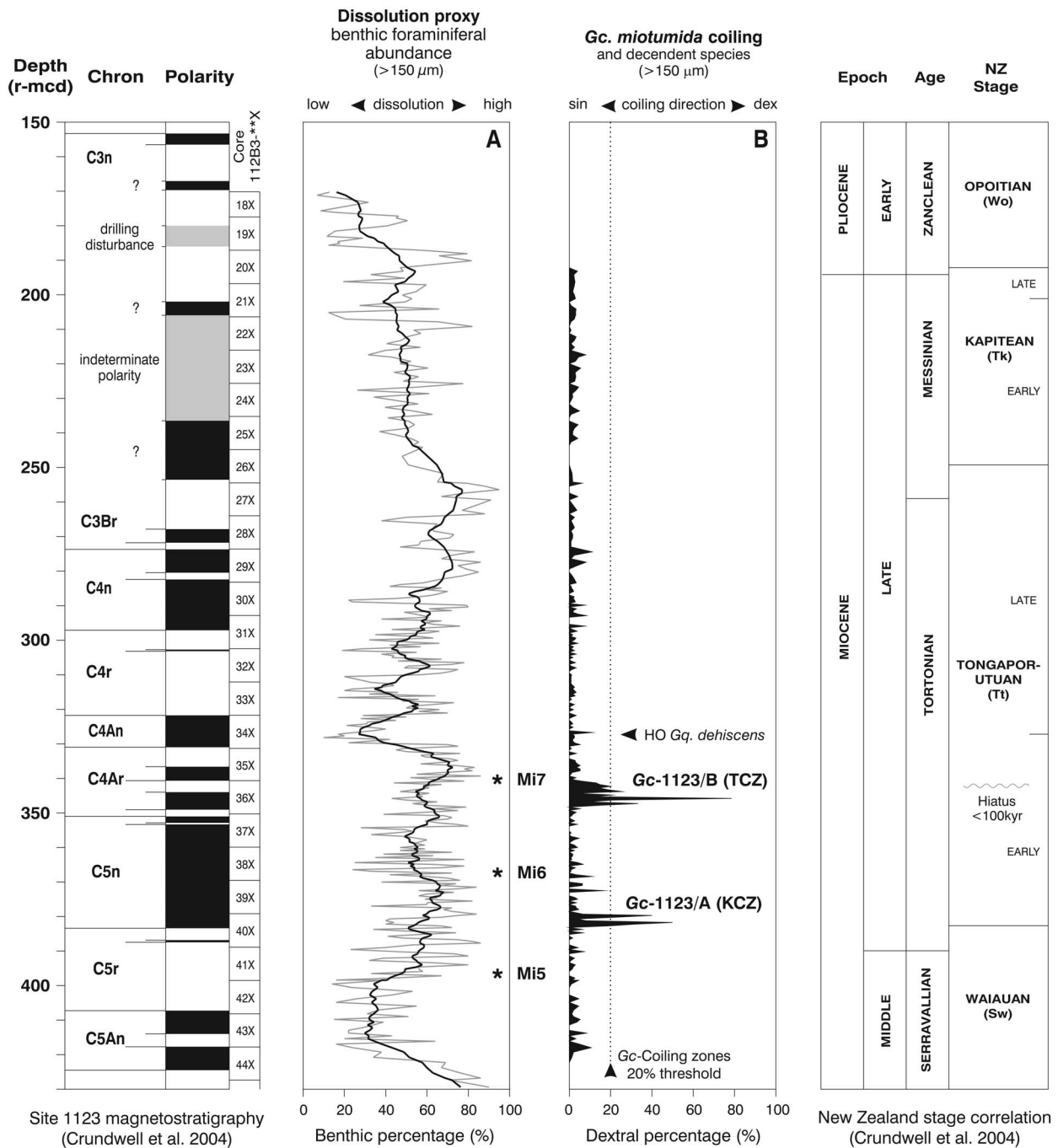
***Bolboforma metzmacheri ornata* occurrence interval (8.45-8.28 Ma):** *Bolboforma metzmacheri ornata* is distinguished from *B. metzmacheri* s.s. by the presence of short aborally-pointing spines at the junctions of the cancellate-ridged ornament (text-fig. 4/2). It first appears in sample 1123-32X-6, 50-55cm and its stratigraphic range extends upward to 1123-32X-2, 50-55cm. *B. metzmacheri ornata* is a relatively common and persistent species that occurs in 12 out of 13 samples that span the species stratigraphic range (Appendix 3). Its lowest occurrence is close to the base of core 1123-32X, for which there was only 91.7% recovery, but downhole logs and shipboard logs of physical parameters suggest the core is relatively complete and the datum is reliably located. The *B. metzmacheri ornata* occurrence interval extends from Chron C4r.2r(0.44) to C4r.2r(0.06) and has an interpolated magnetochronologic age of 8.45 to 8.28 Ma.

***Bolboforma praeintermedia* occurrence interval (8.25-8.21 Ma):** The irregular spiro-concentric ridged ornament of *B. praeintermedia* (text-fig. 4/1) represents a marked morphological change from the cancellate ornament of *B. metzmacheri* species that precede it. It superficially resembles *Bolboforma gruetzmacheri*, but the ridged-ornament tends to be more evenly spaced and better interconnected. At Site 1123, it is confined to a very short interval that extends over three consecutive samples, from 1123B-32X-1, 50-55cm to 1123-31X-7, 0-5cm. The *B. praeintermedia* occurrence interval extends from the base of Chron C4n.1n to C4n.1r(0.81) and it has an interpolated magnetochronologic age of 8.25-8.21 Ma.

The disappearance of *B. praeintermedia* at 8.21 Ma represents the regional extinction of bolboformids in the Southwest Pacific (Grützmacher 1993).

#### **Bolboformid zonation and correlation**

Despite the taxonomic confusion and uncertainty surrounding this enigmatic group of calcareous microfossils (Poag and Karowe 1986), bolboformid assemblages from Site 1123 and other oceanic sites in the temperate Southwest Pacific share many common species with assemblages in the North Atlantic (e.g. Spiegler and Daniels 1991; Spiegler 1999). The order of species appearances and disappearances and ages of important



TEXT-FIGURE 5

Magnetostratigraphy of Site 1123 compared to stratigraphic plots of benthic foraminiferal abundance (dissolution proxy), *Globoconella miotumida* coiling data, and New Zealand Stages. A) High benthic abundances correspond to high dissolution, grey curve (benthic percentage), black curve (11-point moving average), calibrated oxygen isotope events Mi5, Mi6, and Mi7 from Wright and Miller (1992). B) Subzone *Gc*-1123/A corresponds to the Kaiti Coiling Zone (KCZ, Scott 1995), and *Gc*-1123/B corresponds to the Tukemokihi Coiling Zone (TCZ) identified at Site 593 and uplifted marine sections in New Zealand (Crundwell et al. 1997b; Crundwell et al. 2004).

zonal events are also very similar (Table 2). This allows the bolboformid zonation in the North Atlantic and southern Indian Ocean (Spiegler and Daniels 1991) to be used with minimal modification in the Southwest Pacific (Grützmacher 1993).

In this study, four of Spiegler and Daniels bolboformid zones are recognized, although improvements in taxonomy (Crund-

well et al. 2005), the close sampling interval, and the very well defined ranges of most species has necessitated minor changes to the zones to make them easier to apply in the Southwest Pacific. The emended zones include:

1) The *B. subfragoris* s.l. taxon-range zone (BBs-Zone) which extends from the lowest to the highest occurrence of *B.*

*subfragoris* s.l., and includes four occurrence intervals of *B. subfragoris* s.l. separated by three barren intervals without bolboformids (see above). At Site 1123, the BBs-Zone has a magnetochronologic age of 11.56-10.50 Ma. This is similar to the reported age of 11.7-10.6 Ma age for the BBs-Zone in the North Atlantic (Spiegler 1999).

2) The *B. capsula* partial range zone (BBc-Zone) encompasses the interval from immediately above the highest occurrence of *B. subfragoris* s.l. to immediately below the lowest occurrence of *B. metzmacheri* s.s. The BBc-Zone includes the occurrence intervals of *B. gruetzmacheri*, *B. capsula*, *B. pentaspinosa*, and *B. gracilireticulata* and four barren intervals without bolboformids; an interval at the base of the BBc-Zone, intervals between the occurrence intervals of *B. gruetzmacheri* and *B. capsula*, and *B. pentaspinosa* and *B. gracilireticulata*, and an interval at the top of the BBc-Zone. At Site 1123, the BBc-Zone has a magnetochronologic age of 10.50-9.54 Ma. This is similar to the 10.6-9.7 Ma age for the BBc-Zone in the North Atlantic (Spiegler 1999).

3) The *B. metzmacheri* taxon range zone (BBm-Zone) extends from the lowest occurrence of *B. metzmacheri* s.s. to the highest occurrence of *B. metzmacheri ornata* and includes the lower and upper occurrence intervals of *B. metzmacheri* s.s., the occurrence interval of *B. metzmacheri ornata*, and two barren intervals without bolboformids that separate the occurrence intervals. At Site 1123, the BBm-Zone has a magnetochronologic age of 9.54-8.78 Ma. In the North Atlantic the base of the BBm-Zone has a similar age of 9.7 Ma, but the top of the zone at 7.7 Ma is much younger.

4) The *B. intermedia* partial range zone (BBi-Zone) is incomplete in the Southwest Pacific and extends upwards from immediately above the highest occurrence of *B. metzmacheri ornata* to the highest occurrence of *B. praeintermedia*. The upper part of the BBi-Zone is missing in the Southwest Pacific (Grütz-macher 1993); although in the southern Indian Ocean and the North Atlantic the BBi zone extends through to the latest Miocene (5.6 Ma, Spiegler 1999).

The general similarity between the magnetochronologic ages for the bolboformid zones at Site 1123 and the reported ages for the same zones in the North Atlantic (Spiegler 1999) suggest some bolboformid events may be isochronous, or nearly so, between the Southwest Pacific and North Atlantic and are potentially useful for regional and interregional correlation.

#### **Paleoceanographic implications of the bolboformid record**

The well-defined sequence of short-lived appearances and disappearances of monospecific bolboformid populations at Site 1123 is very similar to the sequence of appearances and disappearances at Site 593 (Table 3) – a much shallower oceanic site in the Tasman Sea (text-fig. 1) with very well preserved calcareous microfossil assemblages. Although it is still only possible to speculate about the causes of these appearances and disappearances, the general increase in bolboformid abundance and diversity that occurs between DSDP Sites 590 and 594 (Grütz-macher 1993) points to their introduction from higher southern latitudes. Because the northward transport of bolboformids is orthogonal to the regional paleoceanographic pattern of surface-water circulation and oceanic fronts in the late Miocene (Edwards 1975; Nelson and Cooke 2001) it has been postulated that the bolboformids were entrained in the northward flow of subsurface water masses (Cooke et al. 2002; Crundwell et al.

2005). Furthermore, the presence of bolboformids at relatively shallow oceanic sites where the seafloor is bathed by Antarctic Intermediate Water (AAIW; e.g. Sites 593 and 594) suggests the distribution of bolboformids may have been coextensive with the distribution of this water mass. In this respect, the punctuated record of bolboformid appearances and disappearances at Site 1123 – average duration 150kyr (Table 2) – may record periodic episodes of intensified AAIW formation at the Antarctic Polar Front. In this context, it is speculated that bolboformid abundance spikes, where bolboformid numbers in the >150µm sediment size fraction sometimes reach several thousand specimens per gram, may record condensed intervals, or diastems.

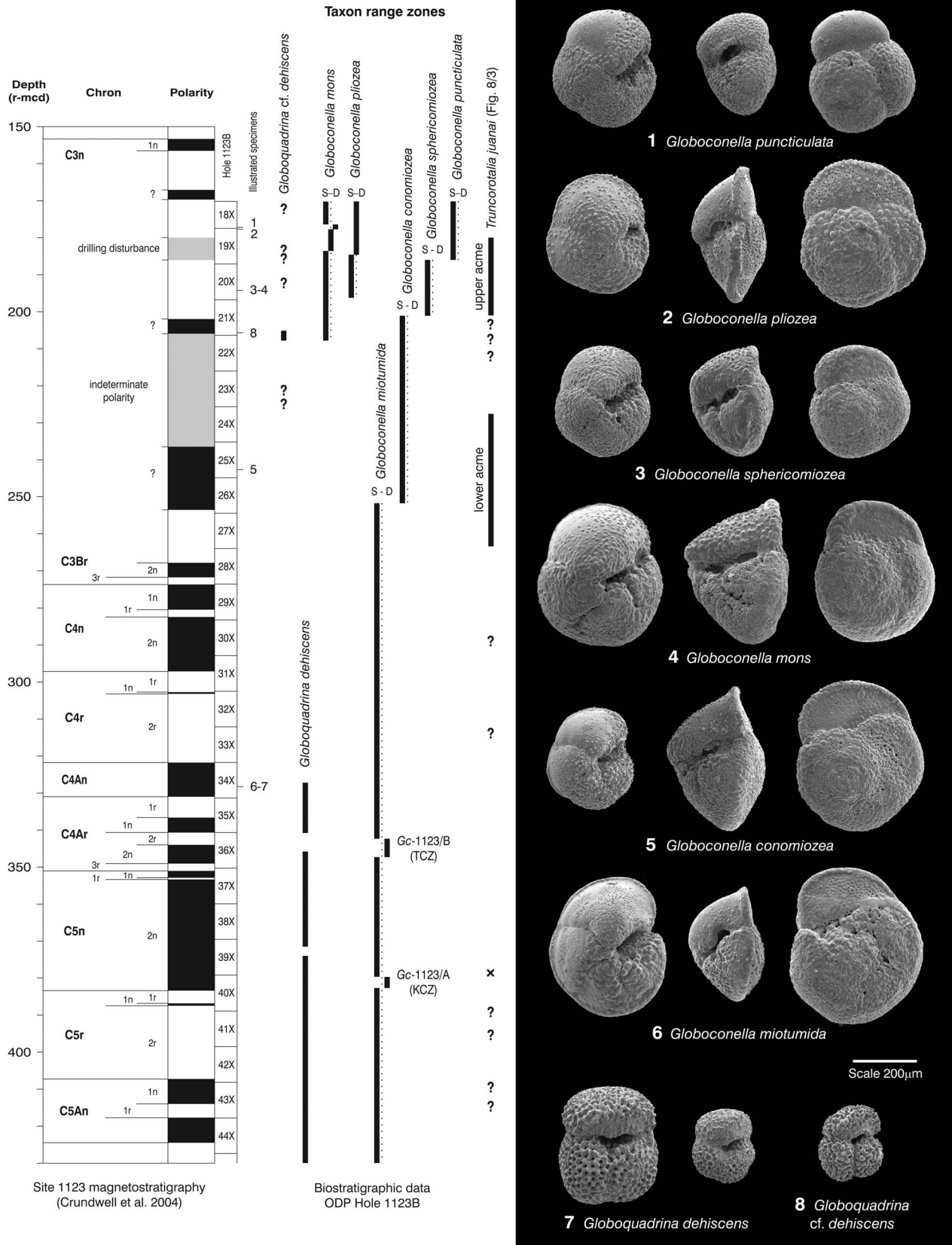
The extinction of bolboformids in the Southwest Pacific at 8.21 Ma occurs about 4myr earlier than their extinction in the southern Indian Ocean, in the late early Pliocene, Zanclean (Spiegler and Daniels 1991; Mackensen and Spiegler 1992), and 5.4myr before their extinction in the North Atlantic (Spiegler 1999). The reason for the early extinction of bolboformids in the Southwest Pacific is not known. We would speculate, however, that the late Miocene restriction of the Indonesian Gateway (Gasperi and Kennett 1993) and subsidence of the Norfolk Ridge (Herzer et al. 1997) may have intensified the counter-flow of higher salinity AAIW that interrupts the northward flow of low-salinity AAIW in the Southwest Pacific and Tasman Sea (e.g. Wyrki 1962). The northward flow of AAIW is unlikely to have ceased completely, but a reduction in the intensity of the flow may have been sufficient to interrupt the entrained supply of bolboformids in such a water mass (Cooke et al. 2002). Further studies of bolboformid distribution patterns are clearly needed on regional and global scales to elucidate the paleoceanographic circulation patterns of intermediate water masses.

#### **PLANKTIC FORAMINIFERS**

Planktic foraminifers, including species that are used for the recognition and correlation of New Zealand stages, are present throughout the upper Miocene section of Site 1123, although their preservation and abundance are highly variable (text-fig. 5). The large number of fragmented and partially dissolved shells in many samples and the dominance of heavily encrusted morphotypes, particularly *Globoconella*, *Zeoglobigerina*, and *Neogloboquadrina*, suggest calcareous faunas were subject to differential dissolution. Faunas that have been severely affected by dissolution contain mostly benthic specimens and they have few whole or nearly whole specimens. This reduces the potential biostratigraphic resolution of some planktic foraminiferal events, particularly those that have a low resistance to dissolution.

#### **Planktic foraminiferal biostratigraphy and biochronology**

The biostratigraphic data from Site 1123 (Appendix 3) identify at least 13 planktic foraminiferal events based on species and morphotypes that have a high resistance to dissolution. They include dextral coiling excursions in *Globoconella miotumida* (Gc-1123/A and Gc-1123/B), the regional disappearance of *Globoquadrina dehiscens*, an acme zone of *Truncorotalia juanai*, and the evolutionary appearances of *Globoconella conomiozea*, *Gc. mons*, *Gc. sphericomiozea*, *Gc. pliozea*, and *Gc. puncticulata*. Taxa that are less resistant to dissolution (e.g. *Neogloboquadrina mayeri* s.l., *Nq. pachyderma*, and *Truncorotalia crassaformis*) are poorly represented at Site 1123, even though they are relatively common in well preserved temperate



TEXT-FIGURE 6  
 Distribution of important dissolution-resistant planktic foraminifera at Site 1123B. The numbered horizons of illustrated specimens (1-8) correspond to the adjacent SEM images. All images are shown to the same scale. *Gc-1123/A* and *Gc-1123/B* (see caption to text-figure 5). S = sinistral-coiled, D = dextral-coiled.

planktic foraminiferal assemblages (Scott et al. 1990). Their poor preservation and patchy distribution at Site 1123 adversely affects their utility as biochronostratigraphic markers, but does not rule out their use for correlating sequences with better preservation.

**Gc-1123/A coiling zone (10.92-10.82 Ma):** The Gc-1123/A coiling zone is clearly defined in coiling data from Site 1123 (text-fig. 5). It is associated with intermittent acmes of dextral-coiled shells that interrupt the long-term succession of sinistrally-dominated populations of *Globoconella miotumida*, near the base of the upper Miocene (Tongaporutuan Stage). Even though the abundance of planktic foraminifers is highly variable through the upper Miocene section, most faunas have sufficient whole and fragmented specimens of *Gc. miotumida* to give reliable estimates of coiling directions. The base of the Gc-1123/A coiling zone is placed at the horizon where populations of *Gc. miotumida* first contain 20% or more of dextral shells. This occurs in 1123B-40X-3, 0-3cm. The datum is correlated with Chron C5n.2n(0.97) and has an interpolated magnetostratigraphic age of 10.92 Ma. Although the relative abundance of dextral shells within the coiling zone sometimes drops below 20%, the top of the zone is placed at the level where there is a persistent return to *Gc. miotumida* populations with less than 20% and in most instances less than 5%, of dextral shells. The top of the Gc-1123/A coiling zone, so defined, occurs in sample 1123B-40X-1, 0-3cm, within Chron C5n.2n(0.87) and has an interpolated magnetostratigraphic age of 10.82 Ma.

On the basis of its position near the base of the upper Miocene, the Gc-1123/A coiling zone is correlated with the Kaiti Coiling Zone (KCZ) – a coiling zone that has been recognized in neritic and marginal oceanic sequences exposed in New Zealand and at oceanic sites in the Tasman Sea, including Site 593 (Scott 1995). The KCZ occurs at the base of the Tongaporutuan Stage (Crundwell et al. 2004), and provides a useful criterion for the stage boundary in oceanic and deep-water sequences lacking age diagnostic species of *Bolivinita*. Morgans et al. (1996) have previously assigned an age of 11.26 Ma to the stage boundary, but on the basis of the present study the boundary is assigned an age of 10.92 Ma.

**Gc-1123/B coiling zone (9.62-9.42 Ma):** The Gc-1123/B coiling zone has previously been identified at Site 593 and at uplifted marine sequences in New Zealand (Crundwell et al. 1997b; Crundwell 2004). It is a very short and well-defined zone associated with acmes of dextrally-coiled *Globoconella miotumida*, similar to the Gc-1123/A coiling zone. An arbitrary 20% threshold of dextral-coiled specimens of *Gc. miotumida* – about four-times the long-term dextral average at Site 1123 – defines the stratigraphic limits of the coiling zone, although the relative abundance of dextral shells within the zone is highly variable and sometimes falls below 20%. It extends from 1123B-36X-5, 60-64cm to 1123B-36X-2, 10-14cm. The base of the coiling zone is correlated with Chron C4Ar.2n(0.71) and the top of the coiling zone with Chron C4Ar.2r(0.41). It has an interpolated magnetostratigraphic age of 9.62-9.42 Ma.

On the basis that the Gc-1123/B coiling zone is closely associated with *Bolboforma metzmacheri* s.s. and the regional disappearance of *Globoquadrina dehiscens*, it is correlated with the Tukemokihi Coiling Zone (TCZ), the youngest of three late Miocene intervals of dextrally-coiled *Gc. miotumida* (Crundwell et al. 2004). The Mapiri Coiling Zone (MCZ), which oc-

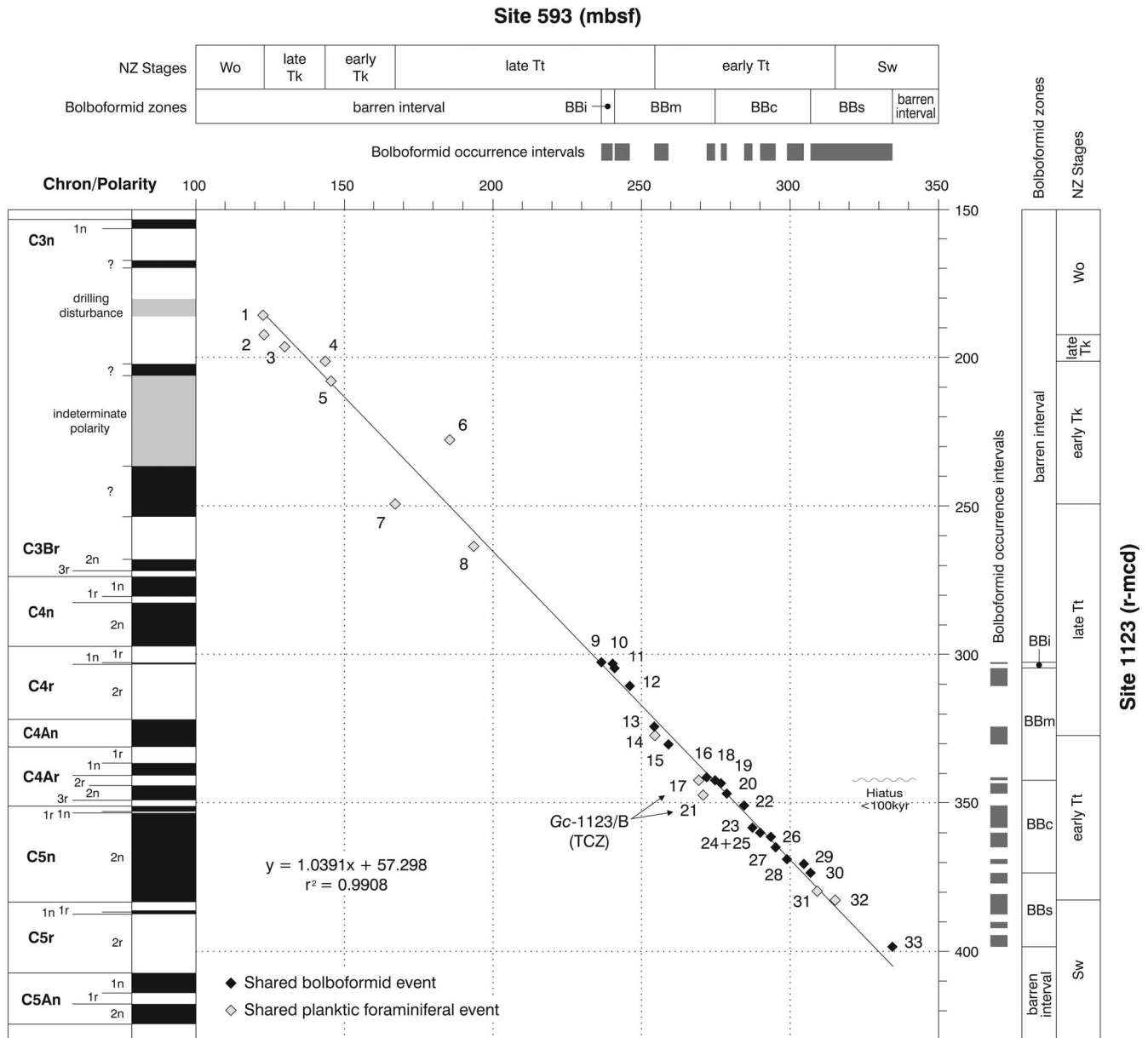
curs between the KCZ and TCZ (Crundwell et al. 2004), is not recognized at Site 1123. It is presumably cut-out by the hiatus in Chron C4Ar.2r (see earlier).

**HO *Globoquadrina dehiscens* (8.88 Ma):** *Globoquadrina dehiscens* is a deep dwelling warm-water species that occurs in low numbers throughout the lower upper Miocene section of Site 1123. It is relatively persistent and is found in 85% of early late Miocene samples, including 19 out of 20 samples in the interval immediately prior to its disappearance (Appendix 3). Most specimens are small and heavily encrusted and this appears to have been a factor in their preservation, particularly in intervals severely affected by dissolution. The highest occurrence of *Gq. dehiscens* is in sample 1123B-34X-4, 100-105cm. In the interval immediately prior to the species disappearance there is an abrupt change from high to low dissolution (text-fig. 5), the largest and most rapid baseline shift in the upper Miocene dissolution curve. The highest occurrence of *Gq. dehiscens* occurs within Chron C4An(0.57) and it has an interpolated magnetostratigraphic age of 8.88 Ma. This is significantly younger than 10.1 Ma reported by (Morgans et al. 1996) and it results in a more-or-less equal subdivision of the Tongaporutuan Stage into lower and upper parts. This ameliorates the paradox whereby most onland sections in New Zealand appeared to have sedimentary thicknesses that were disproportionate to the duration of these intervals.

The highest occurrence of *Gq. dehiscens* is well defined at Site 1123, although very rare specimens of *Gq. cf. dehiscens* occur higher in the late Miocene section, most notably between samples 1123B-22X-1, 140-145cm and 1123B-21X-6, 90-95cm (Appendix 3). These specimens are very small and they resemble the Paleogene taxon *Acarinina primitiva* in having a strongly muricate test and only three to three and one-half chambers in the outer whorl (text-fig. 6/8). Most have a flattened, steeply inclined umbilical face and an exterior-marginal-umbilical aperture, but they lack the well-developed tooth-like projection that is typical of large specimens of *Gq. dehiscens*. As there is no evidence to substantiate reworking, the specimens are considered to be expatriates that have been reintroduced to the New Zealand region from low latitudes, where the range of *Gq. dehiscens* extends up to the Miocene-Pliocene boundary (Kennett and Srinivasan 1983; Berggren et al. 1995; Li et al. 2006).

Similar enigmatic occurrences of *Gq. dehiscens* have also been noted in the latest Miocene and early Pliocene in Marlborough and eastern North Island, New Zealand (Edwards 1987), but there are no records of expatriates in oceanic sequences from similar latitudes in the Tasman Sea (Jenkins and Srinivasan 1986). This suggests that in the latest Miocene there may have been a flow or periodic flow of relatively warm subtropical surface water off eastern New Zealand. This supports a major reorganisation of oceanic circulation in the late Miocene and the development of an early western Pacific warm pool (Li et al. 2006).

**Truncorotalia juanai acme zone (7.23-6.23 Ma):** *Tr. juanai* is a relatively uncommon species and it has a patchy distribution in the upper Miocene section of Site 1123. Persistent records of *Tr. juanai* are only found between 1123B-27X-7, 0-5cm to 1123B-24X-2, 50-55cm, and 1123B-21X-3, 40-45cm to 1123B-17X-7, 0-5cm (text-fig. 6). The lower interval is moderately well defined and it includes spirally-domed morphotypes of *Tr. juanai* similar to those found in the middle acme zone of



TEXT-FIGURE 7

Shaw-plot of shared bolboformid and planktic foraminiferal events from Sites 1123 and 593, bolboformid occurrence intervals, bolboform zonation, and New Zealand Stage correlation at both sites. An explanation of numbered bioevents is given in Table 3.

*Tr. juanai* at Site 593. It extends from Chron C3Br.2r to the lower part of an interval of indeterminate polarity and has an interpolated magnetostratigraphic age of ca. 7.23-6.23 Ma. The upper interval of *Tr. juanai* is in the vicinity of the Miocene-Pliocene boundary and corresponds to the upper *Tr. juanai* acme zone at Site 593 (Crundwell 2004; Crundwell et al. 2004). It is a poorly defined interval and includes a range of biconvex to ventroconical morphotypes (*Truncorotalia* aff. *crassaformis*). The interval is significant in that it marks the permanent colonisation of the New Zealand region by *Trunco-*

*rotalia* and the beginning of an extended period of truncorotalid evolution.

**LO *Globoconella conomiozea* (ca. 6.87 Ma):** There is considerable confusion concerning *Gc. conomiozea*, with some biostratigraphers considering it to be an intraspecific variant of *Gc. miotumida* (Scott 1979; Cifelli and Scott 1986; Scott et al. 1990), while others argue that it evolved from *Gc. miotumida* as a discrete taxonomic entity (Kennett 1966; Malmgren and Kennett 1981, 1982; Hornibrook 1982). Despite these opposing

views, nearly all workers agree that although the degree of conicity may vary within upper Miocene elements of the *Gc. miotumida* plexus, there is a modal decrease in the number of chambers in the outer whorl in successively younger populations. For the purpose of this study, the entry of *Gc. conomiozea* is placed at the horizon where 10% or more of adult specimens in late Miocene populations of *Gc. miotumida-conomiozea* with high-arched apertures have less than four and one-half chambers in the outer whorl (text-fig. 6/5). This occurs in core 1123B-26X-2, 30-35cm, within the lower *Tr. juanai* acme zone, and it is correlated with the lower part of an interval of indeterminate polarity. The lowest occurrence of *Gc. conomiozea* has an interpolated age of ca. 6.87 Ma.

**LO *Globoconella mons* (ca. 5.72 Ma):** The entry of *Gc. mons* is marked by compactly coiled four-chambered variants of the *Gc. miotumida* plexus with reduced or closed umbilici, slit-like apertures, and conical to subconical axial profiles (text-fig. 6/4). The first such specimens are found in 1123B-22X-1, 140-145cm, between the top of the lower *Tr. juanai* acme zone and the lowest occurrence of *Gc. sphericomiozea*. This occurs within the lower part of an interval of indeterminate polarity and the datum has a poorly constrained interpolated age of ca. 5.72 Ma.

**LO *Globoconella sphericomiozea* (ca. 5.53 Ma):** The morphological transformation in populations of *Gc. conomiozea-sphericomiozea* occurs in an interval where globoconellids are relatively common, but most specimens are heavily encrusted and keels are often obscured by calcite overgrowth. This makes identification of the lowest occurrence of *Gc. sphericomiozea* difficult and reduces the reliability of the datum. Very rare non-carinate morphotypes are first noted in sample 1123B-27X-6, 50-55cm, but they become more persistent above 1123B-22X-1, 140-145cm. However, based on the population threshold for the lowest occurrence of *Gc. sphericomiozea* – sensu Scott (1980) where 5% or more of specimens are non-carinate – the species lowest occurrence is identified in 1123B-21X-2, 90-95cm. The datum occurs within an unidentified interval of reversed polarity and has an interpolated age of ca. 5.53 Ma.

At Blind River, an uplifted marine section in New Zealand (text-fig. 1), the lowest occurrence of *Gc. sphericomiozea* occurs within Chron C3r (Roberts et al. 1994) and it has an assigned age of 5.5 Ma (Morgans et al. 1996). Berggren et al. (1995) report a similar age of 5.6 Ma for the appearance of *Gc. sphericomiozea* at subtropical Site 588, in the Southwest Pacific. Despite the potential errors involved in locating the datum at Site 1123, it would appear to be reliably correlated with the GPTS.

**LO *Globoconella pliozea* (ca. 5.39 Ma):** The adopted species concept for *Gc. pliozea* is based on relatively compressed, compactly coiled, biconvex, keeled morphotypes within the *Gc. miotumida* plexus with less than four and one half chambers in the outer whorl of adult specimens (text-fig. 6/2). The entry of such specimens occurs above the lowest occurrence of *Gc. sphericomiozea* in 1123B-20X-2, 9-14cm, within the upper part of an unidentified interval of reversed polarity. In terms of the GPTS-95 time scale (Cande and Kent 1995), the interpolated age of 5.39 Ma is consistent with the datum occurring within the upper part of an interval of reversed polarity (Chron C3r), but is younger than the 5.6 Ma age reported by Berggren et al. (1995) from subtropical Site 588 in the Southwest Pacific.

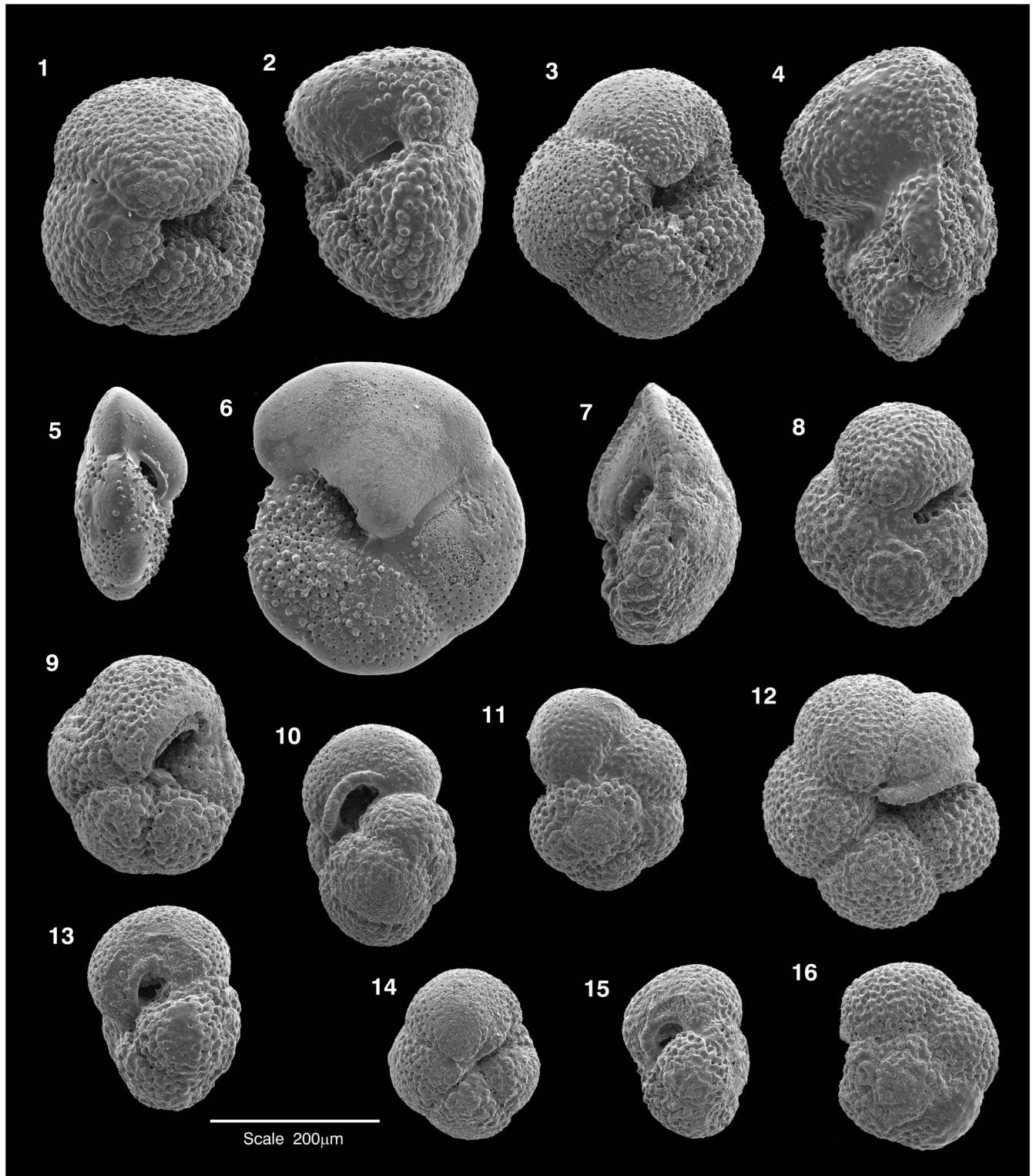
**LO *Truncorotalia crassaformis* (ca. 5.15 Ma):** The lowest occurrence of *Tr. crassaformis* is marked by the first appearance of distinctly ventroconical morphotypes in populations of *Tr. juanai-crassaformis*. This occurs in sample 1123B-20X-1, 10-14cm in an unidentified interval of reversed polarity, and it has an interpolated age of ca. 5.15 Ma. Below this horizon, however, planktic foraminiferal assemblages are very poor and it is unlikely that the lowest occurrence of *Tr. crassaformis* is located accurately.

The morphological transformation between *Tr. juanai* and *Tr. crassaformis* occurs rapidly at Site 1123 and intermediate morphotypes (*Tr. aff. crassaformis*) are confined to an interval of less than 20m (ca. 0.5myr). More detailed study of this plexus is needed, but it may be possible to refine correlations near the Miocene–Pliocene boundary and establish a morphometrically-based phylo-zonation in well-preserved sequences (e.g. Malmgren and Kennett 1982).

#### TEXT-FIGURE 8

SEM images of dissolution resistant globorotalid species from Site 1123B. All images are shown to the same scale.

- |  |   |
|--|---|
| 1 <i>Truncorotalia crassaformis</i> (Galloway and Wissler); 18X-6, 5-10cm    | 8 <i>Neogloboquadrina pachyderma</i> (Ehrenberg); 20X-6, 50-55cm            |
| 2 <i>Truncorotalia crassaformis</i> (Galloway and Wissler); 18X-5, 100-105cm | 9–11 <i>Paragloborotalia mayeri</i> (Cushman and Ellisor); 43X-4, 100-105cm |
| 3 <i>Truncorotalia juanai</i> (Bermúdez and Bolli); 20X-5, 100-105cm         | 12 <i>Neogloboquadrina acostaensis</i> (Blow); 18X-6, 5-10cm                |
| 4 <i>Truncorotalia aff. crassaformis</i> ; 20X-5, 100-105cm                  | 13–16 <i>Paragloborotalia continua</i> (Blow); 43X-4, 100-105cm             |
| 5–6 <i>Hirsutella scitula</i> (Brady); 20X-5, 100-105cm                      |   |
| 7 <i>Hirsutella panda</i> (Jenkins); 1123B-43X-1, 100-103cm                  |   |



**LO *Globoconella puncticulata* (ca. 5.11 Ma):** The lowest occurrence of *Gc. puncticulata* is placed at the level where more than 95% of large adult specimens in *Gc. sphericomiozea-puncticulata* populations are non-carinate. Based on this population concept, the lowest occurrence of *Gc. puncticulata* is identified in 1123B-19X-7, 0-5cm, in an interval with large well-preserved populations of encrusted specimens. The datum, however, is associated with an interval of drilling disturbance and indeterminate polarity and its position is unlikely to be accurate. It has an interpolated age of ca. 5.11 Ma.

At subtropical DSDP Sites 590 and 516, the lowest occurrence of *Gc. puncticulata* occurs close to the base of Chron C3n.4n (Dowsett 1989) and it has an assigned age of 5.2 Ma (Morgans et al. 1996). Given the uncertainty of the magnetostratigraphic correlation associated with the entry of *Gc. puncticulata* at Site 1123 and the difficulty of locating the entry of the species in rapidly evolving populations (e.g. Scott et al. 1980), the species entry would appear to be a more or less synchronous southern mid-latitude event. It also suggests the interval of drilling disturbance and indeterminate polarity at Site 1123 may include Chron C3n.4n and that the underlying interval of reversed polarity, where *Gc. pliozea* and *Gc. sphericomiozea* enter, may correspond to Chron C3r. This interpretation of the magnetostratigraphy is consistent with the entry of the latter species at Blind River (Roberts et al. 1994) and it suggests the magnetostratigraphic age calibration of bioevents at Site 1123 may be improved in the vicinity of the Miocene–Pliocene boundary.

#### COMPARISON OF BIOSTRATIGRAPHIC DATA IN SITES 1123 AND 593

The sequence of bolboformid and planktic foraminiferal bioevents identified at Site 1123 is correlated with Site 593 in the Tasman Sea – a very well preserved late Miocene biostratigraphic reference section (Jenkins and Srinivasan 1986; Lohmann 1986; Hoskins 1990; Scott 1992; Grützmacher 1993; Crundwell et al. 2004). A scatter-plot (text-fig. 7) based on 33 shared bioevents (Table 3) allows a line of correlation to be drawn between the two sections (Shaw 1964; Dowsett 1989).

These biostratigraphic data approximate a linear trendline and indicate the relative rate of sediment accumulation at the two sites was more-or-less constant through the late Miocene, even though the sites were more than 1400km apart and associated with different water masses. The tight grouping of the biostratigraphic data around the line of correlation ( $r^2 = 0.9908$ ) and the consistency of their order, suggest most bioevents are synchronous or nearly so.

In the lower part of the upper Miocene section at Site 1123, the only demonstrably diachronous events relate to the *Gc*-1123/B coiling zone. It plots out of sequence with respect to the highest occurrence of *B. gracilireticulata* s.l., the top and bottom of the lower *B. metzmacheri* s.s. occurrence zone and its associated abundance spike; bolboformid events that plot very close to the linear line of correlation between the sites (text-fig. 7). Although there may be a short hiatus immediately above the *Gc*-1123/B coiling zone (Shipboard Scientific Party 1999b) and there may be some uncertainty about the precise correlation of the lower *B. metzmacheri* occurrence zone, these factors alone would not explain the stratigraphic transposition of the bioevents. The possibility of a hiatus at Site 1123 and the apparent diachrony of the *Gc*-1123/B coiling zone (ca. 320kyr) between Southwest Pacific Site 1123 and Tasman Sea Site 593, place a caveat on the reliability of the coiling zone as a regional biostratigraphic marker, but they do not preclude its use for local correlations.

The upper part of the biostratigraphic sequence at Site 1123, following the disappearance of bolboformids, has a relatively small number of events compared to the lower part of the sequence at the same site (text-fig. 7). Most of the events in the upper part of the sequence are based on the evolutionary appearances of globoconellid species that are relatively common. The dominance, however, of heavily encrusted morphotypes and the high number of broken specimens in dissolution-affected samples make the interpretation of transitional populations difficult. Although this may adversely affect the reliability of some bioevents, most plot close to the linear line of correlation, ex-

#### TEXT-FIGURE 9

SEM images of dissolution resistant globigerine species from Site 1123B. All images are shown to the same scale.

- |   |   |
|---|---|
| 1–3 <i>Sphaeroidinellopsis seminulina</i> (Schwager); 32X-1, 50-55cm        | 10 <i>Zeaglobigerina woodi</i> (Jenkins); 26X-2, 30-35cm                  |
| 4 <i>Globigerinoides quadrilobatus</i> (d'Orbigny); 34X-5, 50-55cm          | 11 <i>Catapsydrax parvulus</i> (Olli, Loeblich, and Tappan); 21X-7, 0-5cm |
| 5 <i>Globigerinoides trilobus</i> (Reuss); 34X-5, 50-55cm                   | 12 <i>Globigerinina glutinata</i> (Egger); 43X-4, 100-105cm               |
| 6 <i>Globoquadrina dehiscens</i> (Chapman, Parr, & Collins); 34X-5, 50-55cm | 13 <i>Globigerina bulloides</i> d'Orbigny; 26X-2, 30-35cm                 |
| 7 <i>Globoquadrina venezuelana</i> (Hedberg); 18X-3, 0-5cm                  | 14 <i>Globigerina</i> sp.; 42X-1, 50-53cm                                 |
| 8 <i>Zeaglobigerina nepenthes</i> (Todd); 34X-5, 50-55cm                    | 15 <i>Globigerina angustumbilicata</i> Bolli; 21X-6, 90-95cm              |
| 9 <i>Zeaglobigerina druryi</i> (Akers); 42X-1, 50-53cm                      | 16 <i>Globigerinopsis obesa</i> (Bolli); 26X-2, 30-35cm                   |

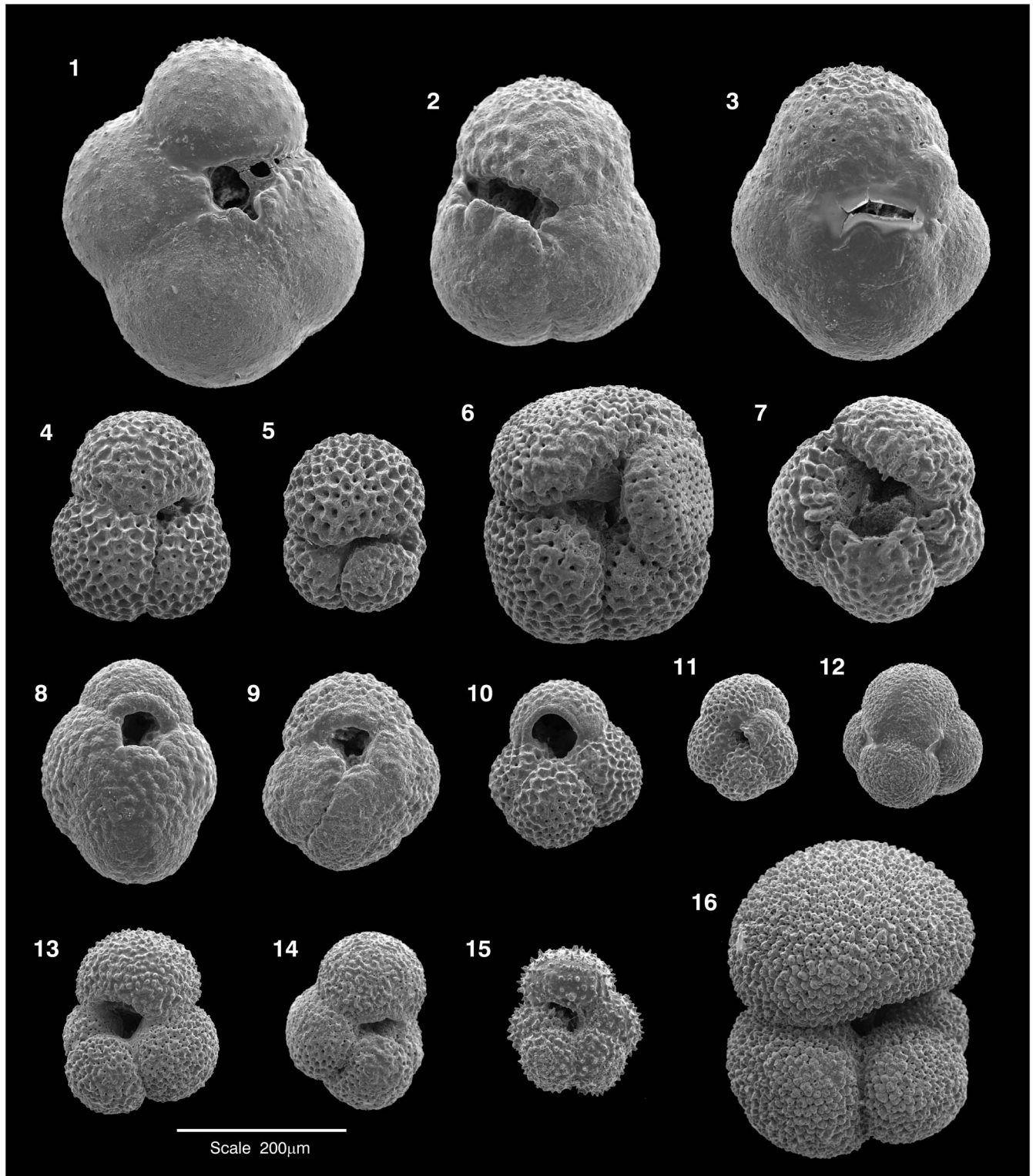


TABLE 1

Coring summary and core splice data Hole 1123B-18X to 44X. Core deformation during the coring and retrieval operation probably accounts for most of the variability in core recovery (average recovery 97.5%). For cores 23X, 26X, and 41X-44X that have less than 90% recovery this table gives a slope (m) and intercept (b) for a linear transformation from reported mbsf to stretched mbsf. Stretched mbsf = (m x mbsf) + b. To subsequently translate a sample to stretched r-mcd (revised-metres composite depth), add the offset in the last column of this table. For the other cores listed in this table, to translate a sample from mbsf to r-mcd, just add the offset.

Hole	Core	Top (mbsf)	Bottom (mbsf)	Recovered core (m)	Section drilled	Recovery (%)	Slope (m)	Intercept (b)	Offset (M)
1123-B	18X	155.40	163.79	8.39	7.30	114.9			14.80
1123-B	19X	162.70	172.41	9.71	9.50	102.2			14.80
1123-B	20X	172.30	182.05	9.75	9.50	102.6			14.80
1123-B	21X	181.90	191.37	9.47	9.50	99.7			14.80
1123-B	22X	191.60	201.47	9.87	9.50	103.9			14.80
1123-B	23X	201.20	208.96	7.76	9.50	81.7	1.2703	-54.40	14.80
1123-B	24X	210.80	220.55	9.75	9.50	102.6			14.80
1123-B	25X	220.40	230.10	9.70	9.50	102.1			14.80
1123-B	26X	230.00	234.18	4.18	9.50	44.0	2.500	-345.06	14.80
1123-B	27X	239.60	249.42	9.82	9.50	103.4			14.80
1123-B	28X	249.20	258.79	9.82	9.50	103.4			14.80
1123-B	29X	258.80	268.59	9.79	9.50	103.1			14.80
1123-B	30X	268.40	278.05	9.65	9.50	101.6			14.80
1123-B	31X	278.10	287.59	9.49	9.50	99.9			14.80
1123-B	32X	287.70	296.41	8.71	9.50	91.7			14.80
1123-B	33X	297.30	306.95	9.65	9.50	101.6			14.80
1123-B	34X	306.90	316.68	9.78	9.50	102.9			14.80
1123-B	35X	316.50	326.12	9.62	9.50	101.3			14.80
1123-B	36X	325.90	335.57	9.67	9.50	101.8			14.80
1123-B	37X	335.50	345.30	9.80	9.50	103.2			14.80
1123-B	38X	345.10	354.89	9.79	9.50	103.1			14.80
1123-B	39X	354.70	364.58	9.88	9.50	104.0			14.80
1123-B	40X	364.40	374.16	9.76	9.50	102.7			14.80
1123-B	41X	374.10	382.30	8.20	9.50	86.3	1.2703	-101.13	14.80
1123-B	42X	383.70	388.54	4.84	9.50	50.9	2.1364	-436.08	14.80
1123-B	43X	393.40	399.62	6.22	9.50	65.5	1.5932	-233.39	14.80
1123-B	44X	403.00	408.42	5.42	9.50	57.1	1.8725	-351.65	14.80

cept for the top of the *Truncorotalia juanai* acme zone and the lowest occurrence of *Globoconella conomiozea* (text-fig. 7, bioevents 6 and 7). The order of these events is transposed and they plot some distance from the line of correlation. This suggests that the stratigraphic level of these events, at Site 1123, may not be reliable.

## CONCLUSIONS

The excellent biostratigraphic correlation between Southwest Pacific Site 1123 and Tasman Sea Site 593, suggests the late Miocene magnetostratigraphically constrained biochronology from Site 1123 can be used in the temperate Southwest Pacific and Tasman Sea regions with a high degree of reliability. It also allows the ages of bioevents that are poorly defined or missing at Site 1123, including those that are associated with other microfossils groups, to be calibrated at other sites in the region by way of second-order GPTS correlations. This will undoubtedly lead to further refinements in late Miocene biochronology in the region. It will also advance the use of modern high-resolution stratigraphic tools and our ability to orbitally-tune and

correlate sedimentary sequences on a refined scale not previously possible.

## ACKNOWLEDGMENTS

This work comprises part of a PhD research programme at University of Waikato by Martin Crundwell and has been undertaken with financial support from the Marsden Fund (UOW523) and the Foundation for Research, Science and Technology through the Global Change Through Time program (CO5X0202).

Thanks are extended to the staff of the Ocean Drilling Program repository in College Station, Texas for providing samples from Site 1123 and Bruce Hayward from Geomarine Research, Auckland for providing shipboard material. Nardia Crosby prepared all samples at the University of Waikato, and Kay Card from Industrial Research provided SEM assistance. We also thank Dorothee Spiegler from Geomar, Germany for assisting with the identification of bolboformids, Gary Wilson from University of Otago for assisting with the integration of magnetostratigraphic data, Penelope Cooke from the University of

TABLE 2

Comparison of dated bolboformid datums between Site 1123 and North Atlantic. North Atlantic bolboformid datums have been dated from interpolations of second-order nannofossil and planktic foraminiferal correlations with GPTS-95 (Spiegler 1999). Bolboformid zonation emended after Spiegler and Daniels (1991) and Grützmacher (1993) for use in the Southwest Pacific. Definitions of biozones are given in Appendix 2. HO = highest occurrence, LO = lowest occurrence.

Event	Site 1123 (Ma)	Interval duration (kyr)	Bolboform zonation	North Atlantic (Ma)
HO <i>Bolboforma praeintermedia</i>	8.21	30	<i>B. intermedia</i> Interval Zone (BBI)	7.7
LO <i>Bolboforma praeintermedia</i>	8.25			
HO <i>Bolboforma metzmacheri ornata</i>	8.28	160	<i>B. metzmacheri</i> Taxon-range Zone (BBm)	
LO <i>Bolboforma metzmacheri ornata</i>	8.44			
HO <i>Bolboforma metzmacheri</i> s.s. (top upper occurrence interval)	8.78	230		
LO <i>Bolboforma metzmacheri</i> s.s. (base upper occurrence interval)	9.01			
HO <i>Bolboforma metzmacheri</i> s.s. (top lower occurrence interval)	9.34	200		9.7
LO <i>Bolboforma metzmacheri</i> s.s. (base lower occurrence interval)	9.54			
HO <i>Bolboforma gracilireticulata</i> s.l.	9.61	140		
LO <i>Bolboforma gracilireticulata</i> s.l.	9.75			
HO <i>Bolboforma pentspinosa</i>	10.08	70	<i>B. capsula</i> Interval Zone (BBc)	
HO <i>Bolboforma capsula</i>	10.13			
LO <i>Bolboforma pentspinosa</i>	10.15	70		
LO <i>Bolboforma capsula</i>	10.20			
HO <i>Bolboforma gruetzmacheri</i>	10.31	150		
LO <i>Bolboforma gruetzmacheri</i>	10.46			
HO <i>Bolboforma subfragoris</i> s.l. (top occurrence interval BBs-1123/D)	10.50	150		10.6
Base occurrence interval BBs-1123/D	10.65			
Top occurrence interval BBs-1123/C	10.77	270	<i>B. subfragoris</i> s.l. Taxon-range Zone (BBs)	
Base occurrence interval BBs-1123/C	11.04			
Top occurrence interval BBs-1123/B	11.15	130		
Base occurrence interval BBs-1123/B	11.28			
Top occurrence interval BBs-1123/A	11.36	200		11.7
LO <i>Bolboforma subfragoris</i> s.l. (base occurrence interval BBs-1123/A)	11.56			

Waikato for discussions about Southwest Pacific paleoceanography, and colleagues from Geological and Nuclear Sciences for their suggested improvements to drafts of the paper. Bob Carter, Bruce Hayward, Mark Leckie, and Chris Hollis are thanked for reviewing drafts of this paper.

## REFERENCES

- BERGGREN, W. A., KENT, D. V., SWISHER, C. C., III. and AUBRY, M.-P., 1995. A revised Cenozoic geochronology and chronostratigraphy. In: Berggren, W. A., Kent, D. V., Aubry, M.-P., and Hardenbol, J., Eds., *Geochronology, Time scales and Global Stratigraphic Correlation*, 129-211. Tulsa, Oklahoma: Society for Sedimentary Geology Special Publication No. 54.
- BOLLI, H.M.; SAUNDERS, J.B., 1985. Oligocene to Holocene low latitude planktic foraminifera. In: Bolli, H. M.; Saunders, J. B.; Perch-Nielsen, K., Ed., *Plankton stratigraphy*, 155-262. Cambridge Earth Science Series, Cambridge University Press.
- CANDE, S. C. and KENT, D. V., 1995. Revised calibration of the geomagnetic polarity time scale for the Late Cretaceous and Cenozoic. *Journal of Geophysical Research*, 100(B4): 6093-6095.
- CARTER, L. and WILKIN, J., 1999. Abyssal circulation around New Zealand – A comparison between observations and a global circulation model. *Marine Geology*, 159: 221-239.
- CARTER, L., GARLICK, R., SUTTON, P., CHISWELL, S.; OIEN, N. A., and STANTON, B. R., 1998. *Ocean Circulation New Zealand*. NIWA Chart Miscellaneous Series, No. 76.
- CHAISSON, W. P. and LECKIE, R. M., 1993. High-resolution Neogene planktic foraminiferal biostratigraphy of ODP Site 806, Ontong Java Plateau (western equatorial Pacific). In: Berger, W. H., Kroenke, L. W., Mayer, L. A., et al. *Proceedings of the Ocean Drilling Program, Scientific Results, volume 130*, 137-178. College Station, Texas: Ocean Drilling Program.
- CHISWELL, S. M., 1994. Acoustic Doppler current profiler measurements over the Chatham Rise. *New Zealand Journal of Marine and Freshwater Research*, 28: 167-178.
- CHISWELL, S. M. and ROEMMICH, 1988. The East Cape Current and two eddies: a mechanism for larval retention? *New Zealand Journal of Marine and Freshwater Research*, 32: 385-397.
- CIFELLI, R. and SCOTT, G., 1986. Stratigraphic record of the Neogene Globorotalid radiation (planktic Foraminiferida). *Smithsonian Contributions to Paleobiology*, 58: 1-101.
- COOKE, P. J., NELSON, C. S., CRUNDWELL, M. P. and SPIEGLER, D., 2002. *Bolboforma* as monitors of Cenozoic palaeoceanographic changes in the Southern Ocean. *Palaeogeography, Palaeoclimatology, Palaeoecology*, 188: 73-100.
- COOKE, P. J., NELSON, C. S., HENDY, C. H. and CRUNDWELL, M. P., in review. Neogene (c. 19-5 Ma) stable isotopic stratigraphies from the southern Tasman Sea, Southwest Pacific (DSDP Site 593):

TABLE 3

Shared bioevents in Sites 1123 and 593. (r-mcd) = revised metres composite depth (G.S. Wilson pers. comm. 2002). Closest = closest constraining sample listed in the range chart (Appendix 3) to a datum. Midpoint = first and last occurrences recorded between the closest samples listed in the range chart. Persistence = presence/absence ratio of a taxon through its occurrence interval leading up to or following a datum; maximum of 20 samples. Chron/subchron = correlations give the proportional position from its younger end. Age = interpolated from the sites magnetostratigraphy (Shipboard Scientific Party 1999a, emended G.S. Wilson pers. comm. 2002), based on GPTS-95 (Berggren et al. 1995; Cande and Kent 1995). Age limit = age difference between samples constraining a datum. Site 593 = biostratigraphic data from Crundwell (2004). LO = lowest occurrence, HO = highest occurrence. \*Bioevents that do not maintain homotaxial order (see text-figure 7).

Site 1123 (Hole B)										Site 593		Ref. Lowest and highest occurrences, coiling zones, and bolboformid abundance spikes	
Core	Sect.	Upp. (cm)	Low. (cm)	Depth (mbsf)	Depth (r-mcd)	Closest (m)	Midpoint (r-mcd)	Persistence	Chron/Subchron	Age (Ma)	Age limit (Ma)		Midpoint (mbsf)
19X	7	0	5	170.82	185.62	1.58	186.41	1.00	indeterminate	5.11	±0.01	123.01	1 LO <i>Globoconella puncticulata</i> s.s. (<5% weakly carinate) Wo/Tk proxy
20X	1	10	14	172.40	187.20	0.90	187.65	0.65	reversed	5.15	±0.01	129.30	2 LO <i>Truncorotalia crassaformis</i>
20X	7	0	5	181.40	196.20	0.90	196.65	1.00	reversed	5.39	±0.01	130.10	3 LO <i>Globoconella plozea</i>
21X	3	140	145	186.30	201.10	0.98	201.59	1.00	reversed	5.53	±0.01	143.69	4 LO <i>Globoconella sphericoiozea</i> s.s. upper-lower Tk proxy
22X	1	140	145	193.00	207.80	1.37	208.49	0.95	indeterminate	5.72	±0.02	145.72	5 LO <i>Globoconella mons</i>
24X	2	50	55	212.80	227.60	-0.90	227.15	0.50	indeterminate	6.23	±0.01	185.27	6* Top <i>Truncorotalia juanai</i> acme zone (middle acme zone Site 593)
26X	2	30	35	231.80	249.24	1.50	249.99	1.00	indeterminate	6.87	±0.03	167.25	7* LO <i>Globoconella conomiozea</i>
27X	7	0	5	248.60	263.40	1.00	263.90	0.80	C3Br.2r	7.23	±0.01	193.71	8 Base <i>Truncorotalia juanai</i> acme zone (middle acme zone Site 593)
31X	7	0	5	287.10	301.90	-0.50	301.65	1.00	C4r.1r(0.81)	8.21	±0.01	236.42	9 HO <i>Bolboforma praeintermedia</i>
32X	1	50	55	288.20	303.00	0.50	303.25	1.00	base C4n.1n	8.25	±0.01	240.42	10 LO <i>Bolboforma praeintermedia</i>
32X	2	50	55	289.70	304.50	-0.50	304.25	0.92	C4r.2r(0.06)	8.28	±0.01	240.82	11 HO <i>Bolboforma metzmacheri ornata</i>
32X	6	50	55	295.70	310.50	1.70	311.35	0.92	C4r.2r(0.44)	8.45	±0.02	246.17	12 LO <i>Bolboforma metzmacheri ornata</i>
34X	2	100	105	309.40	324.20	-0.50	323.95	0.69	C4An(0.25)	8.78	±0.01	254.19	13 HO <i>Bolboforma metzmacheri</i> s.s. (upper occurrence interval)
34X	4	100	105	312.40	327.20	-0.50	326.95	0.90	C4An(0.57)	8.88	±0.01	254.38	14 HO <i>Globoquadrina dehisces</i> (upper-lower T1 proxy)
34X	6	100	105	315.40	330.20	0.50	330.45	0.69	C4An(0.94)	9.01	±0.01	259.17	15 LO <i>Bolboforma metzmacheri</i> s.s. (upper occurrence interval)
36X	1	60	64	326.50	341.30	-0.50	341.05	1.00	C4Ar.2r(0.11)	9.34	±0.02	271.83	16 HO <i>Bolboforma metzmacheri</i> s.s. (lower occurrence interval)
36X	2	10	14	327.50	342.30	-0.50	342.05	0.50	C4Ar.2r(0.41)	9.42	±0.02	269.07	17* Top Gc-1123/B coiling zone >20% Dex (= top TCZ)
36X	2	10	14	327.50	342.30	±0.50	342.30	1.00	C4Ar.2r(0.48)	9.44	±0.04	274.72	18 <i>Bolboforma metzmacheri</i> s.s. abundance spike (lower occurrence interval)
36X	2	110	114	328.50	343.30	0.50	343.55	1.00	C4Ar.2r(0.86)	9.54	±0.02	276.82	19 LO <i>Bolboforma metzmacheri</i> s.s. (lower occurrence interval)
36X	5	10	14	332.00	346.80	-0.50	346.55	0.67	C4Ar.2n(0.51)	9.61	±0.00	278.61	20 HO <i>Bolboforma gracilireticulata</i> s.l.
36X	5	60	64	332.50	347.30	0.50	347.55	0.50	C4Ar.2n(0.71)	9.62	±0.00	270.82	21* Base Gc-1123/B coiling zone >20% Dex (= base TCZ)
37X	1	50	54	336.00	350.80	0.50	351.05	0.67	base C4Ar.3r	9.75	±0.02	284.62	22 LO <i>Bolboforma gracilireticulata</i> s.l.
37X	6	50	54	343.50	358.30	-0.50	358.05	0.75	C5n.2n(0.16)	10.08	±0.01	287.18	23 HO <i>Bolboforma pentaspinosa</i> (excludes Site 1123 outlier)
38X	1	10	14	345.20	360.00	-0.70	359.65	1.00	C5n.2n(0.21)	10.13	±0.01	289.62	24 HO <i>Bolboforma capsula</i>
38X	1	10	14	345.20	360.00	0.40	360.20	0.75	C5n.2n(0.22)	10.15	±0.01	290.42	25 LO <i>Bolboforma pentaspinosa</i>
38X	2	0	4	346.60	361.40	0.50	361.65	1.00	C5n.2n(0.27)	10.20	±0.01	293.61	26 LO <i>Bolboforma capsula</i>
38X	4	50	54	350.10	364.90	-0.50	364.65	0.89	C5n.2n(0.38)	10.31	±0.01	295.22	27 HO <i>Bolboforma gruetzmacheri</i>
38X	7	0	4	354.10	368.90	0.60	369.20	0.89	C5n.2n(0.53)	10.46	±0.01	299.02	28 LO <i>Bolboforma gruetzmacheri</i>
39X	1	100	104	355.70	370.50	-0.50	370.25	1.00	C5n.2n(0.56)	10.50	±0.01	304.57	29 HO <i>Bolboforma subfragoris</i> s.l. (top occurrence interval BBs-1123/D)
39X	4	50	53	359.70	374.50	±0.50	374.50	1.00	C5n.2n(0.71)	10.61	±0.02	306.86	30 <i>Bolboforma subfragoris</i> s.l. abundance spike (occurrence interval BBs-1123/D)
40X	1	50	53	364.90	379.70	-0.40	379.50	1.00	C5n.2n(0.87)	10.82	±0.01	309.05	31 Top Gc-1123/A coiling zone >20% Dex (= top KCZ)
40X	3	0	3	367.40	382.50	0.50	382.45	1.00	C5n.2n(0.97)	10.92	±0.01	315.24	32 Base Gc-1123/A coiling zone >20% Dex (= base KCZ) T1/Sw boundary
41X	6	0	5	381.60	398.42	0.04	398.44	0.60	C5r.2r(0.55)	11.56	±0.00	334.65	33 LO <i>Bolboforma subfragoris</i> s.l. (base occurrence interval BBs-1123/A)

some palaeoceanographic implications. *New Zealand Journal of Geology and Geophysics*.

CRUNDWELL, M. P., 2004. "New Zealand late Miocene biostratigraphy and biochronology – Studies of planktic foraminifers and bolboforms at oceanic Sites 593 and 1123, and selected onland sections." PhD Thesis, University of Waikato, Hamilton, New Zealand, 678 pp.

CRUNDWELL, M. P., COOKE, P. J. and NELSON, C. S., 1997a. Bolboformids: Enigmatic microfossils in New Zealand late Miocene sediments. *Geological Society of New Zealand Miscellaneous Publication*, 95A: 46.

CRUNDWELL, M. P., NELSON, C. S. and SCOTT, G. H., 1997b. Coiling excursions in *Globorotalia miotumida*: A black and white guide to high-resolution biostratigraphy. *Geological Society of New Zealand Miscellaneous Publication*, 95A: 47.

CRUNDWELL, M. P., BEU, A. G., COOPER, R. A., MORGANS, H. E. G., MILDENHALL, D. C. and WILSON, G. S., 2004: Chapter 12, Miocene. In: Cooper, R. A., Ed., *The New Zealand Geological Timescale. Institute of Geological and Nuclear Sciences Monograph*, 22: 164-194.

CRUNDWELL, M. P., COOKE, P. J., NELSON, C. S. and SPIEGLER, D., 2005. Intraspecific morphological variation in late Miocene *Bolboforma*, and implications for their classification, ecology, and biostratigraphic utility. *Marine Micropaleontology*, 56: 161-176.

CRUNDWELL, M. P., SCOTT, G. H., NAISH, T. R. and CARTER, L., in review. Glacial–interglacial ocean climate variability from planktic foraminifera during the Mid-Pleistocene transition in the temperate Southwest Pacific, ODP Site 1123. *Palaeogeography, Palaeoclimatology, Palaeoecology*.

DOWSETT, H. J., 1989. Application of the graphic correlation method to Pliocene marine sequences. *Marine Micropaleontology*, 14: 3-32.

EDWARDS, A. R., 1975. Southwest Pacific Cenozoic paleoceanography and an integrated Neogene paleocirculation model, Deep Sea Drilling Project Leg 29. In: Andrews, J. E., Parkham, G., et al., *Initial Reports of the Deep Sea Drilling Project, volume 30*, 667-684. Washington D.C.: US Government Printing Office

———, 1987. An integrated biostratigraphy, magnetostratigraphy and oxygen isotope stratigraphy for the late Neogene of New Zealand. *New Zealand Geological Survey Record*, 23: 1-80.

GASPERI, J. T. and KENNETT, J. P., 1993. Miocene planktonic foraminifers at DSDP Site 289: Depth stratification using isotopic differences. In: Berger, W. H., Kroenke, L. W., Mayer, L. A., et al., *Proceedings of the Ocean Drilling Program, Scientific Results, volume 130*, 323-325. College Station, Texas: Ocean Drilling Program

GRÜTZMACHER, U. J., 1993. Die veränderungen der paläogeographischen verbreitung von *Bolboforma* – ein beitrag zur rekonstruktion und definition vor wassermassen in Tertiär. *GEOMAR Research Center for Marine Geosciences, Kiel, Report*, 22: 1-104.

- HEATH, R. A., 1985. A review of the physical oceanography of the seas around New Zealand. *New Zealand Journal of Marine and Freshwater Research*, 19: 79-124.
- HERZER, R. H., CHAPRONIERE, G. C. H., EDWARDS, A. R., HOLLIS, C. J., PELLETIER, B., RAINE, J. I., SCOTT, G. H., STAGPOOLE, V., STRONG, C. P., SYMONDS, P., WILSON, G. J. and ZHU, H., 1997. Seismic stratigraphy and structural history of the Reinga Basin and its margins, southern Norfolk Ridge system. *New Zealand Journal of Geology and Geophysics*, 40(4): 425-451.
- HODELL, D. A. and KENNETT, J. P., 1986. Late Miocene-early Pliocene stratigraphy and paleoceanography of the South Atlantic and Southwest Pacific Oceans: a synthesis. *Paleoceanography*, 1: 285-311.
- HORNIBROOK, N. DE B., 1982. Late Miocene to Pleistocene *Globorotalia* (Foraminiferida) from DSDP Leg 29, Site 284, Southwest Pacific. *New Zealand Journal of Geology and Geophysics*, 25: 83-99.
- HORNIBROOK, N. DE B., Brazier, R. C., and Strong, C. P., 1989. Manual of New Zealand Permian to Pleistocene foraminiferal biostratigraphy. *New Zealand Geological Survey Paleontological Bulletin*, 56: 1-175.
- HOSKINS, R. H., 1990. Planktic foraminiferal correlation of the Late Miocene to Early Pleistocene of DSDP Sites 284 and 593 (Challenger Plateau) with New Zealand Stages. *New Zealand Geological Survey Report*, PAL 149: 1-33.
- JENKINS, D. G. and SRINIVASAN, M. S., 1986. Cenozoic planktonic foraminifers from the equator to the sub-antarctic of the Southwest Pacific, Deep Sea Drilling Project Leg 90. In: Kennett, J. P., von der Borch, C. C., et al., *Initial Reports of the Deep Sea Drilling Project, volume 90*, 795-834, Washington D.C.: US Government Printing Office.
- JENKINS, D. G., 1992: The paleogeography, evolution and extinction of Late Miocene-Pleistocene planktonic foraminifera from the Southwest Pacific. In: Ishizaki, K.; Saito, T., Eds., *Centenary of Japanese Micropaleontology*, 27-35. Terra Scientific Publishing Company, Tokyo.
- KENNETT, J. P., 1966. The *Globorotalia crassaformis* bioseries in north Westland and Marlborough, New Zealand. *Micropaleontology*, 12: 235-245.
- KENNETT, J. P. and SRINIVASAN, M. S., 1983. *Neogene planktonic foraminifera: A phylogenetic atlas*. Hutchinson Ross Publishing Company, Stroudsburg, Pennsylvania, 265.
- KENNETT, J. P. and VELLA, P., 1975. Late Cenozoic planktonic foraminifera and paleoceanography at DSDP Site 284 in the cool subtropical South Pacific, Deep Sea Drilling Project Leg 29. In: Kennett, J. P., Houtz, R. E., et al., *Initial Reports of the Deep Sea Drilling Project, volume 29*, 769-799. Washington D.C.: US Government Printing Office.
- LAZARUS, D., SPENCER-CERVATO, C., PIKA-BIOLZI, M., BECKMANN, J.-P., SALIS, K. VON, HILBRECHT, H., THIERSTEIN, H., 1995. Revised chronology of Neogene DSDP holes from the world ocean. *Ocean Drilling Program Technical Note*, No. 24.
- LI, Q., LI, B., ZHONG, G., MCGOWAN, B., ZHOU, Z., WANG, J. and WANG, P., 2006. Late Miocene development of the western Pacific warm pool: Planktonic foraminifer and oxygen isotopic evidence. *Palaeogeography, Palaeoclimatology, Palaeoecology*, 237: 465-482.
- LOHMANN, W. H., 1986. Calcareous nannoplankton biostratigraphy of the southern Coral Sea, Tasman Sea, and southwestern Pacific Ocean, Deep Sea Drilling Project Leg 90: Neogene and Quaternary. In: Kennett, J. P., von der Borch, C. C., et al., *Initial Reports of the Deep Sea Drilling Project, volume 90*, 763-793. Washington D.C.: US Government Printing Office
- MACKENSEN, A. and SPIEGLER, D., 1992. Middle Eocene to early Pliocene *Bolboforma* (Algae?) from the Kerguelen Plateau, southern Indian Ocean. In: Wise, S. W. Jr., Schlich, R., et al., *Proceedings of the Ocean Drilling Program, Scientific Results, volume 120*, 675-682. College Station, Texas: Ocean Drilling Program.
- MALMGREN, B. A. and KENNETT, J. P., 1981. Phyletic gradualism in a Late Cenozoic planktonic foraminiferal lineage: DSDP Site 284, Southwest Pacific. *Paleobiology*, 7: 230-240.
- , 1982. The potential of morphometrically based phylo-zonation: Application of a late Cenozoic planktonic foraminiferal lineage. *Marine Micropaleontology*, 7: 285-296.
- MCCAIVE, I. N. and CARTER, L., 1997. Recent sedimentation beneath the Deep Western Boundary Current off northern New Zealand. *Deep-sea Research I*, 44: 1203-1237.
- MORGANS, H. E. G., SCOTT, G. H., BEU, A. G., GRAHAM, I. J., MUMME, T. C., ST GEORGE, W., STRONG, C. P., 1996. New Zealand Cenozoic time scale (version 11/96). *Institute of Geological and Nuclear Sciences Science Report*, 96/38: 11 pp.
- MORRIS, M., STANTON, B. R. and NEIL, H. L., 2001. Subantarctic oceanography around New Zealand: preliminary results from an ongoing survey. *New Zealand Journal of Marine and Freshwater Research*, 35: 499-519.
- MÜLLER, C., SPIEGLER, D. and PASTOURET, L., 1985. The genus *Bolboforma* Daniels and Spiegler in the Oligocene and Miocene sediments of the North Atlantic and northern Europe, Deep Sea Drilling Project Leg 80. In: Graciansky, P.C. de, Poag, C.W., et al., *Initial Reports of the Deep Sea Drilling Program, volume 80*, 669-675. Washington D.C.: US Government Printing Office
- NELSON, C. S. and COOKE, P. J., 2001. History of oceanic front development in the New Zealand sector of the Southern Ocean during the Cenozoic – a synthesis. *New Zealand Journal of Geology and Geophysics*, 44: 535-553.
- POAG, C. W. and KAROWE, A. L., 1986. Stratigraphic potential of *Bolboforma* significantly increased by new finds in the North Atlantic and South Pacific. *Palaios*, 1(2): 162-171.
- ROBERTS, A. P., TURNER, G. M. and VELLA, P. P., 1994. Magnetostratigraphy chronology of late Miocene to early Pliocene biostratigraphic and oceanographic events in New Zealand. *Geological Society of America Bulletin*, 106: 665-683.
- SCOTT, G. H., 1979. The late Miocene to early Pliocene history of the *Globorotalia miozea* plexus from Blind River, New Zealand. *Marine Micropaleontology*, 22(4): 341-361.
- , 1980. *Globorotalia inflata* lineage and *G. crassaformis* from Blind River, New Zealand: recognition, relationship, and use in uppermost Miocene-lower Pliocene biostratigraphy. *New Zealand Journal of Geology and Geophysics*, 23: 665-677.
- , 1992. Planktonic foraminiferal biostratigraphy (Altonian-Tongaporutuan Stages, Miocene) at DSDP Site 593, Challenger Plateau, Tasman Sea. *New Zealand Journal of Geology and Geophysics*, 35: 501-513.
- , 1995. Coiling excursions in *Globorotalia miotumida*: High resolution bioevents at the middle-upper Miocene boundary in southern temperate water masses? *Journal of Foraminiferal Research*, 25(4): 299-308.

- SCOTT, G. H., BISHOP, S. and BURT, B. J., 1990. Guide to some Neogene Globorotalids (Foraminiferida) from New Zealand. *New Zealand Geological Survey Paleontological Bulletin*, 61: 1-135.
- SHAW, A. B., 1964. *Time in Stratigraphy*. New York: McGraw Hill, 1-365.
- SHIPBOARD SCIENTIFIC PARTY, 1999a. Site 1123: North Chatham Drift – A 20-Ma record of the Pacific Deep Western Boundary Current. In: Carter, R. N., McCave, I. N., Richter, C., Carter, L., et al., *Proceedings ODP, Initial Reports*, 181, 1-184 [CD-ROM]. College Station, TX: Ocean Drilling Program.
- , 1999b. Leg 181: Southwest Pacific paleoceanography. In: Carter, R. N., McCave, I. N., Richter, C., Carter, L., et al., *Proceedings ODP, Initial Reports*, 181, 1-80 [CD-ROM]. College Station, TX: Ocean Drilling Program.
- SPENCER-CERVATO, C., 1999. The Cenozoic deep-sea microfossil record: Explorations of the DSDP/ODP sample set using the Neptune database. *Paleontologica Electronica*, 2. [[http://www.erdw.ethz.ch/~pe/1999\\_2/neptune/issue2\\_99.htm](http://www.erdw.ethz.ch/~pe/1999_2/neptune/issue2_99.htm)]
- SPENCER-CERVATO, C., THIERSTEIN, H. R., LAZARUS, D. B. and BECKMANN, J.-P., 1994. How synchronous are Neogene marine plankton events? *Paleoceanography*, 9(5): 739-763.
- SPIEGLER, D., 1999. *Bolboforma* biostratigraphy from the Hatton-Rockall Basin (North Atlantic). In: Raymo, M. E., Jansen, E., Blum, P., and Herbert, T. D., *Proceedings of the Ocean Drilling Program, Scientific Results, volume 162*, 35-49. College Station, Texas: Ocean Drilling Program.
- SPIEGLER, D. and DANIELS, C. H. VON, 1991. A stratigraphic and taxonomic atlas of *Bolboforma* (Protozoa, incertae sedis, Tertiary). *Journal of Foraminiferal Research*, 21(2): 126-158.
- SPIEGLER, D. and ERLLENKEUSER H., 2001.  $\delta^{18}\text{O}$  and  $\delta^{13}\text{C}$  in foraminiferen und bolboformen de Forschungsbohrung Nieder Octenhausen (Niedersachsen, Nord-Deutschland). *Geolisches Jahrbuch Reihe, A* 152: 440-481.
- SPIEGLER, D. and MÜLLER, C., 1992. Correlation of *Bolboforma* zonation and nannoplankton stratigraphy in the Neogene of the North Atlantic: DSDP Sites 12-116, 49-408, 81-555 and 94-608. *Marine Micropaleontology*, 20: 45-58.
- SPROVIERI, R., DI STEFANO, E., and SPROVIERI, M., 1996. High resolution chronology for late Miocene Mediterranean stratigraphic events. *Revista Italiana di Paleontologia e Stratigrafia*, 102(1): 77-104.
- SUTTON, P. J. H., 2003. The Southland Current: a subantarctic current. *New Zealand Journal of Marine and Freshwater Research*, 37: 645-652.
- UDDSTROM, M. J. and OIEN, N. A., 1999. On the use of high-resolution satellite data to describe the spatial and temporal variability of sea surface temperatures in the New Zealand region. *Journal of Geophysical Research*, 104 (C9): 20,729-20,751.
- STOMMEL, H., STROUP, E. D., REID, J. L. and WARREN, B. A., 1973. Transpacific hydrographic sections at Lats. 43°S and 28°S: the SCORPIO expedition—I. *Deep-sea Research*, 20: 1-7.
- WEISSEL, J. K., HAYES, D. E. and HERRON, E. M., 1977. Plate tectonic synthesis: the displacements between Australia, New Zealand and Antarctica since the Late Cretaceous. *Marine Geology*, 25: 231-277.
- WHITWORTH, T., WARREN, B. A., NOWLIN, W. D., PILLSBURY, R. D. and MOORE, M. I., 1999. On the deep western-boundary current in the Southwest Pacific Basin. *Progress in Oceanography*, 43: 1-54.
- WRIGHT, I. C., ASHBY, J. N. and HOSKINS, R. H., 1985. An age for the sudden disappearance of *Globoquadrina dehiscens* in Mangapoike River Valley, New Zealand. *New Zealand Geological Survey Record*, 9:102-104.
- WRIGHT, J. D. and MILLER, K. G., 1992. Miocene stable isotope stratigraphy, Site 747, Kerguelen Plateau. In: Wise, S. W. Jr., Schlich, R., et al., *Proceedings of the Ocean Drilling Program, Scientific Results, volume 120*, 855-866. College Station, Texas: Ocean Drilling Program.
- WYRTKI, K., 1962. The subsurface water masses in the western South Pacific Ocean. *Australian Journal of Marine and Freshwater Research*, 13:18-47.

Manuscript received September 30, 2006

Manuscript accepted January 20, 2007

## APPENDIX 1

Type references of bolboformids and planktic foraminifers. The original reference for each species identified at Site 1123 is given below. Complete citations for planktic foraminifers can be found in Kennett and Srinivasan (1983) and Bolli and Saunders (1985).

<b>BOLBOFORMS</b>	<b>Original citation</b>
<i>Bolboforma capsula</i>	<i>Bolboforma capsula</i> Spiegler 1987, Mededelingen van de Wekgroep voor Tertiaire Kwartaire Geologie, p. 164, pl. 2, figs. 4-6; pl. 3, figs 1-4
<i>Bolboforma gracilireticulata</i>	<i>Bolboforma gracilireticulata</i> Spiegler (nomen nudum; listed without description or illustration, Spiegler 1998)
<i>Bolboforma gruetzmacheri</i>	<i>Bolboforma gruetzmacheri</i> Crundwell et al. 2004, Marine Micropaleontology 56, p. 174-175, Appendix, fig. 1
<i>Bolboforma laevis</i>	<i>Bolboforma laevis</i> Daniels and Spiegler 1974, Paläontologische Zeitschrift 48, p. 64, pl. 7, figs. 7-9; pl. 10, fig 6, included in <i>B. gracilireticulata</i> s.l. (this paper)
<i>Bolboforma metzmacheri</i>	<i>Lagena metzmacheri</i> Clodius 1922, Archiv Verein der Freunde der Naturgeschichte Mecklenburg. n. 108. pl. 1. fig. 2
<i>Bolboforma metzmacheri ornata</i>	<i>Bolboforma metzmacheri ornata</i> Spiegler (nomen nudum; listed without description or illustration, Spiegler 1998)
<i>Bolboforma pentaspinosa</i>	<i>Bolboforma pentaspinosa</i> Spiegler and Daniels 1991, Journal of Foraminiferal Research 22(2), p. 138, pl. 6, figs. 5-7
<i>Bolboforma praeintermedia</i>	<i>Bolboforma praeintermedia</i> Spiegler (nomen nudum; listed without description or illustration, Spiegler 1998)
<i>Bolboforma subfragoris</i>	<i>Bolboforma subfragoris</i> Spiegler and Daniels 1991, Journal of Foraminiferal Research 22(2), p. 140, pl. 11, figs. 3-6
<b>PLANKTIC FORAMINIFERS</b>	<b>Original citation</b>
<i>Catapsydrax parvulus</i>	<i>Catapsydrax parvulus</i> Olli, Loeblich, and Tappan, 1957, US National Museum Bulletin, no. 215, p. 37, pl. 7, figs. 9a-c
<i>Globigerina angustiumbilocata</i>	<i>Globigerina ciperoensis angustiumbilocata</i> Bolli 1957, US National Museum Bulletin, no. 215, p. 109, pl. 22, figs 12a-13c
<i>Globigerina bulloides</i>	<i>Globigerina bulloides</i> d'Orbigny 1826, Ann. Sci. Nat., Paris, ser. 1, tome 7, p. 277, no. 1
<i>Globigerina eamesi</i>	<i>Globigerina eamesi</i> Blow 1959, Bull. Amer. Paleontology, Ithaca, N.Y. vol. 39, no. 178, p. 176, pl. 9, figs 39a-c
<i>Globigerina quinqueloba</i>	<i>Globigerina quinqueloba</i> Natland 1938, Californian, Univ. Inst. Oceanography Bull. Tech. Ser., p. 149, pl. 6, figs 7a-c
<i>Globigerinella aequilateralis</i>	<i>Globigerina aequilateralis</i> Brady 1879, Quat. Journ. Micr. Sci., n.s., vol. 19, p. 285, (figures in Brady, 1884: Rep. Voy. Challenger, Zool. 9, pl. 80, figs. 18-21)
<i>Globigerinita glutinata</i>	<i>Globigerina glutinata</i> Egger 1893, Akad. Wiss. Munchen, Math. Physik. Cl., Abh. Bd. 18 (1895), Abth. 2, p. 371, pl. 13, figs. 19-21
<i>Globigerinita uvula</i>	<i>Pyloedixia uvula</i> Ehrenberg 1861, K. Preuss. Akad. Wiss. Berlin, Monatsber., Berlin, p. 206, 207, 308; 1873, K. Preuss. Akad. Wiss. Berlin, Abh., Jahre. 1872, pl. 2, figs. 24-25
<i>Globigerinoides bollii</i>	<i>Globigerinoides bollii</i> Blow 1959, Micropaleontology 27(3), p. 189, pl. 10, figs 65a-c
<i>Globigerinoides obliquus</i>	<i>Globigerinoides obliqua</i> Bolli 1957, US National Museum Bulletin, no. 215, p. 113, pl. 25, figs 10a-c
<i>Globigerinoides quadrilobatus</i>	<i>Globigerina quadrilobata</i> d'Orbigny 1846, Paris, Gide et Comp., p. 164, pl. 9, figs 7-10
<i>Globigerinoides ruber</i>	<i>Globigerina rubra</i> d'Orbigny 1839, Histoire physique, politique et naturelle de L'île de Cuba, 8, p. 82, pl. 4, figs. 12-14
<i>Globigerinoides sacculifer</i>	<i>Globigerina sacculifera</i> Brady 1877, Geol. Mag. London, n.s., decade 2, vol. 4, no. 2, p. 604, pl. 80, figs. 11-17, pl. 81, fig. 2, pl. 82, fig. 4
<i>Globigerinoides trilobus</i>	<i>Globigerina triloba</i> Reuss 1850, K. Akad. Wiss. Wien, Math. - Naturw. Cl., Denkschr., Berlin, Bd. 1, p. 374, pl. 477, figs. 11a-c
<i>Globigerinopsis obesa</i>	<i>Globorotalia obesa</i> Bolli 1957, US National Museum Bulletin, no. 215, p. 119, pl. 29, figs. 2a-3

APPENDIX 1  
continued.

<i>Globoconella conomiozea</i>	<i>Globorotalia conomiozea</i> Kennett 1966, <i>Micropaleontology</i> 12(2), p. 235, text figs. 10a-c
<i>Globoconella miotumida</i>	<i>Globorotalia menardii</i> (d'Orbigny) <i>miotumida</i> Jenkins 1960, <i>Micropaleontology</i> 6, p. 362, pl. 4, figs. 9a-c
<i>Globoconella mons</i>	<i>Globorotalia conomiozea mons</i> Hornibrook 1982, <i>New Zealand Journal of Geology and Geophysics</i> 25, p. 91, figs. 3a-g, 4a-i
<i>Globoconella pliozea</i>	<i>Globorotalia pliozea</i> Hornibrook 1982, <i>New Zealand Journal of Geology and Geophysics</i> 25, p. 95, figs. 7a-g
<i>Globoconella puncticulata</i>	<i>Globigerina puncticulata</i> Deshayes 1832, <i>Encyclopédie méthodique: Histoire naturelle des vers</i> , Paris, Mme. v. Agasse, tome 2, pt. 2, p. 170
<i>Globoconella sphericomiozea</i>	<i>Globorotalia puncticulata sphericomiozea</i> Walters, <i>New Zealand Journal of Geology and Geophysics</i> 8(1), 1965, p. 126, figs. 8n-s
<i>Globquadrina dehiscens</i>	<i>Globquadrina dehiscens</i> Chapman, Parr, and Collins 1934, <i>Linn. Soc. London, Jour. Zool.</i> 38(262), p. 569, pl. 11, figs. 36a-c
<i>Globoquadrina venezuelana</i>	<i>Globigerina venezuelana</i> Hedberg 1937, <i>Journal of Paleontology</i> 11(8), p. 681, pl. 92, fig. 72b
<i>Globorotalia linguaensis</i>	<i>Globorotalia linguaensis</i> Bolli 1957, <i>US National Museum Bulletin</i> , no. 215, p. 120, pl. 29, figs. 5a-c
<i>Hirsutella scitula</i>	<i>Pulvinulina scitula</i> Brady 1880, <i>Roy. Soc. Edinburgh, Proc.</i> II (III), p. 716 (Figures in Brady, <i>Rep. Voy. Challenger, Zool.</i> , pl. 103, figs. 7a-c, 1882). Banner and Blow 1960, <i>Contributions from the Cushman Laboratory for Foraminiferal Research</i> , 11, pt. 1, p. 27, pl. 5, fig. 5 (lectotype)
<i>Hirsutella panda</i>	<i>Globorotalia menardii</i> (d'Orbigny) <i>panda</i> Jenkins 1960, <i>Micropaleontology</i> 6(4), p. 364, pl. 4, figs. 10a-c
<i>Neogloboquadrina acostaensis</i>	<i>Globorotalia acostaensis</i> Blow 1959, <i>Bull. Amer. Paleontology</i> , Ithaca, N.Y. vol. 39, no. 178, p. 208, pl. 17, figs. 106a-c
<i>Neogloboquadrina dutertrei</i>	<i>Globigerina dutertrei</i> d'Orbigny 1839, <i>Histoire physique, politique et naturelle de L'île de Cuba</i> , 8, p. 84, pl. 4, figs. 19-21, Banner and Blow, 1960, <i>Contributions from the Cushman Laboratory for Foraminiferal Research</i> , 11, pt. 1, pl. 2, fig. 1 (lectotype)
<i>Neogloboquadrina pachyderma</i>	<i>Aristospira pachyderma</i> Ehrenberg 1861, <i>K. Preuss Akad. Wiss. Berlin, Monatsber.</i> p. 276, 277, 303, Banner and Blow, 1960, <i>Contributions from the Cushman Laboratory for Foraminiferal Research</i> , 11, pt. 1, p. 4, pl. 3, figs. 4a-c (lectotype)
<i>Orbulina universa</i>	<i>Orbulina universa</i> d'Orbigny 1839, <i>Histoire physique, politique et naturelle de L'île de Cuba</i> , 8, p. 3, pl. 1, fig. 1
<i>Paragloborotalia continuosa</i>	<i>Globorotalia opima</i> Bolli, <i>continuosa</i> Blow 1959, <i>Bull. Amer. Paleontology</i> , Ithaca, N.Y. vol. 39, no. 178, p. 218, pl. 19, figs. 125a-c
<i>Paragloborotalia mayeri</i>	<i>Globorotalia mayeri</i> Cushman and Ellisor 1939, <i>Contributions from the Cushman Laboratory for Foraminiferal Research</i> , 15, pt. 1, p. 11, pl. 2, figs. 4a-c
<i>Paragloborotalia nympa</i>	<i>Globorotalia mayeri</i> Cushman and Ellisor, sub sp. <i>nympa</i> Jenkins 1967, <i>New Zealand Journal of Geology and Geophysics</i> , 10(4), p. 1072, fig. 3, no. 7-13
<i>Sphaeroidinellopsis kochi</i>	<i>Globigerina kochi</i> Caudi 1934, <i>Tertiary deposits of Soemba</i> . Amsterdam, Nederland, H.J. Paris, p. 144, Type figures in <i>Eclogae Geol. Helvetiae</i> , Bd 18, no. 2, tf. 8a-b
<i>Sphaeroidinellopsis paenedehiscens</i>	<i>Sphaeroidinellopsis subdehiscens paenedehiscens</i> Blow 1969, <i>Proceedings of the first international conference of planktonic microfossils</i> . Leiden, Netherlands: E. J. Brill, vol. 1, p. 386, pl. 30, figs. 4, 5, 9
<i>Sphaeroidinellopsis seminulina</i>	<i>Globigerina seminulina</i> Schwager 1866, <i>Novara Exped. 1857-1859</i> , Wien, Bd. 2, <i>Geol. Theil.</i> , p. 256, pl. 7, fig. 112
<i>Tenuitella clemenciae</i>	<i>Turborotalia clemenciae</i> Bermudez 1961, <i>Boletín de Geología</i> , Spec. Publ. 3, Caracas, Venezuela, p. 1321, pl. 17, figs. 10a-b

APPENDIX 1  
continued.

---



---

<i>Truncorotalia crassaconica</i>	<i>Globorotalia crassaconica</i> Hornibrook 1981, New Zealand Journal of Geology and Geophysics 24, p. 271, figs. 5g-i, 9a-c
<i>Truncorotalia crassaformis</i>	<i>Globigerina crassaformis</i> Galloway and Wissler 1927, Journal of Paleontology 1, p. 41, pl. 7, fig. 12
<i>Truncorotalia juanai</i>	<i>Globorotalia juanai</i> Bermúdez and Bolli 1969, Bol. Geologia (Venezuela), 10(20), p. 171, pl. 14, figs. 1-6
<i>Truncorotalia ronda</i>	<i>Globorotalia crassaformis</i> (Galloway and Wissler), <i>ronda</i> Blow 1969, Proceedings of the first international conference on planktonic microfossils. Leiden, Netherlands: E. J. Brill, vol. 1, p. 388, pl. 4, figs 4-6, pl. 37, figs. 6-9
<i>Zeaglobigerina apertura</i>	<i>Globigerina apertura</i> Cushman 1918, US Geol. Surv. Bull. 676, p. 57, pl. 12, figs. 8a-c
<i>Zeaglobigerina decoraperta</i>	<i>Globigerina druryi</i> Akers, sub. sp. <i>decoraperta</i> Takayanagi and Saito 1962, Sci. Rep. Tohoku Univ. 2nd Ser. (Geol.), Spec. Vol. 5, p. 72, text figs. 1a-c
<i>Zeaglobigerina druryi</i>	<i>Globigerina druryi</i> Akers 1955, Journal of Paleontology 29(4), p. 654, pl. 65, fig. 1
<i>Zeaglobigerina nepenthes</i>	<i>Globigerina nepenthes</i> Todd 1957, US Geol. Survey Prof. Paper 280-H, p. 301, figs. 7a-b
<i>Zeaglobigerina woodi</i>	<i>Globigerina woodi</i> Jenkins 1960, Micropaleontology 6(4), p. 352, pl. 2, figs. 2a-c

---

APPENDIX 2

Explanation of shared planktic foraminiferal and bolboformid events and bolboformid zones in Sites 1123 and 593.

---

**BOLBOFORMS**

---

***Bolboforma subfragoris* s.l. Taxon-range Zone (BBs):** Based on Spiegler and Daniels (1991). Extends upward from the lowest occurrence of spiro-spinose bolboformids related to *B. subfragoris* s.l. to the highest occurrence of the same group of spiro-spinose bolboforms. The BBs-zone includes several short-lived influxes of spirospinose bolboforms (occurrence intervals BBs-1123/A, BBs-1123/B, BBs-1123/C, and BBs-1123/D) that are separated by barren intervals without bolboformids.

***Bolboforma capsula* Interval Zone (BBc):** Emended after Spiegler and Daniels (1991) for use in the Southwest Pacific as extending from immediately above the highest occurrence of *Bolboforma subfragoris* s.l. to immediately below the lowest occurrence of *Bolboforma metzmacheri* s.s. Includes the occurrence intervals of *Bolboforma gruetzmacheri*, *Bolboforma capsula*, *Bolboforma pentaspinosa*, and *Bolboforma gracilireticulata* s.l. that are separated by barren intervals without bolboformids.

***Bolboforma gracilireticulata* s.l.:** Includes small smooth-walled phases similar to *Bolboforma laevis* that occur in the same occurrence interval as the weakly ornamented species *Bolboforma gracilireticulata* Spiegler and form part of the range of morphological variation associated with that species (Crundwell et al. 2004).

***Bolboforma metzmacheri* Interval Zone (BBm):** Emended after Spiegler and Daniels (1991) for use in the Southwest Pacific as extending upwards from the lowest occurrence of *Bolboforma metzmacheri* s.s. to the highest occurrence of the subspecies *Bolboforma metzmacheri ornata*. Includes the lower and upper *B. metzmacheri* s.s. and *B. metzmacheri ornata* occurrence intervals, and the barren intervals without bolboformids.

***Bolboforma intermedia* Interval Zone (BBi):** Emended after Spiegler and Daniels (1991) for use in the Southwest Pacific as extending upwards from immediately above the highest occurrence of *Bolboforma metzmacheri ornata* up to the lowest occurrence of *Bolboforma costairregularis*. Only the lowermost part of the BBi-zone with *Bolboforma praeintermedia* is represented at Site 1123. The highest occurrence of this species marks the regional extinction of bolboforms in the Southwest Pacific.

---

**PLANKTIC FORAMINIFERS**

---

**HCO *Paragloborotalia mayeri* s.l.:** *Paragloborotalia mayeri* s.l. is a very common and often dominant element of late middle Miocene planktic foraminiferal assemblages in the temperate Southwest Pacific, but its abundance drops rapidly in the early late Miocene before its regional disappearance. The highest common occurrence of *Paragloborotalia mayeri* s.l. is defined here as the highest level of this species prior to its highest occurrence where it comprises at least 5% of planktic foraminifers in the 125-1000 µm size fraction.

***Globoconella miotumida* (dextral coiling excursions):** Two short intervals are identified at Site 1123 where the prevailing sinistral coiling trend in *Gc. miotumida* is interrupted by populations with majorities or significant representations (>20%) of dextral shells. The lower interval that is referred to here as the *Gc*-1123/A coiling zone corresponds to the Kaiti Coiling Zone (Scott 1995). It occurs near the highest common occurrence of *Neogloboquadrina mayeri* s.l. The upper interval that is referred to here as the *Gc*-1123/B coiling zone corresponds to the Tukemokihi Coiling Zone identified at Site 593 and uplifted marine sections in New Zealand (Crundwell et al. 1997b; Crundwell 2004). It occurs near the regional disappearance of *Globoquadrina dehiscens*.

***Truncorotalia juanai* acme zone:** An interval between the highest occurrence of *Globoquadrina dehiscens* and the lowest occurrence of *Globoconella sphericomiozea* where spirally domed variants of *Truncorotalia juanai* are relatively common. Above and below the acme zone, *Truncorotalia juanai* occurs in small numbers and its distribution is very patchy.

**HO *Paragloborotalia mayeri* s.l.:** The highest occurrence of *Paragloborotalia mayeri* s.l. marks the regional disappearance of *Pr. mayeri*, *Pr. nympha* and *Pr. continuosa*. However rare expatriate occurrences of these species occur higher in the section near the *Gc*-1123/B coiling zone. The disappearance of *Paragloborotalia mayeri* s.l. coincides with the regional appearance of *Neogloboquadrina pachyderma*.

**HO *Hirsutella panda*:** Highest occurrence of strongly keeled morphotypes – does not include weakly carinate and non-carinate specimens of *Hirsutella* cf. *ichinosekiensis* (Jenkins) that can sometimes be mistaken for *Hr. panda*.

**HO *Globoquadrina dehiscens*:** The late Miocene disappearance of *Globoquadrina dehiscens* is a well-defined regional event, but rare expatriate occurrences occur in some eastern North Island sequences, near the Miocene-Pliocene boundary.

**LO *Truncorotalia* aff. *crassaformis*:** Marked by the entry of intermediate morphological variants in the rapid anagenetic transformation between biconvex forms of *Truncorotalia juanai* and rounded forms of *Truncorotalia crassaformis*. Closely resembles *Truncorotalia crassaformis* but is more compressed ventrally and the spiral-surface is slightly convex.

**LO *Truncorotalia* aff. *crassaconica*:** Marked by the entry of forms similar to *Truncorotalia crassaformis*, but with more angular, slightly less inflated chambers and rudimentary keels – imperforate bands or slightly raised pustulose ridges around the peripheral margin.

**LO *Truncorotalia crassaformis*:** Marked by the entry of rounded forms of *Truncorotalia crassaformis* (e.g. Hornibrook et al. 1989; Scott et al. 1990).

---















APPENDIX 3  
Continued.

SAMPLES HOLE 1123B										PLANKTIC FORAMINIFERAL DISTRIBUTION (presence/absence)										BOLBOFORMID DISTRIBUTION		P/B DATA		COILING						
Core	Section	Interval (top)	Interval (bottom)	Depth (mbsf)	Depth (mcd) - G. Wilson March 2002	Polarity	Age (Ma)	Position in Chron	Stage	Core	Section	Interval (top)	Interval (bottom)	Depth (mbsf)	Depth (mcd) - G. Wilson March 2002	Polarity	Age (Ma)	Position in Chron	Stage	Planktic species (n)	Bolboformid species	Planktic foraminifers (n)	Benthic foraminifers (n)	Percentage planktics (%)	<i>Globocentella miomunda</i> gp (sinistral)	<i>Globocentella miomunda</i> gp (dextral)	Dextral <i>G. miomunda</i> gp (%)			
43X	1	100	103	394.40	409.77	11.989	0.38	New Zealand Stage	Sw	X	X	X	X	X	X	X	X	X	X	X	X	X	X	X	X	X	X	18	1	5.9
43X	2	0	5	394.90	410.56	12.006	0.49		Sw	X	X	X	X	X	X	X	X	X	X	X	X	X	X	X	X	X	X	26	1	3.7
43X	2	50	55	395.40	411.36	12.023	0.61		Sw	X	X	X	X	X	X	X	X	X	X	X	X	X	X	X	X	X	X	66	34	0.0
43X	2	100	105	395.90	412.16	12.039	0.73		Sw	X	X	X	X	X	X	X	X	X	X	X	X	X	X	X	X	X	X	71	29	3
43X	3	0	5	396.40	412.95	12.056	0.85		Sw	X	X	X	X	X	X	X	X	X	X	X	X	X	X	X	X	X	X	78	22	0.0
43X	3	50	55	396.90	413.75	12.073	0.96		Sw	X	X	X	X	X	X	X	X	X	X	X	X	X	X	X	X	X	X	78	22	0.0
43X	3	100	105	397.40	414.55	12.078	1.04		Sw	X	X	X	X	X	X	X	X	X	X	X	X	X	X	X	X	X	X	10	0	0.0
43X	4	0	5	397.90	415.34	12.088	1.10		Sw	X	X	X	X	X	X	X	X	X	X	X	X	X	X	X	X	X	X	30	1	3.2
43X	4	50	55	398.40	416.14	12.095	1.16		Sw	X	X	X	X	X	X	X	X	X	X	X	X	X	X	X	X	X	X	36	64	0.0
43X	4	100	105	398.90	416.94	12.101	1.21		Sw	X	X	X	X	X	X	X	X	X	X	X	X	X	X	X	X	X	X	84	16	4.8
44X	1	10	13	403.10	417.95	12.109	1.29		Sw	X	X	X	X	X	X	X	X	X	X	X	X	X	X	X	X	X	X	76	24	76
44X	1	80	85	403.80	419.27	12.119	1.38		Sw	X	X	X	X	X	X	X	X	X	X	X	X	X	X	X	X	X	X	62	38	62
44X	2	10	15	404.60	420.76	12.130	1.49		Sw	X	X	X	X	X	X	X	X	X	X	X	X	X	X	X	X	X	X	66	34	66
44X	2	90	95	405.40	422.26	12.142	1.60		Sw	X	X	X	X	X	X	X	X	X	X	X	X	X	X	X	X	X	X	31	69	31
44X	3	100	103	406.20	423.76	12.154	1.71		Sw	X	X	X	X	X	X	X	X	X	X	X	X	X	X	X	X	X	X	24	76	24
44X	3	100	103	407.00	425.26	12.165	1.82		Sw	X	X	X	X	X	X	X	X	X	X	X	X	X	X	X	X	X	X	24	76	24
44X	4	30	35	407.80	426.76	12.177	1.93		Sw	X	X	X	X	X	X	X	X	X	X	X	X	X	X	X	X	X	X	14	86	14
44X	4	30	35	407.80	427.7	12.184	2.04		Sw	X	X	X	X	X	X	X	X	X	X	X	X	X	X	X	X	X	X	57	43	57

# Post-middle Miocene origin of modern landforms in the eastern Piedmont of Virginia

Robert E. Weems and Lucy E. Edwards

926A National Center, U.S. Geological Survey, Reston, VA 20192

---

**ABSTRACT:** Diverse late middle Miocene dinoflagellate floras, obtained from two sites along the western edge of the Atlantic Coastal Plain in central Virginia, indicate that the eastern Virginia Piedmont was covered by marine waters about 12-13 Ma. This transgression extended farther westward across the Virginia Piedmont than any other transgression that has been documented. Extensive fluvial deposits that may be associated with this transgression covered earlier stream patterns in the eastern Piedmont and buried them beneath a thin (probably less than 100 foot-thick) veneer of sand and gravel. During the subsequent regression, a linear down-slope stream-drainage pattern developed. Although it has been somewhat modified by later stream captures, it still is easily recognizable. This interval of marine inundation and deposition explains why modern stream patterns in the eastern Piedmont of Virginia strongly resemble the stream patterns in the Coastal Plain and differ from the structurally adjusted trellis stream patterns typical of the western Piedmont, Blue Ridge, and Valley and Ridge regions. Uplift of the modern Southern Appalachian Mountains began at the time of this transgression and was largely completed by the late Pliocene.

---

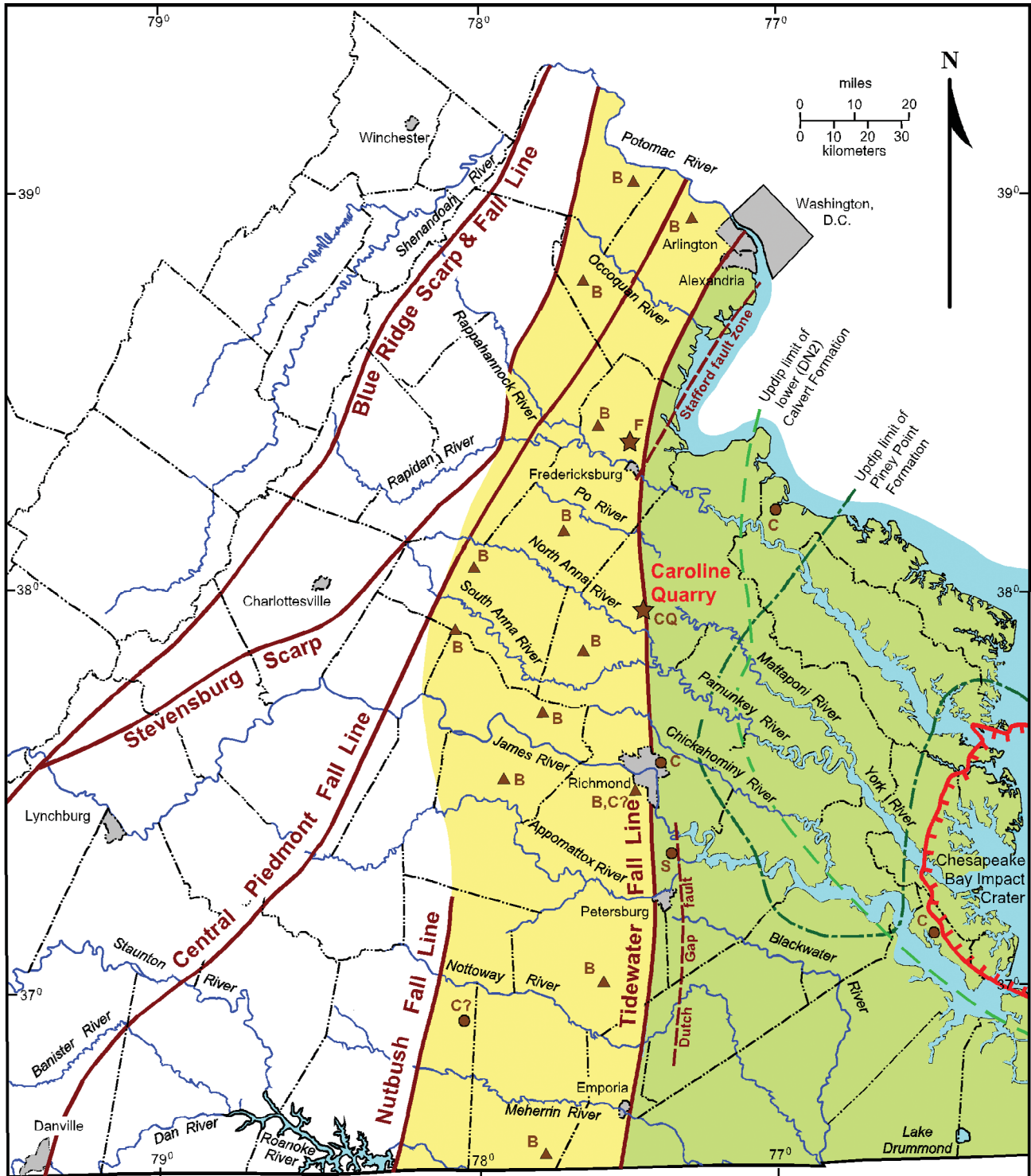
## INTRODUCTION

The boundary between the Coastal Plain and Piedmont provinces of Virginia is the Tidewater Fall Line (Weems 1998), a hinge zone where Piedmont streams flow eastward across fall zones down to the flat or very low gradients that characterize the Coastal Plain (text-fig. 1). This hinge zone separates areas that have undergone long-term regional uplift to the west from areas that have undergone long-term regional subsidence to the east. The Tidewater Fall Line in Virginia was established at least as long ago as late in the Early Cretaceous (about 115 Ma), when the predominantly non-marine Patuxent Formation accumulated across the entirety of the present Virginia Coastal Plain (Spangler and Peterson 1950). Although Late Cretaceous sediments are absent across most of the western and central Virginia Coastal Plain, numerous marine transgressions during the Paleogene and Neogene left sedimentary deposits across this region (Reinhardt and others 1980; Newell and Rader 1982; Mixon and others 1989, among others).

At least once during the Neogene, the eastern Piedmont also was covered by Coastal Plain sediments. Burial can be demonstrated by the occurrence of widespread but now discontinuous patches of a deeply weathered sand and gravel unit, here termed the eastern Piedmont upland gravel unit, up to 70 feet thick (Goodwin 1970). This deposit previously has been called the Bryn Mawr Formation north of Virginia (Lewis 1881; Pazzaglia and Gardner 1993), the Tenley Formation in the District of Columbia and northern Virginia (Wentworth 1930) and the Bon Air gravel in central and southern Virginia (Mathews and others 1965; Johnson and others 1987). The unit occurs on high hill-tops in the eastern Virginia Piedmont at elevations ranging from 300 to 530 feet. The exceptionally high elevations of occurrence and the presence of faults within the unit (Johnson and others 1987) suggest that the eastern Piedmont upland gravel unit was tectonically uplifted and warped after it was deposited. The unit is encountered along the highest interfluvies between major river valleys, so it probably was once continuous over

most or all of the eastern Piedmont (text-fig. 1, yellow area). The age of this unit has remained controversial. At various times, its age has been considered to be Oligocene and Miocene (Pazzaglia and Gardner 1993), Miocene (Owens and Minard 1979; Pazzaglia 1993), middle Miocene or older (Johnson and others 1987), late Miocene (Fleming and others 1994; Drake and Froelich 1997), late Miocene or early Pliocene (Weems 1986), or Pliocene(?) (Wentworth 1930). Until now, the only firm older age limit that could be placed on this unit in the vicinity of Virginia was early Miocene (mid-Burdigalian, ca. 17 Ma), based on the age of the Fairhaven Member of the Calvert Formation that lies unconformably beneath it in the District of Columbia (Fleming and others 1994). The younger age limit is the age of the Thornburg Scarp along the western edge of the Tidewater Fall Line (text-fig. 1) that bounds the unit on its east, which is mid-Pliocene (Piazencian, ca. 3.5 Ma) in age (Mixon and others 1989).

Beneath the western margin of the Coastal Plain, intermittent Cenozoic fault motion has been documented in two areas (text-fig. 1): the northeast-trending Stafford fault system near the city of Fredericksburg (Mixon and Newell 1977) and the north-south trending Dutch Gap fault east of the city of Petersburg (Dischinger 1987). Some of this or similar fault motion formed local sediment traps that preserve remnants of marine stratigraphic units once widespread across the western Virginia Coastal Plain but subsequently removed from most areas by erosion. One such locality is the Caroline Stone Quarry in Caroline County (text-fig. 1, locality CQ, approximately 170 feet original pre-excavation ground-surface elevation). There, six thin Coastal Plain marine units have been recognized in what is probably a fault-bounded trough (Marr and Ward 1987; Dooley 1993). This locality offers an exceptional opportunity to gauge the original extent of a number of major marine transgressions across the western Coastal Plain in Virginia. Additionally, northwest of Fredericksburg, Virginia (text-fig. 1, locality F, approximately 315 feet ground surface elevation), an auger hole



**TEXT-FIGURE 1**  
 Map of much of eastern Virginia, showing the major geomorphic boundaries in that region. Fall lines and scarps are from Weems (1998). Fall lines follow deeply eroded scarps, and are expressed as fall zones (typically several miles long) along major and many minor streams. The Tidewater Fall Line coincides with the Thornburg Scarp. The modern Coastal Plain (shaded green) lies mostly east of the Tidewater Fall Line and is characterized by roughly linear, down-slope stream-drainage patterns. Stream patterns across most of the eastern Piedmont region (shaded yellow) are similar to those found in the Coastal Plain, which suggests a former veneer of Coastal Plain sediments once blanketed that region as well. The star marked "CQ" is the Caroline Stone Quarry. The star marked "F" is an auger hole site where late middle Miocene beds also were encountered. Circles labeled "C" are known localities of the upper Choptank Formation. The triangle marked "B, C?" is an area in Bon Air where the eastern Piedmont upland gravel unit overlies weathered clayey and silty very fine sands that are probably referable to the upper Choptank Formation. The circle marked "C?" is a region in Lunenburg County underlain by Caroline coastal plain soils (McDaniel and others, 1981). Circle marked "S" is the westernmost known outcrop of the St. Marys Formation. Triangles labeled "B" are representative localities of the eastern Piedmont upland gravel unit. Dashed lines show the approximate updip limit of the middle Eocene Piney Point Formation and the lower Miocene Popes Creek Sand Member of the Calvert Formation.

through a sandy phase of the eastern Piedmont upland gravel unit yielded clayey, very fine sandy silt at about 270 feet elevation that contained dinoflagellates. Dinoflagellate data, derived from both of these localities, strongly suggest that the likely age of the eastern Piedmont upland gravel unit is late middle Miocene.

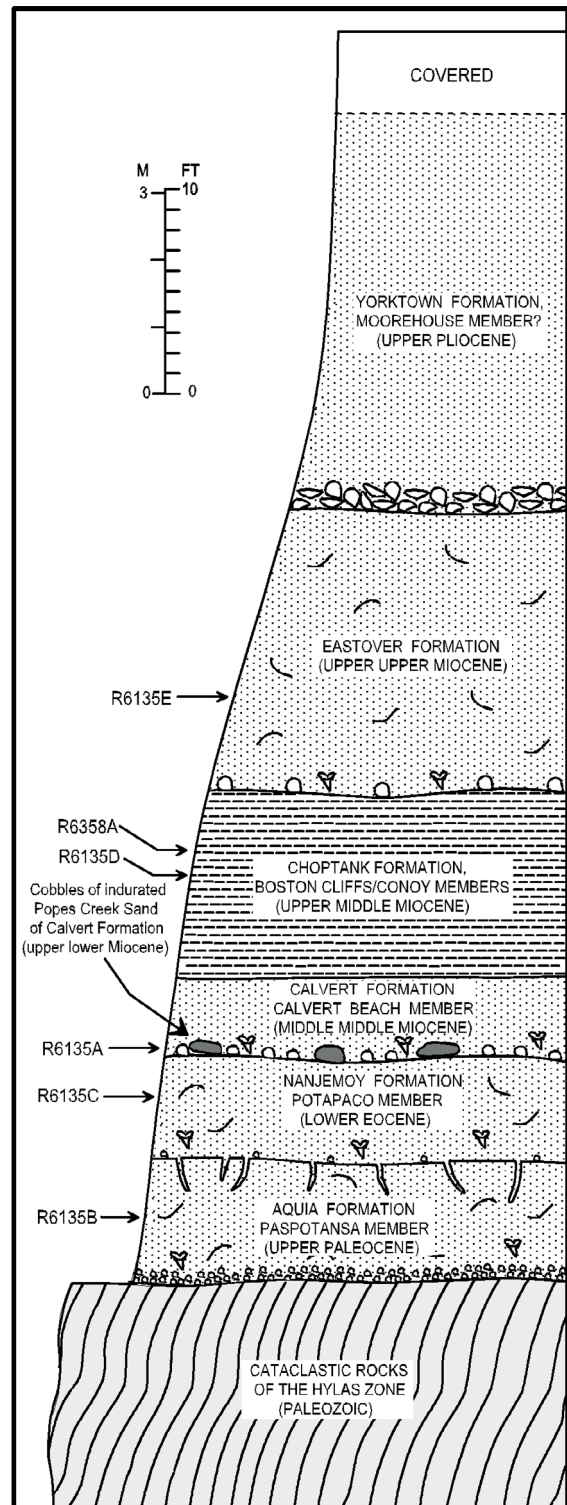
### PRESENT WORK

The strata preserved at the Caroline Stone Quarry are summarized in text-figure 2 and placed chronostratigraphically in text-figures 3 and 4. The dinoflagellate assemblages are shown in Table 1. The preserved sequence includes the upper Paleocene Paspotansa Member of the Aquia Formation, the lower Eocene Potapaco Member (Bed A) of the Nanjemoy Formation (not the Woodstock Member as indicated by Marr and Ward 1987), the middle middle Miocene Calvert Beach Member of the Calvert Formation, the upper middle Miocene Boston Cliffs Member of the Choptank Formation as indicated by Marr and Ward (1987) (not the St. Marys Formation as suggested by Barnes and others, 2004), the upper upper Miocene Eastover Formation, and nearshore strata of the upper Pliocene Yorktown Formation. All of these units formed in marine environments, though the Yorktown sediments grade upward and laterally in areas near the quarry into onshore deltaic deposits of the Brandywine Member of the Yorktown (Weems 1986).

Dinoflagellate cysts in sediments are useful for both biostratigraphy and paleoecology. Because dinoflagellates are planktonic organisms, the patterns of cyst distribution do not reflect water depth. Their patterns of occurrence, however, do relate to factors such as sea-surface temperature, nutrient supply, and fluctuating salinity. In general, nearshore dinoflagellate assemblages have low diversity and are strongly dominated by one or only a few species. Offshore dinoflagellate assemblages tend to be much more diverse and not to be dominated by any particular taxon.

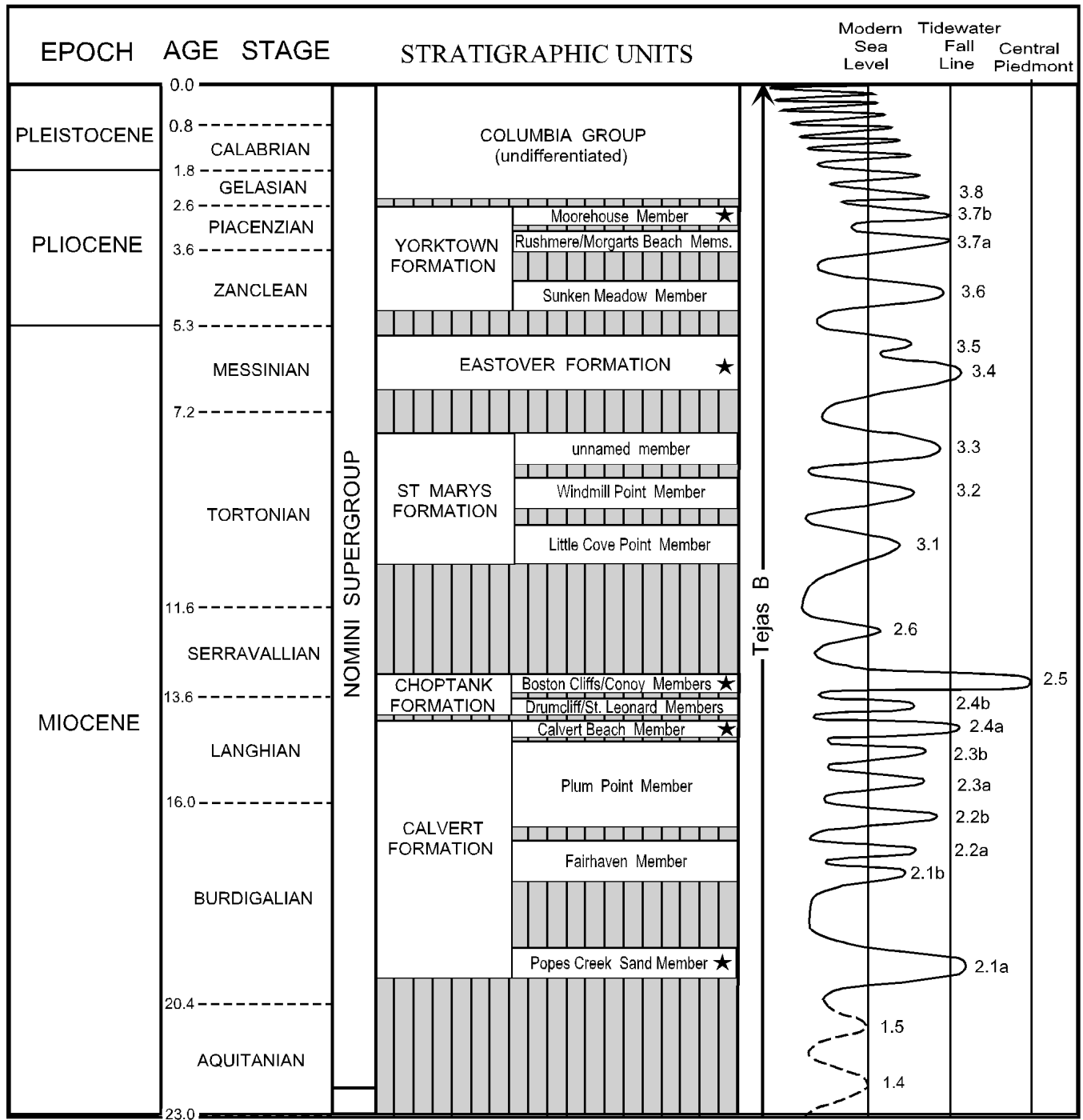
The dinoflagellate floras recovered from the Paspotansa member of the Aquia and the Potapaco (Bed A) member of the Nanjemoy both have moderately high diversity and are not dominated by any single species. This suggests accumulation in offshore (though not far offshore) environments of deposition. At the time these deposits were accumulating, the sea must have transgressed onto the eastern portion of the present Piedmont well beyond the present outcrop limit.

At the base of the Calvert Beach Member, numerous rounded and reworked calcareous sandstone pebbles and cobbles are present that contain unidentified molds of mollusks. A sample from one of these clasts contains dinoflagellate assemblages of at least two different ages (Table 1, R6135 A). *Cerebrocysta satchelliae* de Verteuil and Norris 1996 indicates that material from the early Miocene zone DN2 of de Verteuil and Norris (1996) is included. The only units of this age known from the central and western Virginia Coastal Plain are the Popes Creek Member of the Calvert Formation (Gibson 1983) and the probably coeval Newport News beds of Powars and Bruce (1999). An older assemblage is also present. Its age is restricted to the range of *Corrudinium incompositum* (Drugg 1970) Stover and Evitt 1978, which is middle Eocene to early Oligocene. The only unit of this age known from the central and western Coastal Plain is the middle Eocene Piney Point Formation (Ward 1985). Neither the Piney Point nor the Popes Creek are known within twenty miles of this locality at the present time

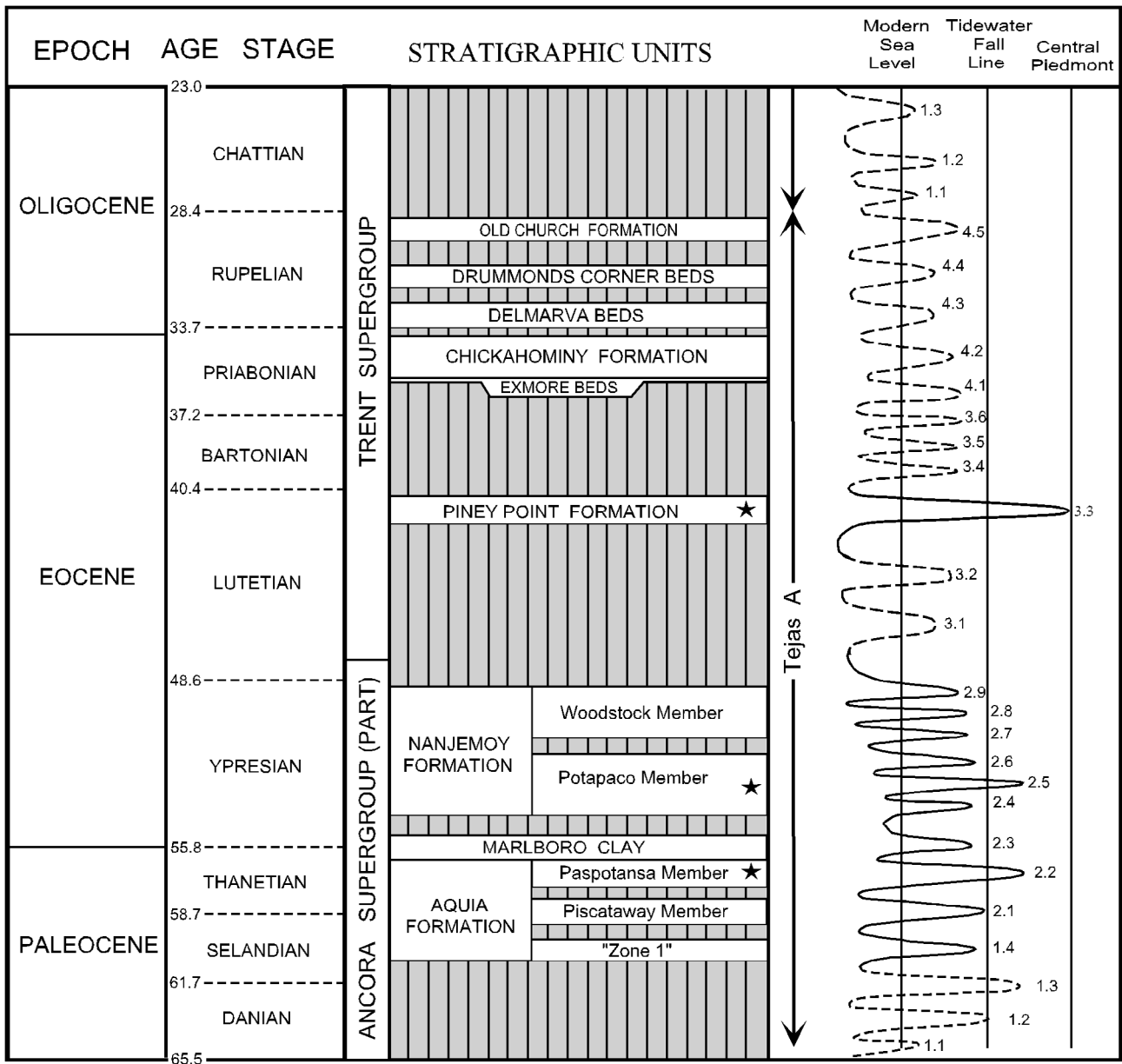


TEXT-FIGURE 2

Columnar section of sediments exposed in the Caroline Stone Quarry, adapted from Marr and Ward (1987) with the following revisions and additions: 1) The Nanjemoy Formation is represented by the Potapaco Member (Bed A) and not by the Woodstock Member as previously reported. 2) The Calvert Beach Member of the Calvert Formation is recognized (Dooley, 1993). 3) The basal lag bed of the Calvert Beach Member of the Calvert Formation contains reworked indurated clasts of the Popes Creek Sand Member of the Calvert Formation. 4) The clasts from the Popes Creek Member also contain reworked dinoflagellates from the Piney Point Formation.



TEXT-FIGURE 3  
 Neogene stratigraphic units known from the central Virginia Coastal Plain. Units marked with a star are represented at the Caroline Stone Quarry. Based on presence or absence of units at this site, and evidence for distance to shore from contained dinoflagellate floras, a curve of relative transgression distances has been created indicating times of maximal inundation. The single strongest transgression that can be documented directly is the upper Choptank transgression about 12-13 Ma. Strong transgressions are inferred also at about 14 Ma and 20 Ma. Solid curves are from evidence available in the western Coastal Plain of central Virginia. Dashed lines are inferred from work done in and near the Chesapeake Bay Crater (Powars and Bruce 1999) for the lower Miocene interval. Numerical ages are from Gradstein and others (2004). Curve numbers are from Haq and others (1988), but their ages and intensities have been modified to fit newer data presented in Billups and Schrag (2002) and Gradstein and others (2004).



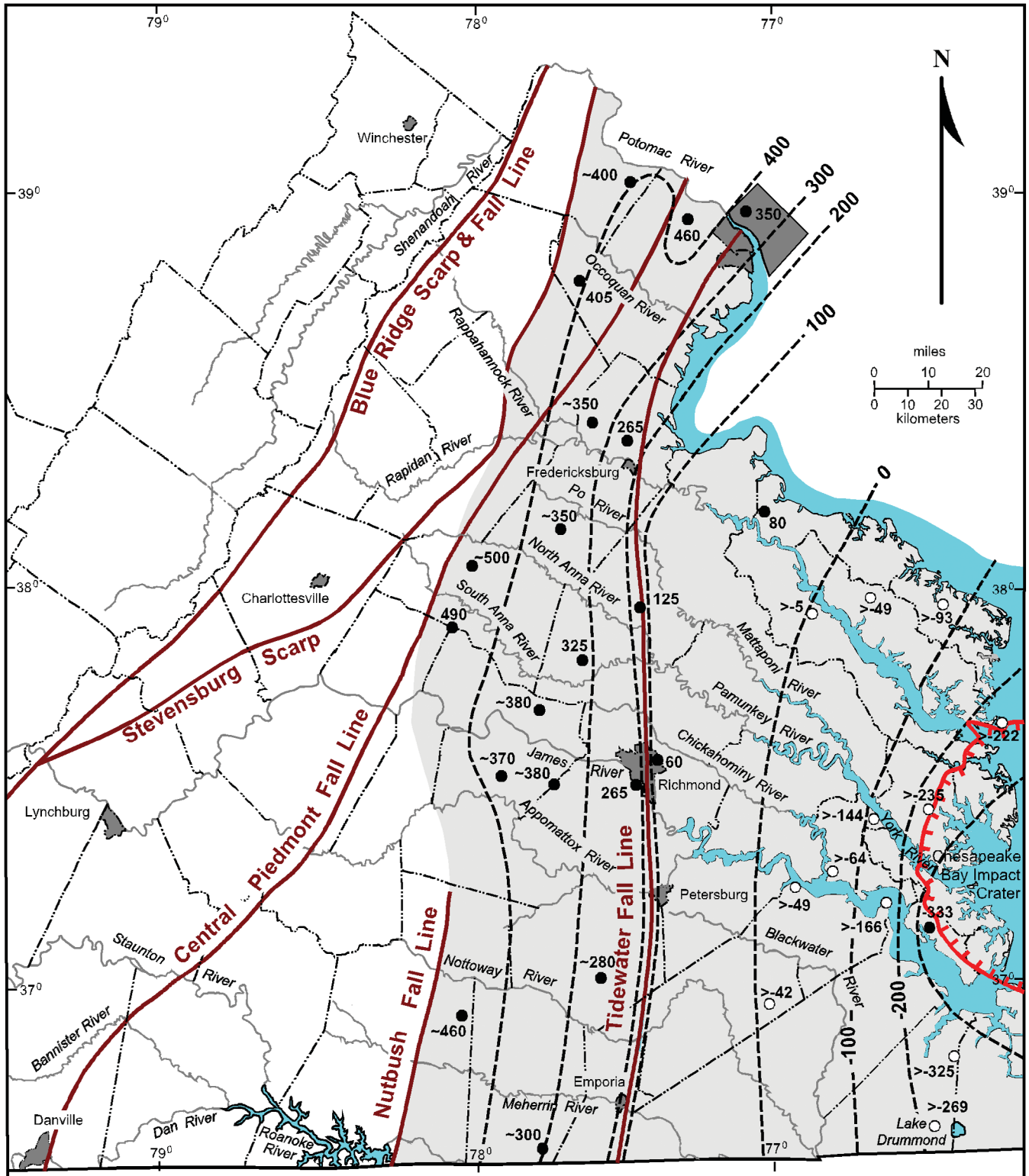
TEXT-FIGURE 4

Paleogene stratigraphic units known from the central Virginia Coastal Plain. Units marked with a star are represented at the Caroline Stone Quarry. Based on presence or absence of units at this site, and evidence for distance to shore from contained dinoflagellate floras, a curve of relative transgression distances has been created indicating times of maximal inundation. An especially strong transgression is inferred at about 42 Ma (Cabe 1984; Ward 1992). Solid curves are from evidence available in the western Coastal Plain of central Virginia. Dashed lines are inferred from work in South Carolina and Georgia (Edwards 2001) and work done in and near the Chesapeake Bay Crater (Powars and Bruce 1999) for the middle Eocene through Oligocene interval. Numerical ages are from Gradstein and others (2004). Curve numbers are from Haq and others (1988).

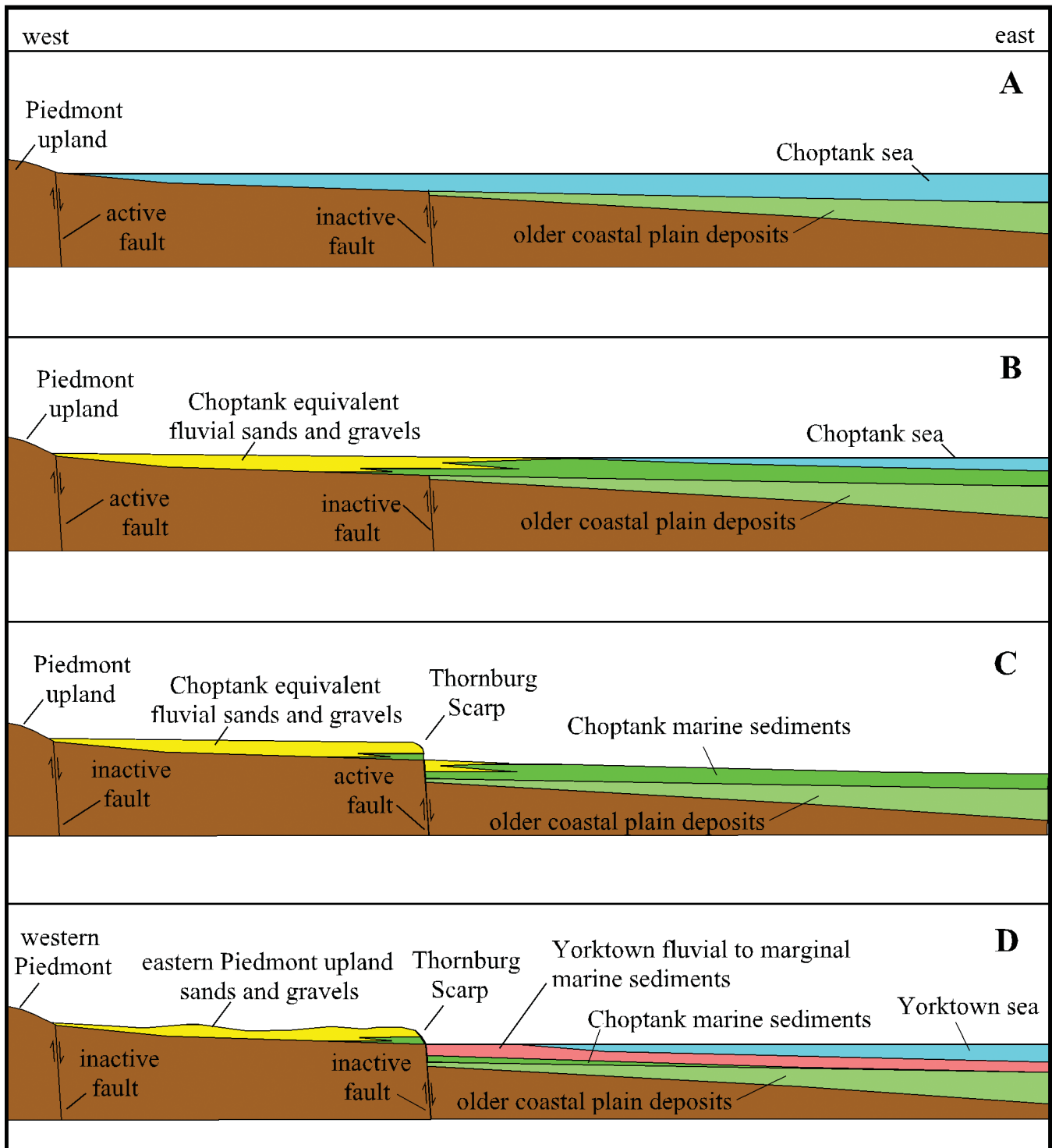
(text-fig. 1), but the preserved clast indicates that both units once were widespread up to the Tidewater Fall Line.

It is difficult to evaluate the depositional environment of the dinoflagellate flora recovered from the indurated nodules of the Popes Creek Sand Member of the Calvert Formation, because this flora includes reworked taxa probably from the Piney Point Formation. Even so, diversity is moderate and no single species dominates the composite assemblage. Therefore, part or all of the eastern Piedmont also probably was covered by these trans-

gressions. This conclusion is supported by data gathered for an extensive middle Eocene transgression in North Carolina southeast of Raleigh (Cabe 1984; Ward 1992), and by data gathered for an early Miocene transgression in the District of Columbia (Fleming and others 1994), and in southern Maryland (Gibson 1983). These data collectively suggest that both the Piney Point and the Popes Creek depositional events represent times of major westward transgression of the Atlantic Ocean across the Coastal Plain and onto the eastern Piedmont (text-fig. 3, text-fig. 4).



**TEXT-FIGURE 5**  
 Approximate structure contour map of the base of the upper Choptank/Bryn Mawr depositional package. Despite sparse data points, a prominent flexure is apparent along the Tidewater Fall Line. This indicates 100-200 feet of tectonic offset on the base of the unit along this feature some time after the middle Miocene, probably during the late Miocene. The slope of the base of this unit averages about 7 feet per mile eastward, both east and west of the Tidewater Fall Line, indicating that most of the tectonic motion was vertical. Steepened gradients in the vicinity of the Chesapeake Bay impact crater may be due to the effect of long-term differential settling and dewatering within the crater fill. Structure contours beneath the Coastal Plain are partially constrained by localities from Powars and Bruce (1999) (white circles), which give current elevations of tops of units that are older than the upper Choptank (usually the top of the Calvert Formation). The base of the upper Choptank must have lain at elevations higher (i.e., greater than) the top of units that lay beneath it. Thus, except in the vicinity of the Watkins School core where the upper Choptank is still preserved, the approximated structure contours could lie east of where they have been placed, but they could not lie much farther west.



TEXT-FIGURE 6

Diagram showing the stages in the development of the modern eastern Piedmont landform in the middle Miocene and Pliocene. A – Late Serravallian transgression of the Choptank sea covers all pre-existing Coastal Plain units in eastern Virginia and spreads far westward into the Piedmont up to a fault-bounded rising upland. B – Late Serravallian deposition partly fills the Choptank sea in the east, and fluvial-deltaic deposits spread eastward across the Choptank marine deposits from a rising fault-bounded upland within the Piedmont. C – Choptank sea retreats eastward, and a reactivation of fault motion occurs along the Thornburg Scarp and the future position of the Tidewater Fall Line. D – Late Pliocene Yorktown sea spreads westward up to the Thornburg scarp, largely reworking the Choptank (and also Eastover) marine deposits east of the Thornburg Scarp and depositing its own sediments in their stead.

TABLE 1

Stratigraphic distribution of dinoflagellates observed in samples from the Caroline Quarry (locality CQ in Fig. 1, 37.9067° N, 77.4797° W). Sample positions shown in text-figure 2. X = present, R = present but presumably reworked.

Dinoflagellate taxa	Eastover Formation R6135E	Choptank Formation R6358A R6135D	Calvert Fm. Popes Creek Sand Mem. R6135A	Piney Point Fm. (reworked into Popes Creek Sand) R6135A	Nanjemoy Fm. Potapaco Mem. (Bed A) R6135C	Aquia Fm. Paspatansa Mem. R6135B
<i>Achomospaera andalouisiensis</i> Jan du Chene 1977	X					
<i>Habibacysta tectata</i> Head et al. 1989	X	X				
<i>Invertocysta lacrymosa</i> Edwards 1984	X	X				
<i>Labyrinthodinium truncatum</i> Piasecki 1980 subsp. <i>truncatum</i>	X	X				
<i>Lingulodinium machaerophorum</i> (Deflandre & Cookson 1955) Wall 1967	X	X	X	X		X
<i>Nematosphaeropsis</i> Deflandre & Cookson 1955 sp.	X					
<i>Operculodinium</i> Wall 1967 sp.	X	X			X	
<i>Operculodinium ?eirikianum</i> Head et al. 1989	X					
<i>Reticulatosphaera actinocoronata</i> (Benedek 1972) Bujak & Matsuoka 1986	X	X				
<i>Spiniferites elongates</i> Reid 1974	X					
<i>Spiniferites</i> Mantell 1850 spp.	X	X	X	X	X	X
<i>Tectatodinium pellitum</i> Wall 1967	X	X				
<i>Tuberculodinium vancampoae</i> (Rossignol 1962) Wall 1967	X	X	X			
<i>Areoligera</i> group	R					
<i>Batiacasphaera sphaerica</i> Stover 1977		X				
<i>Dapsilidinium pseudocolligerum</i> (Stover 1977) Bujak et al. 1980		X				
<i>Hystriospherosis obscura</i> Habib 1972		X				
<i>Impagidinium</i> Stover & Evitt 1978 sp.		X				
<i>Lejeunecysta</i> Artzner & Dorhofer 1978 sp.		X				
<i>Operculodinium centrocarpum</i> (Deflandre & Cookson 1955) Wall 1967		X				X
<i>Palaeocystodinium golzowense</i> Alberti 1961		X	X	X	X	X
<i>Selenopemphix brevispinosa</i> Head et al. 1989 subsp. <i>brevispinosa</i>		X				
<i>Selenopemphix quanta</i> (Bradford 1975) Matsuoka 1985		X				
<i>Sumatradinium druggii</i> Lentin et al. 1994		X				
<i>Sumatradinium soucouyantiae</i> de Verteuil & Norris 1996		X				
<i>Apteodinium spiridoides</i> Benedek 1972			X			
<i>Batiacasphaera hirsuta</i> Stover 1977			X			
<i>Brigantedinium cariacense</i> (Wall 1967) Lentin & Williams 1993			X			
<i>Cerebrocysta satchelliae</i> de Verteuil & Norris 1996			X			
<i>Pentadinium</i> sp. cf. <i>P. laticinctum granulatum</i> Gocht 1969			X			
<i>Spiniferites pseudofurcatus</i> (Klumpp 1953) Sarjeant 1970			X			
<i>Corrudinium incompositum</i> (Drugg 1970) Stover & Evitt 1978				X		

All of these stratigraphic intervals mark major transgressions across the Coastal Plain and onto the eastern edge of the Piedmont. Even so, the flora from the upper Choptank Formation (i.e., strata laterally equivalent to the Boston Cliffs Member and (or) the Conoy Member of the Choptank Formation in Maryland) has a higher diversity of dinoflagellates than any of the other units present at this site. This implies that, during the late middle Miocene (about 12–13 Ma), the Atlantic Ocean transgressed farther across the eastern portion of the Piedmont than at any other time that can be documented adequately at the Caroline Stone Quarry site. Because beds of this age are rarely encountered, occurring in Virginia only as localized remnants (text-fig. 1) near Newport News (Watkins School site; Edwards and others, 2004), near Oak Grove (Gibson and others 1980), and in Shockoe Valley in Richmond (de Verteuil and Norris 1996), it has not been appreciated in the past that this was one of

the major transgressive events in Coastal Plain history. However, the diverse dinoflagellate flora preserved in this unit at the Caroline Stone Quarry site, as well as the consistently very fine-grained, silty, and diatomaceous texture of this unit up to its westernmost preserved edge, attest that this transgression extended farther into the Piedmont than any other transgression that can be documented in the stratigraphic column of the Virginia Coastal Plain.

Above the Choptank, the assemblage from the Eastover Formation is moderately diverse but dominated by a single species (*Operculodinium* Wall 1967 sp.). This pattern indicates that the Eastover transgression was far less expansive westward than the earlier transgressions documented in this area. The highly oxidized upper Yorktown beds were not successfully sampled for dinoflagellates, but the presence of *Ophiomorpha* burrows, me-

TABLE 1  
continued.

Dinoflagellate taxa	Eastover Formation R6135E	Choptank Formation R6135A R6135D	Calvert Fm. Popes Creek Sand Mem. R6135A	Piney Point Fm. (reworked into Popes Creek Sand) R6135A	Nanjemoy Fm. Potapaco Mem. (Bed A) R6135C	Aquia Fm. Pasopansa Mem. R6135B
<i>Heteraulacacyata pustulosa</i> Jan du Chene & Adediran 1985				X		
<i>Histiocysta</i> sp. of Stover and Hardenbol (1993)				X		
<i>Lentinia serrata</i> Bujak 1980				X	X	X
<i>Phthanoperidinium stockmansii</i> (de Coninck 1975) Lentin & Williams 1977				X		
<i>Saturnodinium</i> sp. Brinkhuis et al. 1992				X		
<i>Apectodinium homomorphum</i> (Deflandre & Cookson 1955) Lentin & Williams 1977					X	X
<i>Catillopsis abdita</i> Drugg 1970					X	
<i>Cribroperidinium</i> Neale & Sarjeant 1962 sp.					X	
<i>Deflandrea phosphoriitica/obisfeldensis</i> complex					X	X
<i>Diphyes colligerum</i> (Deflandre & Cookson 1955) Cookson 1965					X	
<i>Eocladopyxis peniculata</i> Morgenroth 1966					X	
<i>Fibrocysta radiata</i> (Morgenroth 1966) Stover & Evitt 1978					X	
<i>Fibrocysta</i> Stover & Evitt sp.					X	
<i>Hafniasphaera septata</i> (Cookson & Eisenack 1967) Hansen 1977					X	X
<i>Heteraulacacysta</i> Drugg & Loeblich 1967 sp.					X	
<i>Hystriochosphaeridium tubiferum</i> (Ehrenberg 1838) Deflandre 1937					X	X
<i>Kallosphaeridium brevibarbatum</i> de Coninck 1969 (2 var.)					X	X
<i>Muratodinium fimbriatum</i> (Cookson & Eisenack 1967) Drugg 1970					X	
<i>Wilsonidium tabulatum</i> (Wilson 1967) Lentin & Williams 1976					X	
miscellaneous areoligeracean forms					X	X
miscellaneous cladopyxiacean forms					X	X
<i>Amphorosphaeridium multispinosum</i> (Davey & Williams 1966) Sarjeant 1981						X
<i>Cordosphaeridium fibrospinosum</i> Davey & Williams 1966						X
<i>Fromea fragilis</i> (Cookson & Eisenack 1967) Stover & Evitt 1978						X
<i>Hystriochokolpoma</i> Klumpp 1953 sp.						X
<i>Phelodinium</i> Stover & Evitt 1978 sp.						X
<i>Spinidinium</i> Cookson & Eisenack 1962 sp.						X
<i>Turbiosphaera</i> sp. aff. <i>T. magnifica</i> of Edwards 1989						X
small peridiniacean forms					X	X

dium-grained sands, and prominent cross-bedding all indicate a nearshore depositional environment during a transgression that peaked in the late Pliocene about at the present Tidewater Fall Line. No later transgressions are known that extended this far inland (Weems 1986).

In the northwest corner of the Fredericksburg, Virginia 7.5-minute quadrangle (text-fig. 1, locality F), an auger hole through the Piedmont upland gravel unit yielded a sample of clayey, very fine sandy silt at approximately 270 feet elevation that contains dinoflagellates (Table 2, right column) characteristic of the same upper Choptank interval (upper middle Miocene, DN7) encountered in the Caroline Stone Quarry at an elevation of approximately 125 feet (Table 1, Choptank Formation column). The high diversity of the sample comes from a large number of protoperidiniacean species (presumed to be

heterotrophic), so this sample may represent a nearshore, nutrient-rich environment. This updip occurrence demonstrates directly that the Piedmont upland gravel unit of the eastern Piedmont cannot be any older than the 12-13 Ma upper Choptank unit exposed at the Caroline Quarry, and additionally suggests that the deposits near Fredericksburg have been uplifted 100-200 feet relative to the Caroline Stone Quarry site due to post-depositional tectonism (text-fig. 5). Weathered unfossiliferous very fine-grained strata, of very similar lithology and at a nearly identical elevation, lie beneath the Piedmont upland gravel unit in Bon Air (Johnson and others 1987). These deposits here are referred to the upper Choptank (text-fig. 1, circle marked B, C?). The eastern Piedmont upland gravel unit at the Fredericksburg site is more sandy than gravelly and contains several subtle fining upward sequences that suggest the fluvial sands lie with some degree of unconformably upon the marine

sandy silts. This apparent angularity could suggest a much younger age for the Piedmont upland gravel unit, but it is just as plausible that the observed unconformable relationships simply reflect the relatively rapid meanderings of delta distributary channels within an offlap depositional sequence, where fluvio-deltaic sands and gravels were prograding into a shallow, high-stand sea. Thus, based only on lithologic criteria, the Piedmont upland gravel unit could be either onshore fluvio-deltaic deposits coeval with the upper Choptank Formation or a distinctly younger unit resting unconformably upon the upper Choptank.

If the eastern Piedmont upland gravel unit is significantly younger than the Choptank, only laterally equivalent marine units older than the upper Yorktown Formation need to be considered as possible correlatives. This is because, by the time that the upper Yorktown deposits at the Caroline Quarry accumulated, the Thornburg Scarp was already in existence and blocked the upper Yorktown transgression from extending any farther inland except for fluvial/estuarine deposits that extend westward along the major rivers (Weems 1998). Where such deposits have been mapped along the James River (Goodwin 1970) they clearly extend up a broad river valley that was already deeply incised into the Bon Air uplands and thus represent deposits distinctly younger than the eastern Piedmont upland gravel unit. Additionally, the gravels associated with the late Yorktown transgression are composed almost entirely of very stable quartzite and vein quartz clasts that appear to have been reworked from the older eastern Piedmont upland gravel unit. The eastern Piedmont upland gravel unit contains ghosts of many other kinds of igneous and metamorphic clasts that are extremely leached and weathered, so those clasts did not survive reworking (Weems 1986). As incisement of the eastern Piedmont upland was already well under way by the time of the late Yorktown (late Pliocene), only units younger than the upper Choptank and older than the upper Yorktown are possible candidates for offshore equivalents to the eastern Piedmont upland gravel. These candidates are, from oldest to youngest, the St. Marys Formation (early late Miocene), the Eastover Formation (late late Miocene), and the Sunken Meadow Member of the Yorktown Formation (early Pliocene).

The early late Miocene, when the St. Marys Formation was deposited (text-fig. 4), was a time of relatively low global sea levels (Haq and others 1988; Miller and others, 2005). The westernmost St. Marys deposit found in this general area, a clayey silt sampled at a site seven miles northeast of Petersburg in Chesterfield County (elevation about 80 feet above sea level, labeled S in text-fig. 1), contains an inshore dinoflagellate flora with abundant pollen and plant debris that accumulated in a low-energy, nearshore depositional setting (Table 2, right column). Therefore, the St. Marys is not a reasonable candidate for correlation with the Piedmont upland gravel unit, because it cannot be associated with a depth of transgression great enough to flood or back up sediment across the eastern Piedmont. In the very late Miocene, global sea levels rose again, and this rise in global eustatic sea level correlates well with the Eastover transgression that produced nearshore deposits at the Caroline Stone Quarry site in the vicinity of the Tidewater Fall Line. Again, however, the near-shore nature of these deposits at the Caroline Quarry does not indicate a depth of transgression great enough to have allowed a regional accumulation of the widespread eastern Piedmont upland gravels. Although no deposits remain in the area, it is worth considering the early Pliocene Sunken Meadow Member of the Yorktown Formation. Gibson (1967)

has provided evidence that the Sunken Meadow transgression was more widespread than its present distribution would suggest, but even so he considered its maximum depth of transgression to be no more than 250 feet above modern sea level. This is slightly less than the maximum depth of the later Yorktown transgression that was blocked by the Thornburg Scarp, and again is insufficient to allow a regional accumulation of the widespread eastern Piedmont upland gravels.

The relatively nearshore flora and depositional fabric in all younger candidate units leaves the upper Choptank unit as the only plausible equivalent to the eastern Piedmont upland gravel unit, because patches of eastern Piedmont upland gravel and sand are found across the Piedmont up to 35 miles west of the Tidewater Fall Line (text-fig. 1, triangles labeled "B") and this westward extent is comparable only to the degree of westward transgression suggested by dinoflagellates for the late middle Miocene upper Choptank transgression.

The abundance and thickness of the upland gravels seem somewhat anomalous when compared to the energy of the depositional regime that formed the very fine grained marine deposits of the upper Choptank, but it needs to be kept in mind that only the lower portion of the original upper Choptank Formation remains east of the Tidewater Fall Line, and that any still-stand progradational deposits that once may have overtopped this sequence are long since gone. Thus, due to the local depositional geometry and setting, toward the east (seaward) only early transgression deposits are preserved and toward the west (landward) mostly progradational still-stand deposits of slightly younger age are preserved. The westernmost extent of these gravel outliers presently is constrained by portions of three geomorphic features, the Nutbush Fall Line, the Central Piedmont Fall Line, and the Stevensburg Scarp (text-fig. 1). As the Piedmont upland gravel unit locally is incised into the Piedmont upland surface west of the Nutbush Fall Line along major rivers such as the Roanoke, it seems likely that these features already existed in the late middle Miocene and constrained the inland extent of the late middle Miocene transgression. The presence of such uplands to the west would help to explain the large volume of pebbles and cobbles in the upland gravel unit, especially those that once were metamorphic or igneous rocks now completely saprolitized. This scenario is compatible with what little is known from the heavy minerals in this part of the section. At the Haynesville core in Richmond County, Virginia the upper Choptank unit is absent, but the immediately underlying Calvert Beach Member of the Calvert Formation is present, as is the immediately overlying St. Marys Formation. In the upper Calvert, hornblende and epidote are only about half as abundant as they are in the St. Marys, indicating a significant influx of first-cycle metamorphic and igneous minerals immediately after the middle Miocene (McCartan, 1989). This indicates that at least the western part of the Piedmont must have been tectonically reactivated during or right after the time of the upper Choptank transgression.

Further support for the association of the eastern Piedmont upland gravel unit with the middle Miocene comes from studies much farther south in Georgia. There, a unit called the Screven Member of the Altamaha Formation (Huddlestun 1988) appears to be of the same age and to have the same characteristics as the eastern Piedmont upland gravel unit in Virginia. The Screven Member, unlike the eastern Piedmont upland gravels, is in the western Atlantic Coastal Plain Province, but this is in an area where the coastal plain deposits have undergone significant up-

TABLE 2

Stratigraphic distribution of dinoflagellates observed in samples from Chesterfield County (locality S in text-fig. 1, 37.3290° N, 77.3629° W) and from Stafford County, Virginia (locality F in text-fig. 1, 38.3709° N, 77.4982° W).

Dinoflagellate taxa	Chesterfield County (St. Marys Fm.)	Stafford County (Choptank Fm.)
<i>Achomosphaera andalouisiensis</i> Jan du Chene 1977	X	
<i>Achomosphaera</i> Evitt 1963 sp.	X	
<i>Bitectatodinium tepikiense</i> Wilson 1973/ <i>Betectatodinium raedwaldii</i> Head 1997	X	
<i>Brigantedinium simplex</i> Wall 1965	X	
<i>Cyclopsiella</i> Drugg & Loeblich 1967 sp.?	X	
<i>Impagidinium</i> Stover & Evitt 1978 sp.	X	
<i>Polykrikos</i> Butschli 1873 sp.?	X	
<i>Sumatradinium</i> Lentin & Williams 1976 sp.	X	
<i>Trinovantedinium papula</i> de Verteuil & Norris 1992	X	
<i>Batiacasphaera hirsuta</i> Stover 1977	X	X
<i>Erymnodinium delectabile</i> (de Verteuil & Norris 1992) Lentin et al. 1994	X	X
<i>Geonettia clinae</i> de Verteuil & Norris 1996	X	X
<i>Habibacysta tectata</i> Head et al. 1989	X	X
<i>Labyrinthodinium truncatum</i> Piasecki 1980 subsp. <i>truncatum</i>	X	X
<i>Lejeunecysta</i> Artzner & Dorhofer 1978 sp.	X	X
<i>Lingulodinium machaerophorum</i> (Deflandre & Cookson 1955) Wall 1967	X	X
<i>Nematosphaeropsis</i> Deflandre & Cookson 1955 sp.	X	
<i>Operculodinium centrocarpum</i> (Deflandre & Cookson 1955) Wall 1967	X	X
<i>Quadrina? condita</i> de Verteuil & Norris 1992	X	
<i>Reticulatosphaera actinocoronata</i> (Benedek 1972) Bujak & Matsuoka 1986	X	X
<i>Selenopemphix brevispinosa</i> Head et al. 1989 subsp. <i>brevispinosa</i>	X	X
<i>Spiniferites</i> Mantell 1850 spp.	X	X
<i>Tectatodinium pellitum</i> Wall 1967	X	X
<i>Trinovantedinium harpagonium</i> de Verteuil & Norris 1992	X	X
<i>Tuberculodinium vancampoae</i> (Rossignol 1962) Wall 1967	X	X
<i>Barssidinium evangelinae</i> Lentin et al. 1994		X
<i>Batiacasphaera sphaerica</i> Stover 1977		X
<i>Brigantedinium</i> Reid 1977 sp.		X
<i>Cannosphaeropsis passio</i> de Verteuil & Norris 1996		X
<i>Cerebrocysta poulsenii</i> de Verteuil & Norris 1996		X
<i>Dapsilidinium pseudocolligerum</i> (Stover 1977) Bujak et al. 1980		X
<i>Hystriochosphaeropsis obscura</i> Habib 1972		X
<i>Operculodinium piaseckii</i> Strauss & Lund 1992		X
<i>Palaeocystodinium golzowense</i> Alberti 1961		X
<i>Selenopemphix dionaeacysta</i> de Verteuil & Norris 1992		X
<i>Sumatradinium druggii</i> Lentin et al. 1994		X
<i>Sumatradinium soucouyantiae</i> de Verteuil & Norris 1996		X
<i>Trinovantedinium glorianum</i> de Verteuil & Norris 1992		X

lift and warping west of the Orangeburg Scarp similar to the pattern seen for the upland gravel unit. Lithologically, the two units are quite similar. Huddlestun (1988) described the Screven as a prominently cross-bedded, feldspathic, pebbly sand that locally contains gravel beds with cobbles up to 7 inches (18cm) in diameter. In Georgia, the Screven Member overlies deposits of the Meigs and the Berryville Clay members of the Coosawhatchie Formation, which Huddlestun assigned to the lower Serravallian. Huddlestun noted that the Screven often lay unconformably upon the Coosawhatchie, but he considered this to be the result of lateral channel migrations that occurred very shortly after deposition of the underlying estuarine to shallow marine strata. In other places, he noted that the Screven sequence seems to be conformable with underlying strata, and also that the fluvial Screven deposits seemed to grade down dip into deposits of either the Meigs Member or the Berryville Member. The Meigs Member and much of the Berryville Clay Member are lower Serravallian in age (containing a DN5 dinoflagellate flora), but it since has been established that there are very similar-looking diatomaceous deposits that are slightly younger and upper Serravallian in age, based on the DN7 dinoflagellate flora that they contain (Weems and Edwards, 2001). We suggest that it is this upper Berryville Member with which the Screven Member intertongues, and that the Screven is time-equivalent to the eastern Piedmont upland gravel unit, with which it is so very similar lithologically and in its depositional setting.

As noted by Huddlestun (1988), the Screven is lithologically very unusual for an Atlantic Coastal Plain unit because it is so predominantly fluvial in character and so areally wide-spread. Except for a few Cretaceous deposits, such as the Patuxent and Potapasco formations in Maryland and Virginia, and the Cape Fear and Tuscaloosa (s.l.) formations in Georgia and the Carolinas, Atlantic Coastal Plain deposits almost all formed in marine shelf environments. Fluvial deposits landward of these units either never formed or were quickly eroded away, leaving only a sparse record of onshore deposition, especially in the Cenozoic. Thus, while the strongly fluvial character of the eastern Piedmont upland gravels in Virginia might suggest that they represent a deposit distinctly different in age than the upper Choptank marine beds, the occurrence of very similar deposits of the same age in Georgia and South Carolina, with a similarly contrasting onshore and offshore character, indicates that the contrast in depositional setting of the onshore and offshore components of the eastern Piedmont upland gravel and upper Choptank depositional packages occurred elsewhere at that time.

The deposition of a widespread, feldspathic fluvial unit across the southern Atlantic Coastal Plain and the eastern Piedmont of Virginia at the same time that a strong late Serravallian transgression was occurring, suggests that this transgression coincided with the beginning of a significant uplift in the entire Appalachian interior region that ultimately produced the modern Southern Appalachians. The abrupt appearance of abundant labile heavy minerals in the sands of the immediately younger (Tortonian) St. Marys Formation (McCartan 1989) also supports this age for the beginning of uplift in the interior modern Appalachian region. This transgression, in conjunction with the presence of the uplifted Thornburg Scarp by 3.5 Ma (Mixon and others 1989), brackets the interval of major modern Appalachian uplift to between 13 Ma and 3.5 Ma, or the latest Middle Miocene to early Pliocene.

This same time interval also brackets the timing of uplift of the eastern Piedmont in Virginia. Interestingly, the presence of a sand and gravel unit up to 70 feet thick across the eastern Piedmont during the early phase of this uplift meant that the river and stream systems that formed after the Choptank regression in this area were incised into an unconsolidated, broadly planar-bedded substrate. This resulted in a linear, down-slope stream-drainage pattern that is nearly identical to the stream flow patterns developed on the Atlantic Coastal Plain farther east. The total amount of uplift, while sufficient to block any further marine transgressions across this region, has been insufficient to allow most of the drainage patterns to adjust to the structural grain of the Piedmont rocks that lie beneath the Coastal Plain cover that once blanketed the region. This explains why the stream drainage patterns in the eastern Piedmont of Virginia are very much like the stream drainage patterns found in the Coastal Plain and contrast sharply with the predominantly bedrock-adjusted drainage patterns found in the western Piedmont of Virginia.

## CONCLUSIONS

Based on available direct evidence, a major marine transgressive event in the late middle Miocene (late Serravallian) resulted both in the deposition of the upper Choptank Formation and the onshore to nearshore deposits of the eastern Piedmont upland gravel unit in Virginia. This transgression was the most westward that can be documented so far for any time interval within the Cenozoic Era. Remnant patches of these gravels extend westward far enough to indicate that the eastern Piedmont of Virginia at one time was completely buried beneath these deposits. During the subsequent regression, the eastern Piedmont region developed a linear, down-slope stream-drainage pattern on this thick gravel deposit that is similar to that seen throughout the Coastal Plain. This sand and gravel depositional event, and the subsequent stream flow pattern developed upon it, best explains the strong geomorphic contrast between the eastern and western Piedmont regions of Virginia and the lack of geomorphic contrast between the eastern Piedmont and Coastal Plain. If the upper Choptank Formation is age equivalent to the eastern Piedmont upland gravel unit, then the present geomorphology of the eastern Piedmont in Virginia must have developed between 13 Ma and 3.5 Ma. This matches the timeframe for uplift of the modern Appalachian Mountains in the southeastern United States.

## ACKNOWLEDGMENTS

The authors wish to thank C. Scott Southworth and Jean M. Self-Trail (U.S. Geological Survey, Reston), W. Burleigh Harris (University of North Carolina, Wilmington), and an anonymous reviewer for *Stratigraphy* for their insightful reviews of the manuscript of this paper.

## REFERENCES

- BARNES, L., DOOLEY, A. C., Jr. and FRASER, N. C., 2004. A new Miocene sperm whale (Cetacea; Physeteridae) from Virginia. *Journal of Vertebrate Paleontology*, 24 (supplement):36A.
- BILLUPS, K. and SCHRAG, D. P., 2002. Paleotemperatures and ice volume of the past 27 Myr revisited with paired Mg/Ca and  $^{18}\text{O}/^{16}\text{O}$  measurements on benthic foraminifera. *Paleoceanography*, 17(1):1-11.
- CABE, S., 1984. "Cretaceous and Cenozoic stratigraphy of the upper and middle Coastal Plain, Harnett County area, North Carolina."

- Ph.D. dissertation, University of North Carolina at Chapel Hill, 101 pp.
- DE VERTEUIL, L. and NORRIS, G., 1996. Miocene dinoflagellate stratigraphy and systematics of Maryland and Virginia. *Micro-paleontology*, 42 (supplement):1-172.
- DISCHINGER, J. B., Jr., 1987. Late Mesozoic and Cenozoic stratigraphic and structural framework near Hopewell, Virginia. *United States Geological Survey Bulletin*, 1567:1-48.
- DOOLEY, A. C., Jr., 1993. The vertebrate fauna of the Calvert Formation (middle Miocene) at the Caroline Stone Quarry, Caroline County, Va. *Journal of Vertebrate Paleontology*, 13 (supplement):33A.
- DRAKE, A. A., Jr. and FROELICH, A. J., 1997. *Geologic map of the Falls Church quadrangle, Fairfax and Arlington Counties and the City of Falls Church, Virginia, and Montgomery County, Maryland*. United States Geological Survey Geologic Quadrangle Map GQ-1734 with text, scale 1:24,000.
- EDWARDS, L. E., 1989. Dinoflagellate cysts from the lower Tertiary formations, Haynesville cores, Richmond County, Virginia. In: Mixon, R.B., Ed., *Geology and Paleontology of the Haynesville cores — Northeastern Virginia Coastal Plain*, C1-C12. U.S. Geological Survey Professional Paper 1489.
- , 2001. *Geology and paleontology of five cores from Screven and Burke Counties, eastern Georgia*. United States Geological Survey Professional Paper 1603.
- EDWARDS, L. E., POWARS, D.S., GOHN, G.S., HORTON, J.W., JR., LITWIN, R.J. AND SELF-TRAIL, J.M., 2004. Inside the crater, outside the crater: comparison of two cores from the Chesapeake Bay impact structure. *Geological Society of America Abstracts with Programs*, 36:266.
- FLEMING, A. H., DRAKE, A. A., JR. and MCCARTAN, LUCY, 1994. *Geologic map of the Washington West quadrangle, District of Columbia, Montgomery and Prince Georges counties Maryland, and Arlington and Fairfax counties Virginia*. United States Geological Survey Geologic Quadrangle Map GQ-1748, with text, scale 1:24,000.
- GIBSON, T. G., 1983. Stratigraphy of Miocene through Lower Pleistocene Strata of the United States central Atlantic Coastal Plain. In: Ray, C. E., Ed., *Geology and Paleontology of the Lee Creek Mine, North Carolina, Part 1*. *Smithsonian Contributions to Paleobiology*, 53:35-80.
- GIBSON, T. G., ANDREWS, G. W., BYBELL, L. M., FREDERIKSEN, N. O., HANSEN, T., HAZEL, J. E., MCLEAN, D. M., WITMER, R. J. and NIEUWENHUISE, D. S. VAN, 1980. Biostratigraphy of the Tertiary strata of the core. In: *Geology of the Oak Grove core*, 14-30. Virginia Division of Mineral Resources Publication, 20(2).
- GOODWIN, B.K., 1970. Geology of the Hylas and Midlothian quadrangles, Virginia. *Virginia Division of Mineral Resources Report of Investigations*, 23:1-51, 2 maps.
- GRADSTEIN, F. M., OGG, J. G., SMITH, A. G., BLEEKER, WOUTER and LOURENS, L.J., 2004. A new geologic time scale, with special reference to Precambrian and Neogene. *Episodes*, 27:83-100.
- HAQ, B. U., HARDENBOL, J. AND VAIL, P. R., 1988. Mesozoic and Cenozoic chronostratigraphy and cycles of sea-level change. In: Wilgus, C. K., Hastings, B. S., Ross, C. A., Posamentier, H. W., Van Wagoner, J., and Kendall, C.G. St. C., Eds., *Sea-level changes; an integrated approach*, 72-108. Society of Economic Paleontologists and Mineralogists Special Publication, 42.
- HUDDLESTUN, P. H., 1988. A revision of the lithostratigraphic units of the Coastal Plain of Georgia; the Miocene through Holocene. *Georgia Geologic Survey Bulletin*, 104:1-162.
- JOHNSON, G. H., GOODWIN, B. K., WARD, L. W. and RAMSEY, K.W., 1987. Tertiary and Quaternary stratigraphy across the Fall Zone and western Coastal Plain, southern Virginia. In: Whittecar, G. R., Ed., *Geological excursions in Virginia and North Carolina. Southeastern Section*, 87-144. Geological Society of America 36th Annual Meeting. Norfolk, Virginia, Department of Geological Sciences, Old Dominion University.
- LEWIS, H. C., 1881. The Trenton gravel and its relation to the antiquity of man. *Proceedings of the Academy of Natural Sciences of Philadelphia*, 32:296-309.
- MARR, J. D., Jr. and WARD, L. W., 1987. Geology of the Caroline Stone Quarry. *Virginia Minerals*, 33(4):29-33.
- MATHEWS, H. L., HODGES, R. L. AND AMOS, D. F., 1965. Some geological and geomorphical observations of Chesterfield County. *Virginia Journal of Science*, 16:380-381.
- MCCARTAN, L., 1989. Mineralogy of the Haynesville, Virginia, cores. In: Mixon, R.B., Ed., *Geology and Paleontology of the Haynesville cores — Northeastern Virginia Coastal Plain*, B1-B9. United States Geological Survey Professional Paper, 1489.
- MCDANIEL, J. C., GILLISPIE, H. L. and ALI, JAMES, 1981. *Soil survey of Lunenburg County, Virginia*. United States Department of Agriculture, Soil Conservation Service: 1-109.
- MILLER, K. G., KOMINZ, M. A., BROWNING, J. V., WRIGHT, J. D., MOUNTAIN, G. S., KATZ, M. E., SUGARMAN, P. J., CRAMER, B. S., CHRISTIE-BLICK, NICHOLAS and PEKAR, S. F., 2005. The Phanerozoic record of global sea-level change. *Science*, 310:1293-1298.
- MIXON, R. B., BERQUIST, C. R., Jr., NEWELL, W. L., JOHNSON, G. H., POWARS, D. S., SCHINDLER, J. S. and RADER, E. K., 1989. *Geologic map and generalized cross sections of the coastal plain and adjacent parts of the Piedmont, Virginia*. United States Geological Survey, Report of Investigations I-2033, 2 map sheets and text.
- MIXON, R. B. and NEWELL, W. L., 1977. Stafford fault system; structures documenting Cretaceous and Tertiary deformation along the Fall Line in northeastern Virginia. *Geology*, 5(7):437-440.
- NEWELL, W. L. and RADER, E. K., 1982. Tectonic control of cyclic sedimentation in the Chesapeake Group of Virginia and Maryland. In: Lyttle, P.T., Ed., *Central Appalachian geology*, 1-27. Falls Church, Virginia: American Geologic Institute.
- OWENS, J. P. and MINARD, J. P., 1979. *Upper Cenozoic sediments of the lower Delaware Valley and the northern Delmarva Peninsula, New Jersey, Pennsylvania, Delaware, and Maryland*. United States Geological Survey Professional Paper, 1067-D, 47p.
- PAZZAGLIA, F. J., 1993. Stratigraphy, petrography, and correlation of late Cenozoic middle Atlantic Coastal Plain deposits: implications for late-stage passive-margin geologic evolution. *Geological Society of America Bulletin*, 105:1617-1634.
- PAZZAGLIA, F. J. and GARDNER, T. W., 1993. Fluvial terraces of the lower Susquehanna River. *Journal of Geomorphology*, 8:83-113.
- POWARS, D. S. and BRUCE, T. S., 1999. *The effects of the Chesapeake Bay Impact Crater on the Geological framework and correlation of*

*hydrogeologic units of the lower York-James Peninsula, Virginia.* United States Geological Survey Professional Paper, 1612, 82p.

REINHARDT, JUERGEN, NEWELL, W.L. and MIXON, R.B., 1980. Tertiary lithostratigraphy of the core. In: Geology of the Oak Grove core. *Virginia Division of Mineral Resources Publication*, 20(1):1-13.

SPANGLER, W. P., PETERSON, J. J., 1950. Geology of the Atlantic Coastal Plain in New Jersey, Delaware, Maryland, and Virginia. *American Association of Petroleum Geologists*, 34:1-99.

STOVER, L. E., and HARDENBOL, JAN, 1993. Dinoflagellates and depositional sequences in the lower Oligocene (Rupelian) Boom Clay Formation, Belgium. *Bulletin de la Société Belge de Géologie* 102 (1-2):5-77.

WARD, L. W., 1985. *Stratigraphy and characteristic mollusks of the Pamunkey Group (lower Tertiary) and the Old Church Formation of the Chesapeake Group, Virginia coastal plain.* United States Geological Survey Professional Paper, 1346, 78p.

———, 1992. Middle Eocene and upper Pliocene sea level events; maximum high-stands during the Tertiary. In: Zullo, V.A., Harris, W.B.

and Price, V. Jr., Eds., *Proceedings of the Bald Head Island Conference on Coastal Plains Geology.* Wilmington, University of North Carolina: 2:143.

WEEMS, R. E., 1986. Geology of the Ashland quadrangle, Virginia. *Virginia Division of Mineral Resources Publication 64*, text and 1:24,000 scale map.

———, 1998. *Newly recognized en echelon fall lines in the Piedmont and Blue Ridge provinces of North Carolina and Virginia, with a discussion of their possible ages and origins.* United States Geological Survey, Open-File Report 98-0374, 40p.

WEEMS, R. E., and EDWARDS, L. E., 2001. Geology of Oligocene, Miocene, and younger deposits in the coastal area of Georgia. *Georgia Geologic Survey Bulletin*, 131:1-124.

WENTWORTH, C. K., 1930. Sand and gravel resources of the Coastal Plain of Virginia. *Virginia Geological Survey Bulletin*, 32:1-146.

Manuscript received February 7, 2007

Manuscript accepted April 13, 2007

# Early-Cenomanian terrestrial facies and paleoclimate records of the Lower Tuscaloosa Formation, southwestern Mississippi

David F. Ufnar

Department of Geography and Geology, University of Southern Mississippi, Hattiesburg, Mississippi  
email: david.ufnar@usm.edu

---

**ABSTRACT:** Sphaerosiderite oxygen isotope values from the Early Cenomanian Lower Tuscaloosa Formation, or LTF, extend a mid-Cretaceous meteoric  $\delta^{18}\text{O}$  latitudinal gradient  $9^\circ$  south to  $25^\circ$  N paleolatitude, and contribute to a better understanding of the hydrologic cycle in North America during a “greenhouse” period in Earth history. Sphaerosiderites have been used to reconstruct paleolatitudinal trends in meteoric  $^{18}\text{O}$  values throughout western North America, and the  $^{18}\text{O}$  values have been used in a stable isotope mass balance model to produce quantitative estimates of mid-Cretaceous precipitation rates and latent heat flux values. The LTF meteoric  $^{18}\text{O}$  values help constrain the critical subtropical values on the coastal plain bordering Tethys and the southeastern coast of the Western Interior Seaway. The LTF, an important subsurface petroleum unit (2800–4000 m depths) in southern Mississippi, contains amalgamated pedogenically modified, sphaerosiderite-bearing mudstones and sandstones. Cored intervals of the Early-Cenomanian Stringer Sandstone Member of the Lower Tuscaloosa Formation (LTF) of Southwestern Mississippi are characterized by 6 lithofacies units. The descriptive lithofacies units include: (1) thickly-bedded sandstones; (2) thinly bedded sandstones; (3) carbonaceous mudstones and siltstones; (4) red-mottled mudstones; (5) purple and yellow mottled mudstones; and (6) flaser and lenticular bedded carbonaceous muddy sandstones. The sphaerosiderites are most commonly observed in gleyed domains of the red-mottled mudstones. These mudstones were clays, and silty clay loam soils, and are characterized by prominent red mottles in a gleyed matrix with an abundance of translocated clays, pedogenic slickensides, carbonaceous debris, and root traces. The sphaerosiderites yield  $\delta^{18}\text{O}$  vs.  $\delta^{13}\text{C}$  values, meteoric sphaerosiderite lines (MSLs), that may be used as a proxy for paleoprecipitation  $\delta^{18}\text{O}$  values. The MSL ( $\delta^{18}\text{O}$ ) values range from  $-3.31\text{‰}$  to  $-5.22\text{‰}$  (VPDB). Estimated meteoric water values for the LTF have an average value of  $-4.69\text{‰}$  VSMOW.

## INTRODUCTION

### Study Objectives

The objectives of this study are to: (1) describe the lithofacies and sphaerosiderite-bearing paleosols of the Lower Tuscaloosa Formation (LTF) in southwestern Mississippi, and (2) to present new sphaerosiderite isotopic values from paleosols of the LTF that provide a proxy record of ancient meteoric  $\delta^{18}\text{O}$  values along the southeastern margin of the Western Interior Seaway during the Cenomanian greenhouse warming.

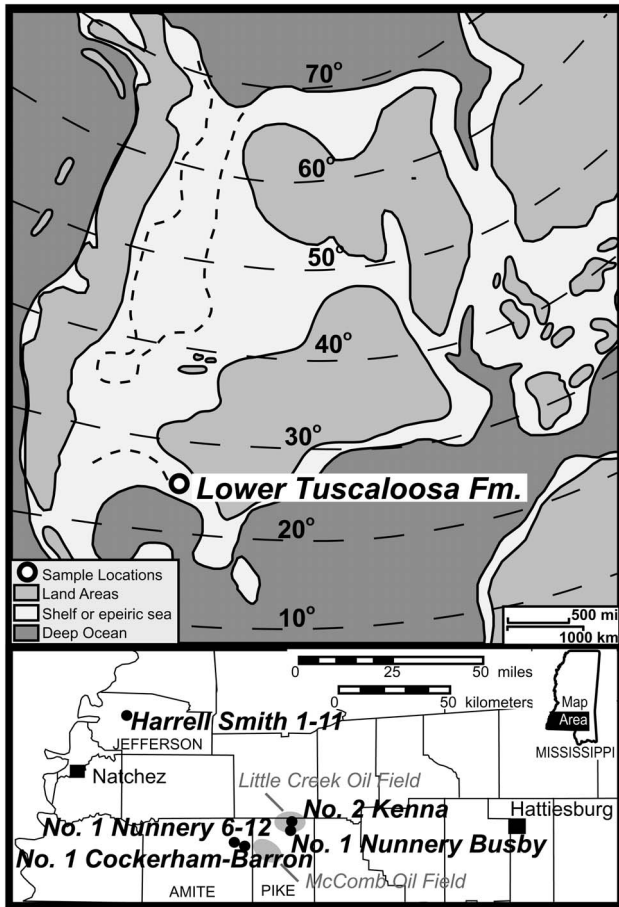
The stable isotopic values of the sphaerosiderites presented in this study provide proxy records of meteoric  $^{18}\text{O}$  values from  $25^\circ\text{N}$  paleolatitude (Ludvigson et al. 1998; White et al. 2000; Ufnar et al. 2002). These meteoric  $\delta^{18}\text{O}$  values extend a paleolatitudinal reconstruction from  $34^\circ\text{N}$  to  $25^\circ\text{N}$ , so that the trend now covers  $50^\circ$  of latitude ( $25^\circ$ – $75^\circ\text{N}$  paleolatitude). These new  $\delta^{18}\text{O}$  values will better constrain modeled precipitation rates and latent heat flux during the mid-Cretaceous greenhouse warming in North America (Ufnar et al. 2002, 2004), and contribute to a strictly Cenomanian Stage paleohydrological reconstruction (Ufnar et al., in press). A critical component of using the sphaerosiderite proxy records for paleoclimatological reconstructions is understanding the litho- and chronostratigraphic framework, and paleopedological context of the proxy materials (e.g. Ufnar et al. 2001, 2005 and White et al. 2005). This investigation describes the lithofacies assemblage of the LTF, provides new palynological age constraints, and describes the

pedogenic development of the LTF sphaerosiderite-bearing paleosols.

### The Lower Tuscaloosa Formation

The Upper Cretaceous LTF trend in southwestern Mississippi is situated along the southern flank of the Mississippi Salt Dome Basin (text-fig. 1; Klicman et al. 1988; Corcoran et al. 1993). The LTF is divided into two members, the basal Massive Sandstone, and the overlying Stringer Sandstone (Womack 1950; Watkins 1962; Klicman et al. 1988). The 5 cores described in this study were all obtained from the Stringer Sandstone Member between depths of approximately 3000–4000 meters (Hersch 1987, Klicman et al. 1988). The Stringer Sandstone Member of the LTF is generally composed of meandering coastal plain fluvial and delta plain deposits (Karges 1962; Hamilton and Cameron 1986). However, the upper McComb Sand unit of the Stringer Sandstone Member, is interpreted to be marine (Klickman et al. 1988). The LTF in the type area of west-central Alabama is assigned to the *Compliopolis-Atlantopolis* zone of the late Cenomanian to early Turonian (Christopher 1982). The LTF in southwestern Alabama is Late Cenomanian (Mancini et al. 1987), and Dunn et al. (1985), using taxonomic assignments of Pessagno (1967), observed foraminifera similar to *Heteromorphani* and *Rotalipora greenhornensis*, and also assigned the LTF to the Late Cenomanian (Hamilton and Cameron 1986).

Palynomorph data obtained for this investigation from the Harrell Smith #1-11 Core of the Lower Tuscaloosa Formation



TEXT-FIGURE 1  
Paleogeographic reconstruction of North America during the Cenomanian indicating the paleolatitudinal position of the sphaerosiderite-bearing formations used in this study and the core locations in southwestern Mississippi (modified from Witzke 2003).

suggests that the Stringer Sandstone Member is Early Cenomanian in age (Table 1). Numerous specimens of the gymnosperm pollen genus *Rugubivesiculites*, the fern-related spore species *Cicatricosisporites goniodontos* and rare angiosperm pollen, and the lack of well-documented North American late Albian assemblages in (e.g., Brenner 1963; Norris 1967; Singh 1971; Playford 1971; Phillips & Felix 1972; Srivastava 1977; Wingate 1980; Ravn 1995), suggests an early Cenomanian age. *C. goniodontos* is a species first described by Phillips and Felix (1972) from Tuscaloosa strata in Louisiana.

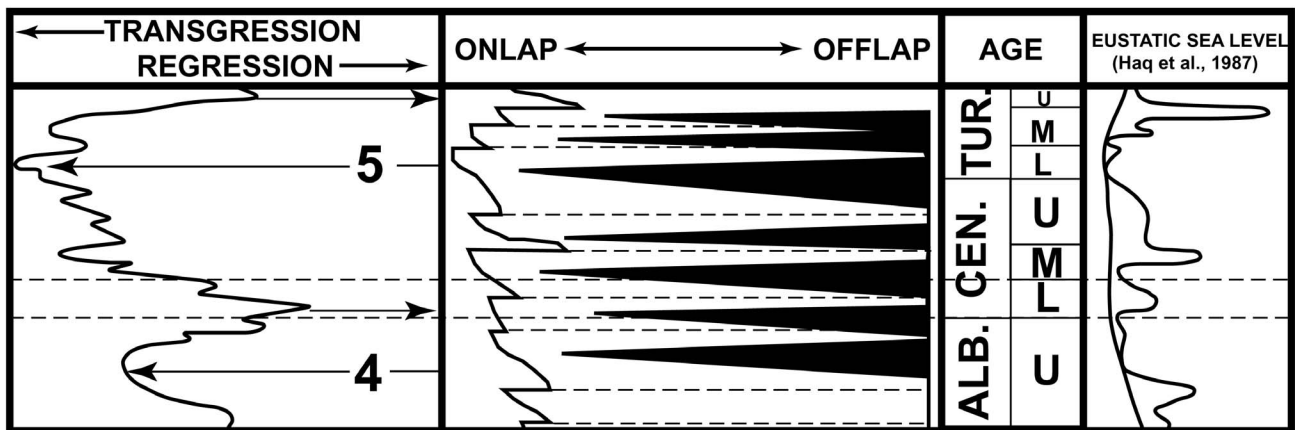
The LTF is generally composed of detritus eroded from the southern Appalachian and Ouachita orogenic belts (Corcoran et al. 1993). LTF sedimentation began during a significant base level fall that occurred during the regression separating the Kiowa-Skull Creek and the Greenhorn sea-level cycles of the Cretaceous Western Interior Basin (KWIB) (text-fig. 2; Kauffman and Caldwell 1993). The sea-level fall at the end of the Kiowa Skull Creek Cycle resulted in an unconformity (Salvador 1991) with widespread erosion in the northern GOM area (Mancini et al. 2002a). The subsequent rise in sea-level and accumulation of the LTF deposits precedes the T-R K5 cycle of Mancini and Puckett (2005) and the middle

Cenomanian to Upper Turonian Cycle 17 of Western Europe (Hardenbol et al. 1998; Jacquin et al. 1998b). The Tuscaloosa Group is a complete depositional sequence (Corcoran et al. 1993), and the LTF formed during the earliest transgressive phases of the Greenhorn cycle (Mancini and Puckett 2005; Kauffman and Caldwell 1993).

Two sandstones units, the Denkman and Dykes are petroleum reservoirs in the updip portions of the LTF (Klickman et al. 1988). The Denkman and the overlying Dykes sandstones are the updip pay zones (Garrison and Chancellor 1991), and several investigations suggest a fluvial depositional origin (Scully et al. 1966; Berg and Cook 1968; Chasteen 1983; Hamilton 1986; Stancliffe and Adams 1986; Young 1987). The fluvial character of these deposits is suggested by the presence of: (1) upward fining sandstone units with scoured basal contacts, (2) a lack of marine indicators, and (3) a close association between sandstone bodies and mottled, rooted, variegated mudstones (Klickman et al. 1988). The facies relationships (e.g. Eisenstatt 1960; Busch 1974; Hamilton and Cameron 1986), and diagenetic history of the LTF sandstone bodies (e.g. Hearn and Lock 1985; Watkins 1985; Stancliffe and Adams 1986; Hamlin and Cameron 1987; Klickman et al. 1988) have been well studied, however very few studies have assessed the pedogenically-modified mudstones (e.g. Cameron et al. 1992).

The Stringer Sandstone Member of the LTF in southwestern Mississippi contains pedogenically modified floodplain deposits consisting of mottled and rooted paleosols and pedocomplexes. Of particular interest is the occurrence of sphaerosiderite nodules in several of the mudstone intervals of the cores used in this investigation. Sphaerosiderites are observed in paleosols throughout the Cretaceous KWIB and the North Slope, Alaska (e.g. Leckie et al. 1989; Hart et al. 1992; Ludvigson et al. 1998; McCarthy and Plint 1998; Ufnar et al. 2004a). The  $\delta^{18}\text{O}$  and  $\delta^{13}\text{C}$  stable isotopic values of sphaerosiderites have been used as a mid-Cretaceous paleoclimatological archive throughout North America; however few analyses have been obtained south of  $34^\circ\text{N}$  paleolatitude (e.g. Ludvigson et al. 1998; White et al. 2000a; Ufnar et al. 2002). The numerous sphaerosiderite-bearing intervals of the LTF were formed at approximately  $25^\circ\text{N}$  paleolatitude (text-fig. 3), and provide the opportunity to: (1) extend a mid-Cretaceous paleolatitudinal trend in sphaerosiderite  $\delta^{18}\text{O}$  values (Ufnar et al. 2002), and (2) build a robust data set to begin reconstructing a paleolatitudinal trend in sphaerosiderite  $\delta^{18}\text{O}$  values for just the Cenomanian Stage.

Sphaerosiderites are millimeter-scale  $\text{FeCO}_3$  nodules that formed in ancient saturated, reducing wetland soils (Ludvigson et al. 1998; White et al. 2000; Ufnar et al. 2002). The  $\delta^{18}\text{O}$  values of the sphaerosiderites are dominated by that of the soil groundwater which was primarily recharged through local precipitation; thus the sphaerosiderites are used as a proxy for the  $\delta^{18}\text{O}$  values of precipitation (Ludvigson et al. 1998, Ufnar et al. 2001). Multiple isotopic analyses from one paleosol horizon tend to yield trends of invariant  $\delta^{18}\text{O}$  values, and more variable  $\delta^{18}\text{O}$  values (Ludvigson et al. 1998). These trends are meteoric sphaerosiderite lines (MSLs), and are analogous to the meteoric calcite lines of Lohmann (1988). The trends of invariant  $\delta^{18}\text{O}$  values and more variable  $\delta^{18}\text{C}$  values suggests that the sphaerosiderites developed during early meteoric phreatic diagenesis in a stable ground water system where the mean annual temperature changed little and the  $\delta^{18}\text{O}$  values reflect the



TEXT-FIGURE 2

The curves illustrate mid-Cretaceous eustatic sea level (Haq et al. 1987) and the transgressive-regressive cycles defined by Kauffman and Caldwell (1993) in the KWIB. The 3 indicates the Clearwater cycle, 4 the Kiowa-Skull Creek Cycle, and 5 the Greenhorn Cycle, and the faint dashed lines the age range of the Lower Tuscaloosa Cores investigated in this study (modified from Kauffman and Caldwell 1993).

mean  $\delta^{18}\text{O}$  values of rainfall (Ludvigson et al., 1998; White et al. 2001; Ufnar et al. 2002). The  $\delta^{18}\text{C}$  values are more variable and reflect incorporation of dissolved  $\text{CO}_2$  from degrading organic matter or methanogenesis (Ludvigson et al. 1998).

Using independently-determined empirical paleotemperature estimates (e.g., Wolfe and Upchurch 1987), and the temperature-dependent fraction factor for siderite and water (Carothers et al. 1988), the MSLs are used to estimate the average meteoric  $\delta^{18}\text{O}$  values for a given paleolatitude (Ludvigson et al. 1998). From multiple locations in North America investigators have reconstructed a paleolatitudinal trend in mid-Cretaceous (primarily Albian) meteoric  $\delta^{18}\text{O}$  values (White et al. 2001; Ufnar et al. 2002). The new data obtained for this investigation are coupled with the results of previous investigations to extend the paleolatitudinal trend in meteoric  $\delta^{18}\text{O}$  values  $9^\circ$  further south in the KWIB. This investigation will contribute to modeling experiments designed to understand the dynamics of the hydrologic cycle during “greenhouse” phases of Earth history (e.g. White et al. 2000, Ufnar et al. 2002; 2004c).

## METHODS

Five cores from Amite, Pike, and Jefferson Counties, Mississippi (text-fig. 1) were sampled and described for this investigation (Table 2). Micromorphological analyses of sphaerosiderite bearing horizons followed the methods of Bullock et al. (1985).

Siderite powder microsamples (a few micrograms) were obtained from nodules exposed on polished core-slabs using a dental drill (Miltex Instrument Company, Bethpage, NY, bur size 0.5mm) under a binocular microscope. At least ten siderite powder microsamples were obtained from each selected siderite-bearing horizon (Table 1). Stable isotope-ratio mass spectrometry was conducted at the University of Kansas Stable Isotope Research lab. The micro samples were initially roasted *in vacuo* at  $380^\circ\text{C}$  to remove any volatile contaminants. After roasting, samples were then reacted with anhydrous phosphoric acid at  $75^\circ\text{C}$  in a Kiel III automated carbonate reaction device coupled to the inlet of a Finnigan MAT 253 isotope ratio mass spectrometer. All siderite stable

isotope ratios are reported relative to the Vienna PeeDee Belemnite (VPDB) standard.

Electron Microprobe analysis were conducted on selected sphaerosiderites using a JEOL Superprobe 733 electron microprobe at the LSU Department of Geology and Geophysics to quantify the chemical composition of the sphaerosiderites. Siderite analyses were conducted (transects of 1-5 points across each sphaerosiderite sample) simultaneously using wavelength dispersive spectrometry at an accelerating voltage of 15 kV, and beam current of 10 nA, and a beam diameter of  $5\mu\text{m}$ . The following standards were simultaneously measured: SCA (Smithsonian sericite), MG1 (Smithsonian dolomite), SSID (Smithsonian siderite), SR1 (LSU strontianite), and MN2 (LSU rhodonite).

## RESULTS

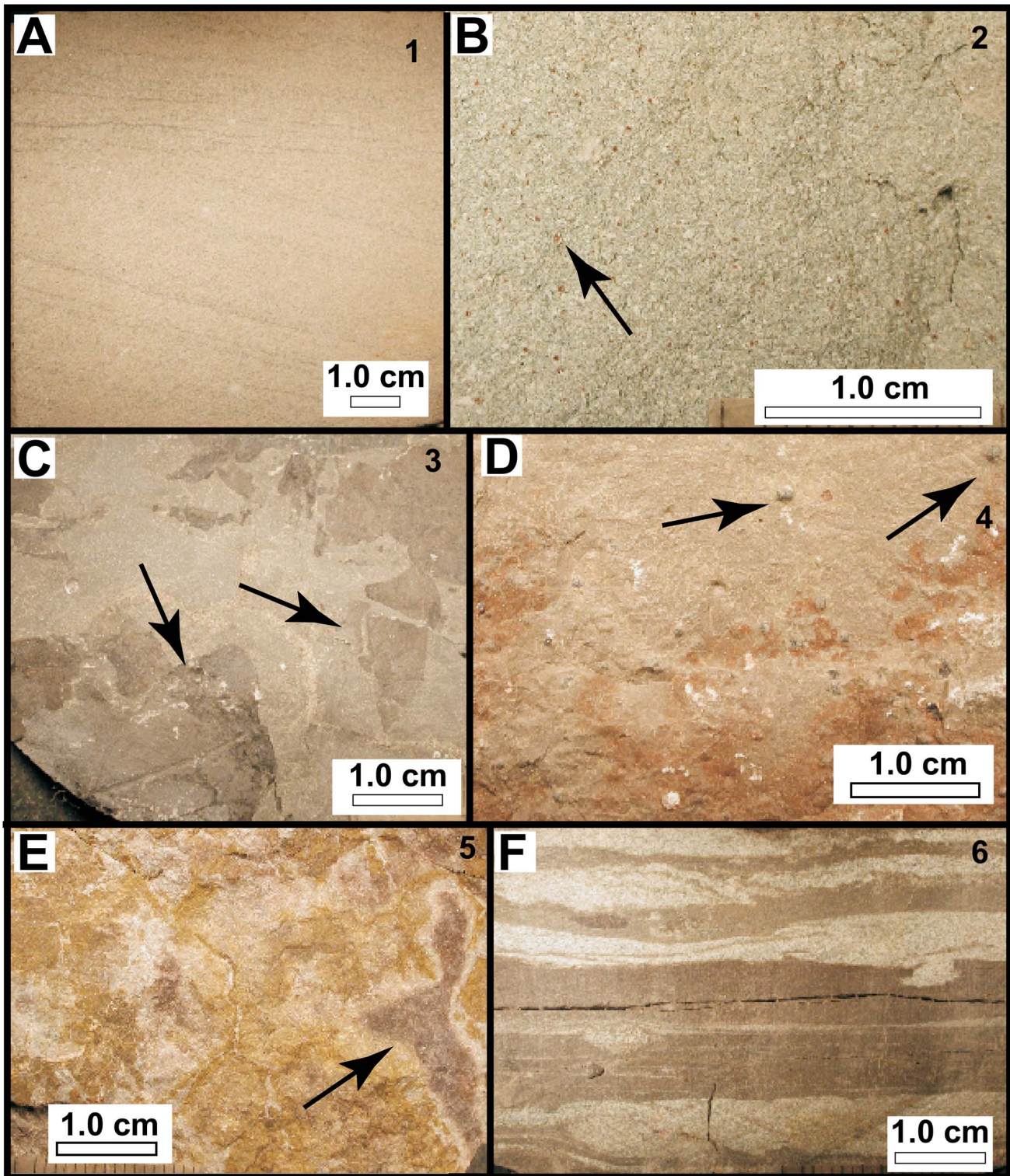
### Lithofacies

The Lower Tuscaloosa Formation is generally composed of thick (1-10m), massive to large-scale cross-stratified, quartzose sandstones interbedded with carbonaceous mudstones, complexly color-mottled mudstones and claystones, and thin (<1m thick) fine-grained sandstones. Six lithofacies units have been identified in the cored intervals of the LTF. The descriptive lithofacies units include: (1) thickly-bedded sandstones; (2) thinly-bedded sandstones; (3) carbonaceous mudstones and siltstones; (4) red-mottled mudstones; (5) purple and yellow mottled mudstones; and (6) flaser and lenticular bedded carbonaceous muddy sandstones.

#### *Lithofacies 1: Thickly-bedded Sandstones*

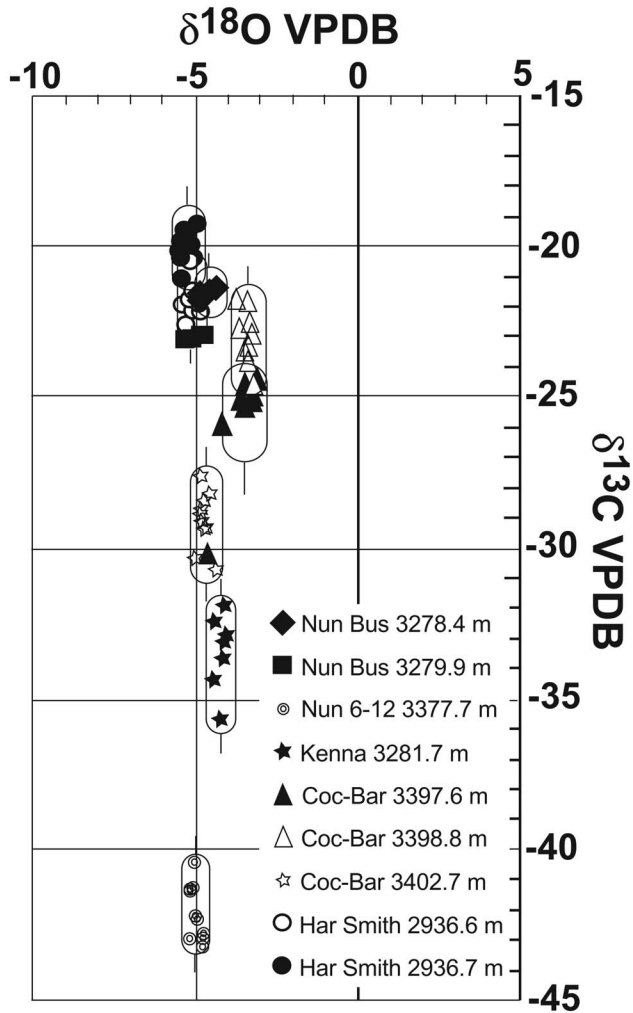
The thickly-bedded sandstones are generally 3-6 meters thick and consist of quartz with minor amounts of chert, feldspars, and micas. The sandstones are generally composed of well-sorted, subrounded to subangular fine-grained sand particles; however some medium- and coarse-grained, and normally-graded intervals are noted. Large-scale trough (?) cross-stratification, horizontal laminations, and wavy laminations are observed in many of the thickly bedded sandstones. Commonly, foresets and thin laminations are mantled with





TEXT-FIGURE 4

The photographs illustrate the macromorphological features observed in the lithofacies of the Lower Tuscaloosa Formation of southwestern Mississippi. The numbers in the top right of each photograph indicate the designated lithofacies unit. (A) The core slab exhibits large-scale cross-stratification in fine - to medium-grained sandstone of lithofacies 1, the thickly-bedded sandstones. (B) The gleyed, fine-grained sandstone with sphaerosiderites (arrow) is representative of the thinly-bedded sandstones of lithofacies 2. (C) The arrows in this photograph indicate carbonaceous leaf-fossils preserved in carbonaceous siltstones (lithofacies 3). (D) the photograph illustrates a gleyed, mudstone with sphaerosiderites (arrows) that is representative of lithofacies 4, the red mottled mudstones. (E) The mudstone illustrated in this photograph is representative of the purple and yellow mottled mudstones (lithofacies 5), and the arrow is pointing to a purple rhizaloe that is surrounded by a gray (gleyed) halo within the predominantly yellow mottled matrix. (F) The photograph illustrates lenticular bedded very fine-grained sandstones and carbonaceous mudstones that are representative of lithofacies 6, the flaser and lenticular bedded carbonaceous muddy sandstones.



TEXT-FIGURE 5

The carbon and oxygen isotope cross plot illustrates the  $\delta^{18}\text{O}$  vs.  $\delta^{13}\text{C}$  values of multiple sphaerosiderites (10 or more) from 9 separate sphaerosiderite-bearing paleosol horizons in the Lower Tuscaloosa Formation of southwestern Mississippi. The sphaerosiderite stable isotope values from any given horizon tend to yield trends of invariant  $\delta^{18}\text{O}$  values ( $\pm 1.0\text{‰}$ ) and more variable  $\delta^{13}\text{C}$  values (3 to 5‰), or meteoric sphaerosiderite lines (MSLs; Ludvigson et al. 1998). The pill-shaped domains encapsulate the sphaerosiderite  $\delta^{18}\text{O}$  vs.  $\delta^{13}\text{C}$  values for an individual paleosol horizon, and the vertical lines projecting from the pills are representative of the MSL value or average  $\delta^{18}\text{O}$  value for that particular sphaerosiderite-bearing paleosol horizon.

carbonaceous debris. Sphaerosiderite nodules are sometimes observed in the dark gray (gleyed), thinly bedded sandstones. The sphaerosiderites are generally <1.5mm in diameter and appear to have engulfed quartz grains as they grew in the interstitial pores (text-fig. 4B).

#### Interpretations, Lithofacies 2

This lithofacies displays characteristics of floodplain crevasse splays and/or levee deposits within a meandering or anastomosing fluvial system (Miall 1977, 1981, 1992; McCarthy et al. 1997). Thin bedding and common pedogenic features (mottling, carbonaceous debris, burrows, and root traces) suggest deposition as levees in distal floodbasin settings, where stable pedogenic processes overprint sedimen-

tary structures (Miall 1992; McCarthy 1997). Anastomosing fluvial deposits are characterized by restricted channel deposits within thick floodplain and common splay deposits, and generally experience stable conditions, during which sphaerosiderite precipitation could have occurred (Miall 1992; Ufnar et al. 2001). Common, upward coarsening trends within these thin sand lenses are typical of crevasse splay deposits within a meandering fluvial system (Miall 1981).

#### Lithofacies 3: Carbonaceous Mudstones and Siltstones

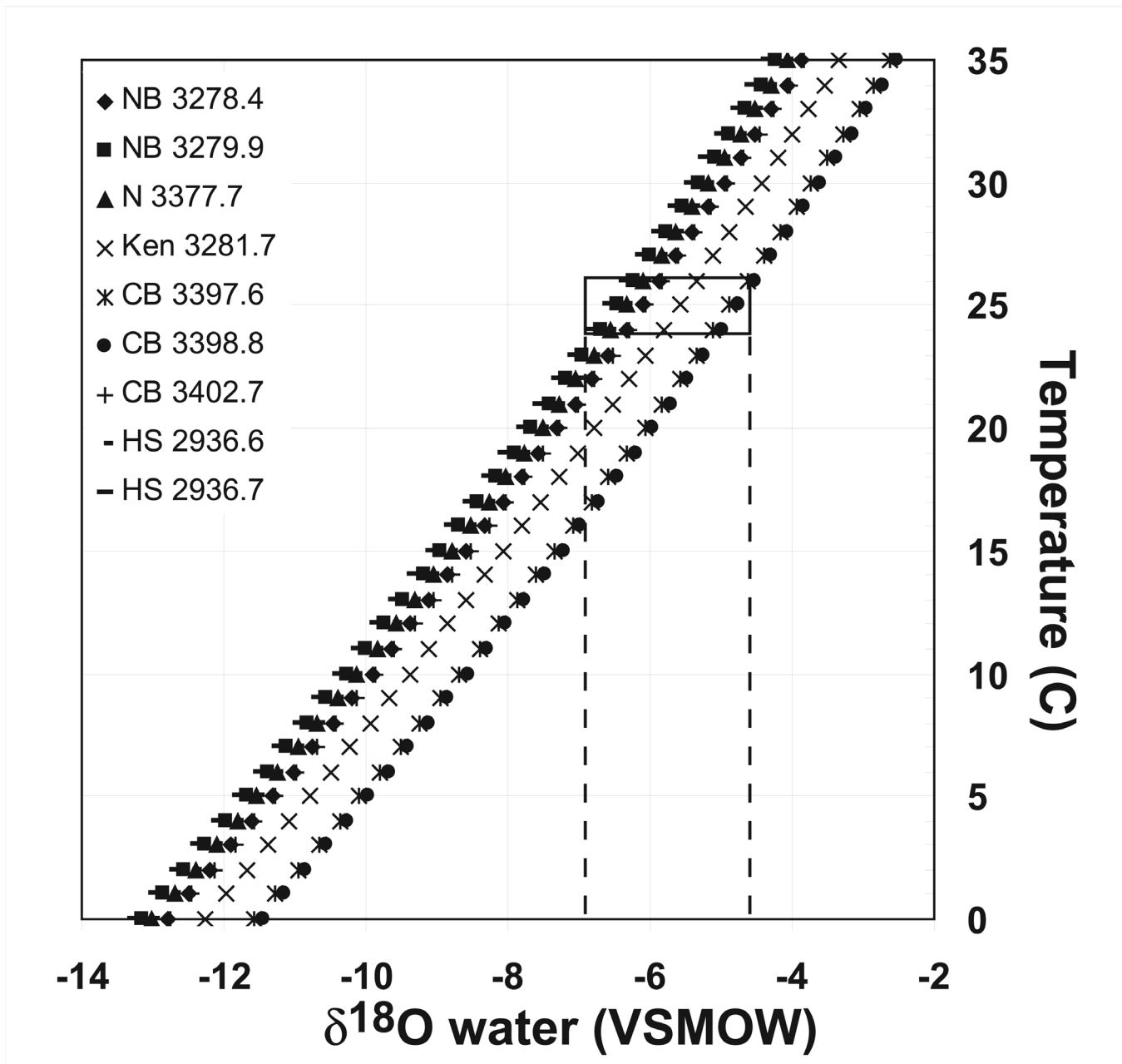
The carbonaceous mudstones consist of massive, dark bluish-grey to black mudstones that vary between claystones and clayey-siltstones in texture. These intervals are often friable, and break easily along subhorizontal, irregular parting surfaces. Commonly, well-preserved plant macrofossils are preserved in this lithofacies. The matrix has gleyed colors and contains an abundance of opaque, very finely-comminuted organic debris. Rarely, this lithofacies exhibits burrow mottling, root traces, and pedogenic slickensides (text-fig. 4C). Rare, very thin (<0.35m thick) coaly intervals are also observed that are up to 70% carbonaceous debris.

#### Interpretations, Lithofacies 3

This lithofacies is interpreted to have been deposited within the floodplain backswamps of a meandering to anastomosing fluvial system (Miall 1977; 1981; 1992). Close association with upward fining sandstones and upward coarsening splay deposits, abundant carbonaceous material, and gleying suggests a swampy, low-lying alluvial/coastal plain fluvial setting with hydromorphic pedocomplexes and high rates of organic matter accumulation (McCarthy 2002; McCarthy et al. 1999; Plint 1996). The texture of the coaly intervals, coupled with the friable structure may be classified as Fusain-like coal (Ward 1984). Close association with carbonaceous siltstones and mudstones implies deposition in floodplain settings where organic accumulation rates were very high (McCarthy 2002; Ward 1984).

#### Lithofacies 4: Red-Mottled Mudstones

Red-mottled mudstones are a common lithofacies unit in the cored intervals, and individual units may reach 2-3m in thickness. The red-mottled mudstones range from claystones to clayey coarse-siltstones and very fine-grained sandstones in texture. The mottling is the dominant feature and generally consists of prominent, coarse red mottles (1 OR 3/3 to 3/6 Munsell colors), that account for 10 to >75% of the coloring (text-fig. 4D). The background matrix colors are typically dark bluish to dark greenish grey. The mottling patterns are very complex. Often, the background colors are predominantly red and contain vein-like gleyed domains that may represent rhizcretions, or more appropriately rhizohaloes (Kraus and Hasiotis 2006). Mottled domains often appear to stain (red) laminated burrows or crescent-shaped infillings. The red mottled mudstones often exhibit a subangular blocky structure, and the parting surfaces between individual blocks are coated with clay and pedogenic slickensides. Tubular clay coatings and carbonaceous root traces are also observed. Commonly, siltstone and very fine-grained sandstone filled burrows are observed. In domains of decreased red-mottling (<30%), sphaerosiderite nodules are often observed (text-fig. 4D arrows). The sphaerosiderites are generally irregular to spherical in shape, and range from <0.5 to 1.5mm in diameter. Individual nodules exhibit a radial-concentric crystalline microstructure, and the nodules are typically oxidized around



TEXT-FIGURE 6

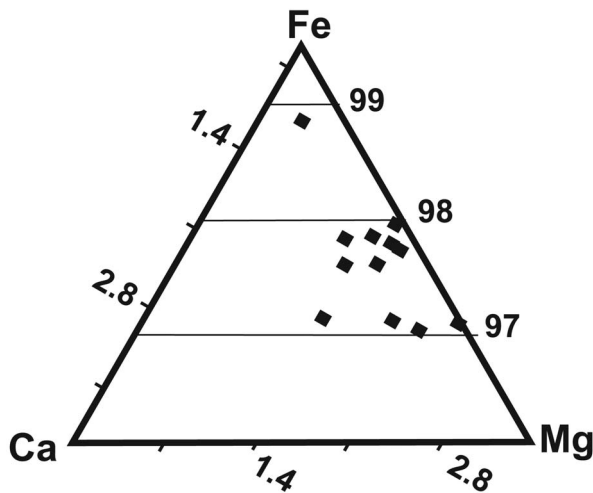
The graph illustrates the meteoric water  $\delta^{18}\text{O}$  values calculated from the sphaerosiderite  $\delta^{18}\text{O}$  values over a range of temperatures using the experimentally-determined siderite-water fractionation factor of Carothers et al. (1988). The rectangle with the dashed line projections represents the estimated range of meteoric water  $\delta^{18}\text{O}$  values based upon the paleotemperature estimates of 25°N paleolatitude of Wolfe and Upchurch (1987).

the margins. The nodules generally occur as randomly distributed individuals, or occur in linear arrays along root traces, or as small clusters of three or more individuals. The nodules appear to have displacive growth fabrics as they sometimes exhibit thin clay coatings around the nodules.

The best preserved nodules are observed in the gleyed mudstone domains. Those which occur in the red-mottled domains are often partially to completely oxidized.

#### *Interpretations, Lithofacies 4*

This lithofacies represents moderately- to heavily-weathered floodplain deposits with evidence for pedogenic modifications. Prominent red mottling, burrows, infillings, and illuvial clay accumulations suggest the pedogenically-modified floodplain was a stable, well-drained geomorphic surface (Ufnar et al. 2002; McCarthy 1997; Schwetermann 1993). Pedogenic slickensides, blocky structures, and clay



TEXT-FIGURE 7

The ternary diagram illustrates the Fe, Mg, and Ca concentrations of representative spherosiderites from the 2936.6-2936.8m interval of the Harrell Smith #1-11 core. The nodules analysed were all >95% FeCO<sub>3</sub>.

coatings also suggest alternating periods of wetting and drying (Wilding and Tessier 1988; Kraus and Hasiotis 2006).

The gleyed mudstone domains formed during times when the soil was saturated, and depleted of oxygen. The available ferrous iron was reduced and subsequently removed from areas of the soil matrix (Fanning and Fanning 1989; Kraus and Hasiotis 2006). Sphaerosiderite precipitation occurred during hydromorphic, saturated, reducing conditions (Stoops 1983; Landuyt 1990; Ludvigson et al. 1998; Ufnar et al. 2001).

#### *Lithofacies 5: Purple and Yellow-Mottled Mudstones*

The purple and yellow mottled mudstones range from claystone to coarse-siltstone in texture, with minor amounts of very fine-grained quartz sand. These mudstone intervals are generally 1-2m in thickness. The mudstones are predominantly gleyed, with dark gray-green to gray-blue colors, complexly mottled with medium, to coarse, prominent red and purple and yellow mottled domains. The mottling generally accounts for 20-40% of the coloration, with the background color predominantly gray. Rhizohaloes are commonly observed in these intervals as well as pedogenic slickensides. The mudstone exhibits some blocky structures and clay void-coatings. Some siltstone-filled burrows are also noted in these mudstones (text-fig. 4E).

#### *Interpretation, Lithofacies 5*

This lithofacies is interpreted to be pedogenically modified floodplain deposits. The purple mottling in these paleosols may result from slight depletions of Fe<sub>2</sub>O<sub>3</sub> and MnO<sub>2</sub> (Kraus and Hasiotis 2006; Stolt et al. 1994; Wright et al. 2000). Yellow mottling may be comprised of goethite (FeO(OH)), which may indicate that hematite was removed preferentially from some domains (Stolt et al. 1994; Kraus and Hasiotis 2006). The localized removal of hematite indicates weakly reducing conditions, often in the presence of organic matter (Macedo and Bryant 1989; Stolt et al. 1994;

Kraus and Hasiotis 2006). The purple and yellow mottling suggests that intermediate drainage conditions existed (Farnham and Kraus 2002; Simonson and Boersma 1972; Schwetermann and Fanning 1976; Macedo and Bryant 1987; Kraus and Hasiotis 2006). Rhizohaloes and pedogenic slickensides indicate alternating periods of wetting and drying (Wilding and Tessier 1988; Joeckel 1995; Farnham and Kraus 2002; Kraus and Hasiotis 2006; McCarthy et al. 1998).

#### *Lithofacies 6: Flaser and Lenticular Bedded Carbonaceous Muddy-Sandstones*

A few intervals that are generally less than 1 meter thick are characterized by very thinly interbedded very fine-grained sandstones and carbonaceous mudstones. The sandstones and mudstones are often characterized by flaser, lenticular, and wavy bedding. The sandstone intervals are commonly small-scale ripple cross-stratified, and some of the cross-stratification exhibits herringbone, reverse-oriented foresets. Individual ripple-sets are often capped by carbonaceous mudstone flasers or drapes. Some reactivation surfaces are noted in the sandstone-dominated, ripple cross-stratification. The mudstone intervals often exhibit very small "stringers" or lenticular domains of coarse siltstone to very fine-grained sandstone. The mudstones are generally very dark grey and contain an abundance of fossil plant debris (large fragments as well as finely-comminuted debris). The mudstone-sandstone interbeds exhibit cyclic changes between mud and sand-dominated deposition (text-fig. 4F). A few intervals consist of burrow-mottled silt- to very fine-grained sandstones. Intense burrowing is evident from the color changes in burrow back-filled domains as compared to the surrounding matrix materials. These beds often exhibit crude laminations that have been highly disrupted by the burrowed fabrics.

#### *Interpretations, Lithofacies 6*

Hamilton and Cameron (1986) interpreted an overall transgressive phase resulted in the transition from non-marine fluvial (Stringer Sand Member) to estuarine and marine sedimentation (McComb Sand) in the Lower Tuscaloosa Formation. The rhythmic nature of the interbedded sandstones and carbonaceous mudstones, and rare herringbone cross-laminations suggests deposition under cyclically-changing flow conditions with changing (possibly reversing) flow directions (de Raaf and Boersma 1971; Visser 1980). This lithofacies may represent deposition within the upper, fluvial-dominated zones of an estuary where tidal influences affected textural patterns (Reinson 1992). Flaser, lenticular, and wavy bedding features, with herringbone cross-stratification and reactivation surfaces, may be indicative of tidally-influenced deposition (Kvale and Archer 1991; DeMowbray and Visser 1984). Tidally-influenced point bars or intrachannel bars feature rhythmic mud drapes that indicate alternating low flow regime conditions (Dalrymple 1992; Kvale and Archer 1990, 1991). The interbedded sandstones and carbonaceous mudstones of the LTF may have been deposited near the tidal limit of influence in a coastal plain fluvial system (Dalrymple 1992; Clifton 1982). The burrowing within these deposits resembles characteristic tidal channel margin, overbank, and tidal flat bioturbation (Crimes and Harper 1970; Clifton 1982; Davis 1985).

## LTF Stable Isotopes

### Harrell-Smith # 1-11 Core

A total of 48 stable isotope analyses were completed from the 9,632' sphaerosiderite-bearing horizon of the Harrell-Smith 1-11 core of Jefferson County, MS. The  $\delta^{18}\text{O}$  values for the 2,935.8m (9,632') sphaerosiderite-bearing horizon of this core range from -5.22 and  $-5.00\text{‰} \pm 0.051\text{‰}$  (VPDB). The average  $\delta^{18}\text{O}$  values of each sampled horizon (2935.8m and 2935.9m; 9,632' and 9,632'4") represent the meteoric sphaerosiderite lines (MSLs) for those horizons and are -5.0 and -5.2‰ (VPDB) respectively (text-fig. 5). The  $\delta^{18}\text{C}$  values of the 2935.8m sphaerosiderite-bearing horizon are more variable than the oxygen isotope values. Average  $\delta^{18}\text{O}$  values range from -22.617 to  $-19.315\text{‰} \pm 0.028\text{‰}$  (VPDB).

### Cockerham-Barron No. 1 core

A total of 29 stable isotope analyses were completed from the sphaerosiderite-bearing horizons of the Cockerham-Barron core of Amite County, MS. The  $\delta^{18}\text{O}$  values for sphaerosiderite-bearing horizons of this core range from -4.72 and  $-3.40\text{‰} \pm 0.054\text{‰}$  (VPDB). The MSLs of each sampled horizon (3401.8m, 3398.1m, and 33,96.7m; 11,161', 11,148'9", and 11,144') are -4.715, -3.407, and -3.525‰ (VPDB), respectively (text-fig. 5) The average  $\delta^{18}\text{C}$  values range from -30.53 to  $-21.734\text{‰} \pm 0.032\text{‰}$  (VPDB).

### Kenna #2 Core

A total of 8 stable isotope analyses were completed from the 10,802'6" sphaerosiderite-bearing horizon of the Kenna #2 core of Pike County, MS. The  $\delta^{18}\text{O}$  values for the 3,292.6m (10,802'6") sphaerosiderite-bearing horizon of this core range from -4.47 and  $-4.01\text{‰} \pm 0.044\text{‰}$  (VPDB). The MSL for the 3,292.6m interval is -4.232‰ (VPDB; text-fig. 5). The  $\delta^{18}\text{C}$  values range from -35.684 to  $-30.674\text{‰} \pm 0.0285\text{‰}$  (VPDB).

### Nunnery 6-12 core

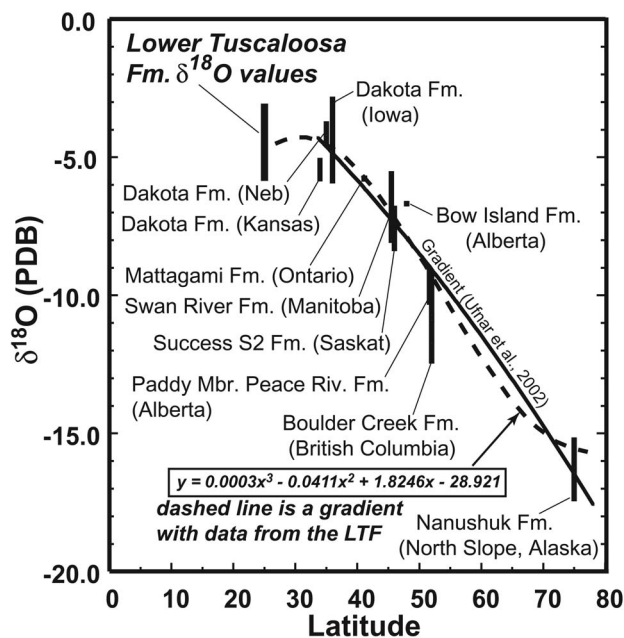
A total of 10 stable isotope analyses were completed from the 11,079' interval. The  $\delta^{18}\text{O}$  values for the 3,376.8m (11,079') sphaerosiderite-bearing horizon of this core range from -5.46 and  $-4.73\text{‰} \pm 0.048\text{‰}$  (VPDB). The MSL for the 3,376.8m (11,079') sphaerosiderite-bearing horizon of the Nun 6-12 core of Amite County, MS, is  $-4.973\text{‰}$  (VPDB; text-fig. 5). The  $\delta^{18}\text{O}$  values range from -42.98 to  $-40.56\text{‰} \pm 0.0334\text{‰}$  (VPDB).

### Nunnery-Busby No. 1 core

A total of 20 stable isotope analyses were completed from the sphaerosiderite-bearing horizons of the No. 1 Nunnery-Busby core of Pike, MS. The  $\delta^{18}\text{O}$  values for the sphaerosiderite-bearing horizons of this core range from -5.12 and  $-4.76\text{‰} \pm 0.045\text{‰}$  (VPDB). The MSLs for the 3,278.9m (10,757'9") and 3,277.5m (10,753') intervals are -5.119 and -4.761‰ (VPDB) respectively (text-fig. 5). The  $\delta^{18}\text{O}$  values range from -23.1411 to  $-21.659\text{‰} \pm 0.03\text{‰}$  (VPDB).

### Estimated LTF Meteoric Water Values

Using the MSLs obtained in this study, the independently determined empirical paleotemperature estimates for (25°N) during the Cenomanian from Wolfe and Upchurch (1987) and Spicer and Corfield (1992), and the experimentally determined  $^{18}\text{O}$  fractionation equation of Carothers et al. (1988), an approximated range of groundwater  $\delta^{18}\text{O}$  values have



TEXT-FIGURE 8

The graph illustrates a mid-Cretaceous paleolatitudinal trend in siderite  $\delta^{18}\text{O}$  values (primarily Albian) that has been constructed from over 150 individual paleosols throughout the KWIB and North Slope, Alaska. The range of Lower Tuscaloosa Formation siderite  $\delta^{18}\text{O}$  values has been added along with a revised gradient that includes the new lower latitude data from this investigation.

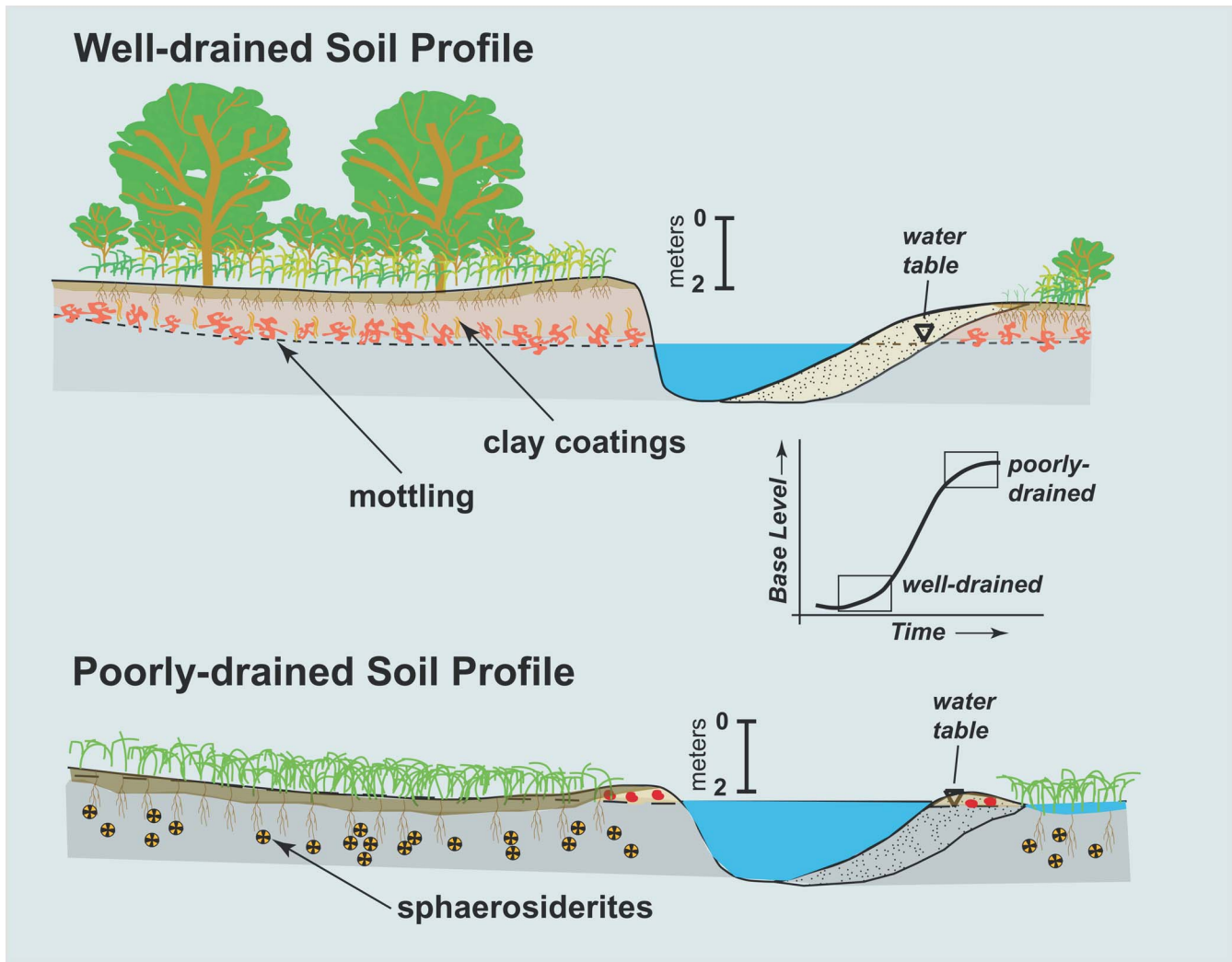
been estimated for the Lower Tuscaloosa (text-fig. 6). The meteoric  $\delta^{18}\text{O}$  values estimated from the LTF sphaerosiderite proxy records range from -6.8‰ to -4.5‰ (VSMOW).

### LTF Minor Elements

The elemental compositions of the sphaerosiderites were analyzed to determine if the siderite was pure, and if later-diagenetic mineral replacement had occurred. Although sphaerosiderites have been shown to be fairly refractory minerals (Ufnar et al. 2004b), the presence of alteration minerals might alter the early-diagenetic stable isotope values of the siderite. The sphaerosiderites analyzed were approximately 97 mol %  $\text{FeCO}_3$ , with very minor enrichments in Ca and Mg (text-fig. 7).

### DISCUSSION

The stable isotopic data obtained from sphaerosiderites in the Lower Tuscaloosa Formation of southwestern Mississippi provide a proxy record of meteoric water  $\delta^{18}\text{O}$  values during the Late Cenomanian Stage. The isotopic trends from each sphaerosiderite-bearing interval yield trends of invariant  $\delta^{18}\text{O}$  values and more variable  $\delta^{18}\text{C}$  values (MSLs of Ludvigson et al. 1998). Although the LTF sustained significant diagenetic alteration (e.g. Hearn and Lock 1985; Hamlin and Cameron 1987) there is little evidence for diagenetic alteration of the sphaerosiderite textures and chemistries. The electron microprobe results suggest that the nodules are composed of >95%  $\text{FeCO}_3$ , and lack evidence of chemical alteration during later diagenesis. Calcite and dolomite cements in the LTF sandstones yield  $\delta^{18}\text{O}$  values ranging from -11.8 to -9‰



TEXT-FIGURE 9

The cartoon illustrates how changes in base level over time may have generated the contrasting pedogenic features observed in the sphaerosiderite-bearing paleosols and pedocomplexes that suggest a polygenetic pedogenic history. The earlier, well-drained phase of pedogenesis was characterized by well-drained soils with illuvial features (clay coatings) and color mottling due to cyclic wetting and drying and excursions of the water table. The latter phase of pedogenic development was characterized by saturated, reducing conditions, a high water table, and generation of sphaerosiderites. Vertical accretion through overbank flooding altered the relative height of the water table and led to either isolation of the former geomorphic surface, soil welding, or started a new cycle of pedogenic development in the freshly deposited materials.

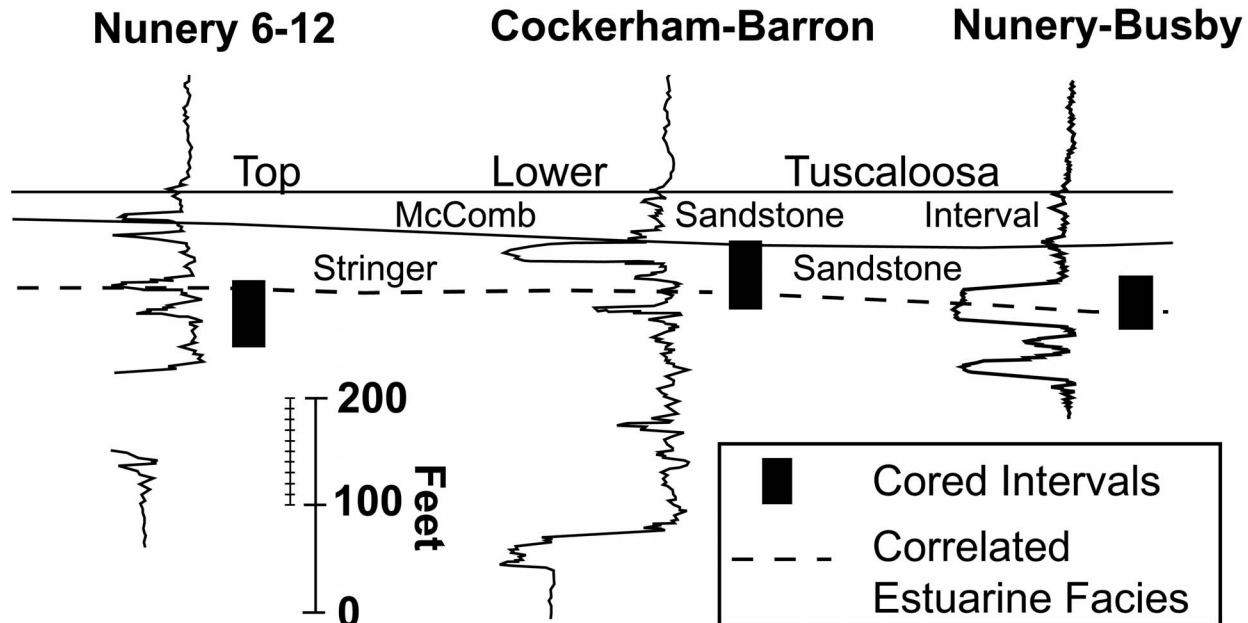
VPDB (Weedman et al. 1996), significantly lighter than the siderite  $\delta^{18}\text{O}$  values. If the formation waters that precipitated these cements had interacted with the sphaerosiderites, the  $\delta^{18}\text{O}$  values would have likely formed covariant trends in  $\delta^{18}\text{O}$  vs  $\delta^{13}\text{C}$  values.

The  $\delta^{18}\text{O}$  values of the LTF sphaerosiderites range from -5.2 to -3.4‰ VPDB. The  $\delta^{18}\text{O}$  values extend a latitudinal trend in mid-Cretaceous  $\delta^{18}\text{O}$  values 9° south, yielding a transect from 25° to 75°N paleolatitude (text-fig. 8; Ludvigson et al. 1998; White et al. 2000; Ufnar et al. 2002).

Stable Isotope mass-balance modeling experiments (Ufnar et al. 2002) have yielded estimates of low latitude precipitation and evaporation fluxes and latent heat transport (Ufnar et al. 2004c). However, those estimates are not confirmed with low-latitude empirical data. The extended gradient in meteoric  $\delta^{18}\text{O}$  values from the LTF will refine estimates of

mid-Cretaceous precipitation rates and atmospheric heat transport (Ufnar et al. 2002, 2004).

The pedogenic features observed in the sphaerosiderite-bearing mudstone intervals suggest a polygenetic history of soil development. The striated birefringence fabrics are indicative of well-drained conditions, and extensive shrink-swell reorganization of the soil materials (Brewer 1976). Extensive color mottling, particularly the red mottles, suggest that there were periodic excursions of the water table, thus the soil experienced multiple cycles of poor and well-drained conditions (McCarthy and Plint 1998). The presence of clay coatings and infillings suggests illuvial accumulations of clay that were translocated through the soil profile (FitzPatrick 1984; McCarthy and Plint 1998). The degradation of the clay coatings and assimilation into the matrix suggests periods of prolonged landscape stability on the floodplain (McCarthy et al. 1998, 1999). The ferruginous hypocoatings observed superim-



TEXT-FIGURE 10

The illustration shows correlated well-logs from three of the cored intervals (Nunery 6-12 core, Cockerham Barron, and the Nunery-Busby core). The well logs are hung off of the top of the Lower Tuscaloosa and the cored intervals are illustrated. The dashed line indicates an interpreted stage of marine influence on the Lower Tuscaloosa depositional system where estuarine conditions may have persisted briefly within a fluvial dominated system. Unfortunately, well-logs could not be obtained for the other 2 cored intervals of the Lower Tuscaloosa Formation.

posed on the clay coatings are also indicative of cyclic wetting and drying, and fluctuating redox conditions (McCarthy et al. 1998).

The red and dark gray mottling is a redoximorphic feature where the groundmass is characterized by domains of redox (primarily iron) accumulations (red mottles), and gleyed domains of redox depletions (Vepraskas 1994; Birkeland 1999). The color mottling indicates cyclic changes in the soil moisture regime and excursions of the water table (Vepraskas 1994; Buol et al. 1997).

The gleyed colors, the abundance of sphaerosiderite, and the abundance of preserved organic matter all suggest that the paleosols were poorly drained, hydromorphic soils (Landuydt 1990; Driese et al. 1995; McCarthy et al. 1997; Ludvigson et al. 1998). The co-occurrence of pedogenic features indicative of well-drained conditions and prolonged hydromorphism suggests that the paleosols had a polygenetic history of pedogenic development. The paleosols were at first well-drained, with cyclic wetting and drying periods evidenced by the abundant clay coatings, pedogenic slickensides, and the striated matrix fabrics. The degraded clay coatings further suggests that this phase of pedogenesis was fairly long (McCarthy et al. 1998, 1999). The color mottling, rhizhaloes (Kraus and Hasiotis 2006), and ferruginous hypoc coatings all indicate excursions of the water table and fluctuating redox conditions (Vepraskas 1994). The presence of the well-preserved sphaerosiderites, extensively gleyed domains, and well-preserved organic materials suggest that the latter stages of pedogenesis were characterized by a high water table, with poorly-drained, anoxic conditions (McCarthy et al. 1998;

Ludvigson et al. 1998). The oxidation rinds on the sphaerosiderites may indicate a return to well-drained conditions, or may be the result of later diagenesis.

The evidence for a polygenetic history of pedogenesis is common in sphaerosideritebearing paleosols throughout the KWIB (McCarthy and Plint 1998; White et al. 2000; Ufnar et al. 2001, 2004, 2005). These paleosols likely mark coastal plain interfluvial landscape surfaces that developed very close to sea-level along the margins of the Cretaceous Western Interior Seaway. The polygenetic developmental history of the paleosols may reflect cumulative pedogenesis under slow, continuous sedimentation rates and changing base-level conditions (McCarthy and Plint 1998; Ufnar et al. 2001). While base-level was lower, the soils were generally well-drained and dominated by eluvial and illuvial pedogenic processes. Under conditions of rising and high base level, the paleosols became boggy wetlands characterized by saturated, reducing conditions (text-fig. 9; Ufnar et al. 2001). Periodic overbank flooding and sedimentation increases the floodplain elevation relative to the water table and leads to improved drainage conditions (Aslin and Autin 1998). Over time, the sphaerosiderite-bearing paleosols occur as amalgamated sets of paleosols and pedocomplexes developed in an aggradational coastal floodplain paleoenvironment (Ufnar et al. 2001; 2005; White et al. 2005). The amalgamated paleosols and pedocomplexes show micromorphological evidence of periodic changes in drainage conditions as the floodplain aggraded. The sphaerosiderite-bearing intervals particularly denote interfluvial domains characterized by a prolonged period of well-drained conditions followed by prolonged hydromorphism, then subsequent burial with incipient soil

TABLE 1

Palynomorph species identified from three depth intervals in the Harrell Smith #1-11 core.

Harrell Smith #1-11 Core	Early Cretaceous		
	2957 m	2947.9 m	2933.2 m
<i>Deltoidospora</i> spp. - <i>indet.</i>	•	•	●
<i>Cicatricosisporites</i> spp. - <i>indet.</i>	•	•	•
<i>Corollina torosa</i>	•	•	•
<i>Cicatricosisporites goniodontos</i>		•	•
<i>Cicatricosisporites venustus</i>		•	•
<i>bisaccate gymnosperm pollen</i> - <i>indet.</i>			●
<i>Rugubivesiculites rugosus</i>			•
<i>Rugubivesiculites reductus</i>			•
<i>Triporoletes reticulatus</i>			•
<i>Laevigatosporites</i> spp. - <i>indet.</i>			•
<i>Cicatricosisporites cf. aralicus</i>			•
<i>Tricolpites crassimurus</i>			•
<i>Rousea</i> sp. - <i>indet.</i> , small			•
<i>Deltoidospora minor</i>			•
<i>Concavissimisporites punctatus</i>			•
<i>Quadricolpites cf. cruciformis</i>			•
<i>Osmundacidites wellmanii</i>			•
<i>Taxodiaceapollenites hiatus</i>			•
<i>Foveosporites labiosus</i>			•
<i>Gleicheniidites senonicus</i>			•
<i>Densosporites</i> sp. - <i>indet.</i>			•
<i>Foveosporites</i> sp. - <i>indet.</i>		•	
<i>Lygodiosporites amboglebosus</i>		•	
<i>Echinatisporis</i> sp. - <i>indet.</i>		•	
<i>Foraminisporis asymmetricus</i>	•		

welding. Perhaps these preserved geomorphic surfaces denote stratigraphically-significant surfaces such as para-sequence boundaries (marine flooding surfaces) within a transgressive systems tract (Van Wagoner et al. 1988; Blum and Price 1998). The changing drainage conditions may have resulted from high-frequency sea-level changes coupled with increasing accommodation space and high sedimentation rates during the earliest stages of the Greenhorn Cycle of the KWIB (text-fig. 2; Kauffman and Caldwell 1993; Mancini et al. 1987; Mancini and Puckett 2005).

At times, the floodplain aggradation may have been punctuated by minor marine flooding, converting the fluvial system to an estuarine paleoenvironment. Well-logs for the Nunery Busby, Nunery 6-12, and Cockerham Barron wells show a correlation of burrowed and tidally-influenced facies (Lithofacies 6) across the area at approximately the same stratigraphic level (text-fig. 10). This correlated (marine-influenced interval) also separates the stringer sandstone Member of these cores into a lower, mudstone dominated floodplain and an upper, sandstone dominated floodplain (text-fig. 3, 10). The soil micromorphology indicates that the mudstone dominated interfluvial areas developed under cyclic changes in drainage conditions, as described above. However, the entire lithofacies assemblage suggests that there was a significant change in the rates of sediment accumulation and creation of accommodation space above vs. below the interpreted marine-influenced deposits. The mudstone-dominated portion of the Stringer Sandstone Member may have developed through increased accommodation under rising

base-level (Blum and Tornquist 2000; Schumm 1993). The depositional system was characterized by the accumulation of floodbasin mudstones and thin crevasse channel and splay sandstone bodies produced during channel avulsions (Lithofacies 2, 4, and 5; Smith et al. 1989; Blum and Tornquist 2000; Schumm et al. 2000). The thin avulsion sandstone bodies are separated by pedogenically modified mudstones and cumulative paleosols that represent alternating periods of slow, continuous sedimentation on the floodplains between avulsion events (Aslin and Autin 1998; Blum and Tornquist 2000). The marine-influenced interval may reflect a period where base-level rise or subsidence exceeded sediment accumulation rates, and minor marine inundation (estuarine) occurred (Leckie and Singh 1991). The upper, sandstone-dominated domains may have resulted from a base-level fall that lead to increased channel sinuosity, and lateral migration of channel sands due to a decrease in accommodation space (Blum and Tornqvist 2000; Schumm et al. 2000). A subsequent rise in base-level, resulted in channel and valley back-filling and eventually lead to marine inundation and deposition of the McComb Sand (Chasteen 1983; Klicman et al. 1988). The upper 1 meter of the Cockerham Barron core contains a coaly interval overlain by burrowed, wavy and lenticular-bedded sandstone (lithofacies 6). The increased marine-character at the top of this core may mark the transition from the non-marine Stringer Sandstone member to the marine McComb Sandstone (Cameron et al. 1992).

## CONCLUSIONS

(1) Sphaerosiderites within the Lower Tuscaloosa Formation paleosols yield  $\delta^{18}\text{O}$  values that are a proxy record for ancient groundwater values from paleosols that were primarily re-charged from precipitation. The siderite MSLs yield meteoric water  $\delta^{18}\text{O}$  values ranging from  $-6.80\text{‰}$  to  $-4.5\text{‰}$  (VSMOW) during the Cenomanian.

(2) The sphaerosiderite-bearing paleosols of the Lower Tuscaloosa Formation show evidence for a polygenic pedogenic history characterized by an early well-drained phase overprinted by a later phase of hydromorphism.

(3) Correlation of core lithofacies and electric well-logs from the Lower Tuscaloosa Formation suggest that the Stringer Sandstone member of the LTF developed through: (a) an initial aggradational phase characterized by a dominance of pedogenically-modified floodplain deposits composed of cumulative paleosols and pedocomplexes; capped by interbedded sandstones and mudstones with evidence of marine influence (estuarine deposits); followed by (b) a progradational phase characterized by a dominance of fluvial sandstone deposits that likely developed following a base-level fall, followed by (c) a transgressive phase characterized by deposition of the marine McComb Sandstone.

## ACKNOWLEDGMENTS

The author thanks Michael Haney for his assistance on this project and support provided by The American Chemical Society Petroleum Research Fund Grant #42251-GB2

## REFERENCES

- ASLAN, A., WHITNEY, J.A. and BLUM, M.D., 2005. Causes of River Avulsion: Insights from the Late Holocene avulsion history of the Mississippi River, USA. *Journal of Sedimentary Research* 75, 650-664.

TABLE 2  
Lithofacies descriptions

No.	Name	Descriptions	Interpretations
1	Thickly-bedded sandstones	fg-cg, well-sorted, subrnd, qtz arenite w/ minor chert, flds, and micas; large-scale cross-strat., hor. lams., minor, opaque finely-comm. organic fossil debris; units 3-6 m in thickness	Fluvial point bar and intra-channel bar deposits
2	Thinly-bedded sandstones	vfg-fg, well-sorted, rnded, qtz arenite w/ minor chert and micas; massive, to hor lams, gleyed colors common, and some faint, medium red mottles; sphaerosiderites noted in some beds; minor org. debris; individual units less than 2m thick.	floodplain crevasse splays and or/ levee deposits within a meandering or anastomosing fluvial system
3	Carbonaceous mudstone	dark blue-grey/black claystones and clayey-siltstones; friable; common well-preserved plant macrofossils; gleyed colors; rare burrows, root traces, and pedogenic slickensides, some units are coally with finely-comm charcoal particles to cm-scale carbonaceous plant fragments	floodplain backswamps or wetlands of a meandering to anastomosing fluvial system
4	Red-mottled mudstones	claystones to clayey coarse-siltstones and vfg sandstones; prominent, coarse red mottles (10R 3/3 to 3/6 Munsell colors), matrix colors are dark blue to green grey; rott traces, blocky structures, slickensides, rhizohaloes, sphaerosiderites, and clay coatings are common	moderately- to heavily-weathered floodplain deposits with evidence for pedogenic modifications
5	Purple and yellow mottled mudstones	mudstones w/ dark gray-green to blue colors, mottled with medium, to coarse, prominent red, purple, and yellow (2.5Y 4/4 to 5/6) domains; rhizohaloes, pedogenic slickensides, blocky structures and clay coatings are common.	pedogenically modified floodplain deposits with intermediate drainage conditions
6	Flaser and lenticular bedded carbonaceous muddy sandstones	vfg-fg, well-sorted, rnded, qtz arenites, interbedded w/ drk gray to black carb mudstones; flaser, lenticular, and wavy bedding. Small-scale ripple cross-strat., herringbone cross-strat, reactivation surfaces; mudstone has abundant fossil plant fragments. Some domains are burrow mottled.	tidally-influenced channel margin/overbank deposits

- BAR-MATTHEWS, M., AYALON, A., GILMOUR, M., MATTHEWS, A. and HAWKESWORTH, C.J., 2003. Sea-land oxygen isotopic relationships from planktonic foraminifera and speleothems in the Eastern Mediterranean region and their implication for paleorainfall during interglacial. *Geochimica et Cosmochimica Acta* 67:3181-3199.
- BARRON, E. J., 1983. A warm equable Cretaceous: the nature of the problem. *Earth Science Review* 19: 305-338.
- BELL, W. A., 1963. Upper Cretaceous floras of the Dunvegan, Bad Heart and Milk River formations of western Canada. *Geological Survey of Canada Bulletin* 94.
- BERG, R.R. and COOK, B.C., 1968. Petrography and origin of Lower Tuscaloosa sandstones, Mallalieu field, Lincoln County, Mississippi. *Gulf Coast Association of Geological Societies Transactions*, 18: 242-255.
- BERNER, R. A., 1981. A new classification of sedimentary environments. *Journal of Sedimentary Petrology*, 51: 359-365.
- BIRKELAND, P. W., 1999. *Soils and Geomorphology*. New York: Oxford University Press, 430 p.
- BOGGS, S., Jr., 1995. *Principles of Sedimentology and Stratigraphy, 2nd edition*. New Jersey: Prentice Hall, 774 p.
- BOWEN, G. J. and WILKINSON, B., 2002. Spatial distribution of  $\delta^{18}\text{O}$  in meteoric precipitation. *Geology*, 30: 315-318.
- BRENNER, G. J. 1963. The spores and pollen of the Potomac Group of Maryland. *Maryland Department of Geology, Mines and Water Research Bulletin* 27: 1-215.
- BREWER, R., 1964. *Fabric and Mineral Analysis of Soils*. New York: John Wiley & Sons, 470 p.
- BULLOCK, P, FEDEROFF, N., JONGERIUUS, A., STOOPS, G., TURSINA, T. and BABEL, U., 1985. Handbook for soil thin section description. England, Waine Research Publications, 152 p.
- BUOL, S. W., SOUTHARD, R. J., GRAHAM, R. C. and MCDANIEL, P. A., eds., 1997. *Soil Genesis and Classification*. Iowa City: Iowa State University Press, 494 p.
- BURNS, S. J., FLEITMANN, D., MATTER, A., NEFF, U. and MANGINI, A., 2001. Speleothem evidence from Oman for continental pluvial events during interglacial periods. *Geology*, 29: 623-626.
- BUSCH, DANIEL A., 1974. *Stratigraphic traps in sandstones – exploration techniques*. American Association of Petroleum Geologists Memoirs.

- CAMERON, C. P., PATRICK, D. M. and KEITH, C. D., 1992. Authigenic clay mineral distribution, Lower Tuscaloosa Formation, southwest Mississippi: impact on sandstone reservoir quality in the North Hustler Field area. *Transactions, Gulf Coast Association of Geological Societies* 42: 47-59.
- CAROTHERS, W. W., LANFORD, H. A. and ROSENBAUER, R. J., 1988. Experimental oxygen isotope fractionation between siderite-water and phosphoric acid liberated CO<sub>2</sub> siderite. *Geochemica et Cosmochemica Acta*, 52: 2445-2450.
- CHASTEEN, H. R., 1983. Reevaluation of the Lower Tuscaloosa and Dantzer formations (Mid-Cretaceous) with emphasis on depositional environments and time-stratigraphic relationships: *Transactions, Gulf Coast Association of Geological Societies* 33: 31-40.
- CHRISTOPHER, R. A., 1982. The occurrence of the *Complexiopollis-Atlantopollis* Zone (palynomorphs) in the Eagle Ford Group (upper Cretaceous) of Texas. *Journal of Paleontology*, 56: 525-541.
- CLIFTON, H. E., 1982. Estuarine deposits. In: Scholle, P.A. and Spearing, D., Eds., *Sandstone Depositional Environments*, 179-189. The American Association of Petroleum Geologists Memoir No. 31.
- CRIMES, T.P. and HARPER, J.C., 1970. *Trace Fossils I*. Liverpool: Steel House Press, 547 p.
- DAANSGARD, W., 1964. Stable Isotopes in Precipitation. *Tellus*, 16: 436-468.
- DALRYMPLE, R. W., 1992. Tidal depositional systems, in Walker, R. G. and Noel, J. P., Eds., *Facies Models: response to sea level change*, 195-218. St. Johns, NL: Geological Association of Canada.
- DAVIS, R. A. Jr., Editor, 1985. *Coastal Sedimentary Environments*. New York: Springer Verlag, 716 p.
- DECONTO, R. M., BRADY, E. C., BERGENGREN, J. and HAY, W.W., 2000. Late Cretaceous climate, vegetation and ocean interactions. In: Huber, B. T., MacCleod, K. G. and Wing, S. L., *Warm Climates in Earth History*. Cambridge: Cambridge University Press.
- DEMOWBRAY, T. and VISSER, M.J., 1984. Reactivation surfaces in subtidal channel deposits, Oosterschelde, southwest Netherlands. *Journal of Sedimentary Petrology* 54: 811-824.
- DENNISTON, R. F., GONZALEZ, L. A., ASMEROM, Y., BAKER, R. G., REAGAN, M. K. and BETTIS, E. A., III, 1999a. Evidence for increased cool season moisture during the middle Holocene. *Geology* 27: 815-818.
- DENNISTON, R. F., GONZALEZ, L. A., BACKER, R. G., ASMEROM, Y., REAGAN, M. K., EDWARDS, R. L. and ALEXANDER, E. C., 1999b. Speleothem evidence for Holocene fluctuation of the prairie-forest ecotone, north-central USA. *The Holocene* 9: 671-676.
- DENNISTON, R. F., GONZALEZ, L. A., ASMEROM, Y., POLYAK, V., REAGAN, M. K. and SALTZMAN, M. R., 2001. A high-resolution speleothem record of climatic variability at the Allerod-Younger Dryas transition in Missouri, central United States. *Palaeogeography Palaeoclimatology Palaeoecology* 176: 147-155.
- DORALE, J. A., GONZALEZ, L. A., REAGAN, M. K., BAKER, R. G., PICKETT, D. A. and MURRELL, M. T., 1992. A high resolution record of Holocene climate changes in speleothem calcite from Coldwater Cave, northeast Iowa. *Science*, 258: 1626-1630.
- DUCHAFOR, P., 1982. *Pedology*. London: Allen and Unwin, 443 p.
- DUNN, D. A., COOLEY, U. and PETTWAY, C., 1985. "Micropaleontology of selected samples from wells in the Lower Tuscaloosa Formation in the McComb, Sand Hill and Stewart Fields, Mississippi." Unpublished report submitted to ARCO Exploration Company, Southeastern Region, USA.
- DRIESE, S. G., SIMPSON, E. L. and ERIKSSON, K. A., 1995. Redoximorphic paleosols in alluvial and lacustrine deposits, 1.8 Ga Lochness Formation, Mount Isa, Australia: pedogenic processes and implications for paleoclimate. *Journal of Sedimentary Research* A65: 675-689.
- EISENSTATT, P., 1960, Little Creek Field, Lincoln and Pike counties, Mississippi. *Transactions, Gulf Coast Association of Geological Societies* 10: 207-213.
- FANNING, D. S. and FANNING, M. C. B., 1989. *Soil: Morphology, Genesis and Classification*. New York: John Wiley and Sons, 395 p.
- FARNHAM, T. M. and KRAUS, M. J., 2002. The stratigraphic and climatic significance of Paleogene alluvial paleosols in synorogenic strata of the Denver basin, CO. *Rocky Mountain Geology* 37: 201-213.
- FITZPATRICK, E. A., 1984. *Micromorphology of Soils*. New York: Chapman and Hall, 433 p.
- FRAKES, L. A., 1979. *Climates Throughout Geologic Time*. New York: Elsevier, 310 pp.
- FRAKES, L. A., FRANCIS, J. E. and SYKTUS, J. I., 1992. *Climate modes of the Phanerozoic: the history of the earth's climate over the last 600 million years*. Cambridge: Cambridge University Press.
- FRUMKIN, A., CARMİ, I., GOPHER, A., FORD, D. C., SCHWARCZ, H. P. and TSUK, T., 1999. A Holocene millennial-scale climatic cycle from a speleothem in Nahal Qanah Cave, Israel. *The Holocene*, 9:677-682.
- GROCKE, D. R., LUDVIGSON, G. A., WITZKE, B. J., ROBINSON, S. A., JOECKEL, R. M., UFNAR, D. F. and RAVN, R. L., 2006. Recognizing the Albian-Cenomanian (OAE1 d) sequence boundary using plant carbon isotopes. Dakota Formation, Western Interior Basin, USA. *Geology* 34: 193-196.
- HAMILTON, W. S. and CAMERON, C. P., 1987. Facies relationships and depositional environments of the Lower Tuscaloosa Formation reservoir sandstones in McComb and Little Creek Field areas, southwest Mississippi. Gulf Coast Association of Geological Societies and Gulf Coast Section of SEPM Meeting, Baton Rouge, LA. *American Association of Petroleum Geologists Bulletin* 70: 1182.
- HORVANTINÈÏÈ, N., BRONIC, I. K. and OBELIC, B., 2003. Differences in the 14C age, δ<sup>14</sup>C and δ<sup>18</sup>O of Holocene tufa and speleothem in the Dinaric Karst. *Palaeogeography Palaeoclimatology, Palaeoecology*, 193: 139-157.
- JOECKEL, R. M., 1995. Tectonic and paleoclimatic significance of a prominent Upper Pennsylvanian (Virgillain/Stephanian) weathering profile, Iowa and Nebraska, USA. *Palaeogeography, Palaeoclimatology, Palaeoecology*, 118: 159-179.
- KAMPF, N. and SCHWETERMANN, U., 1982. Goethite and hematite in a climosequence in southern Brazil and their application in classification of kaolinitic soils. *Geoderma*, 29: 27-39.

- KAUFFMAN, E. G. and CALDWELL, W. G. E., 1993. The Western Interior Basin in space and time. In: Caldwell, W. G. E. and Kauffman, E. G., Eds., *Evolution of the Western Interior Basin*, 1-30. Geological Association of Canada Special Paper 39.
- KOPPELHUS, E. B. and PEDERSEN, G. K. 1993. A palynological and sedimentological study of Cretaceous floodplain deposits of the Atane Formation at Skansen and Igdlunguaq, West Greenland. *Cretaceous Research*, 14: 707-734.
- KRAUS, M. J. and ASLAN, A., 1993. Eocene hydromorphic paleosols: significance for interpreting ancient floodplain processes. *Journal of Sedimentary Petrology*, 63: 453-463.
- KRAUS, M. J. and HASIOTIS, S. T., 2006. Significance of different modes of rizo lith preservation to interpreting paleoenvironmental and paleohydrologic settings: Examples from paleogene paleosols, Bighorn Basin, Wyoming, U.S.A. *Journal of Sedimentary Research*, 76: 633-646.
- KVALE, E. P. and ARCHER, A. W., 1990. Tidal deposits associated with low-sulphur coals, Brazil Formation (Lower Pennsylvanian), Indiana. *Journal of Sedimentary Petrology* 60: 563-574.
- KVALE, E. P. and ARCHER, A. W., 1991. Characteristics of two Pennsylvanian-age semidiurnal tidal deposits in the Illinois Basin, USA. *Canadian Society of Petroleum Geologists Memoirs* 16: 179-188.
- LACHNIET, M. S., ASMEROM, Y., BURNS, S. J., PATTERSON, W. P., POLYAK, V. J. and SELTZER, G. O., 2004. Tropical response to the 8200 yr B.P. cold event? Speleothem isotopes indicate a weakened early Holocene monsoon in Costa Rica. *Geology* 32: 957-960.
- LANDUYDT, C. J., 1990. Micromorphology of iron minerals from bog ores of the Belgian Campine area, in Douglas, L.A., ed., *Soil Micromorphology: A basic and applied science. Developments in Soil Science*, 19: 289-294.
- LINGE, H., LAURITZEN, S.-E., LUNDBERG, J. and BERSTAD, I. M., 2001. Stable isotope stratigraphy of Holocene speleothems; examples from a cave system in Rana, Northern Norway. *Palaeogeography Palaeoclimatology Palaeoecology* 167: 209-224.
- LOHMANN, K.C., 1988. Geochemical patterns of meteoric diagenetic systems and their application to studies of paleokarst. In: James, N. P. and Choquette, P. W., Eds., *Paleokarst*, 58-80. Berlin: Springer Verlag.
- LUDVIGSON, G. A., GONZALEZ, L. A., METZGER, R. A., WITZKE, B. J., BRENNER, R. L., MURILLO, A. P., WHITE, T. S., 1998. Meteoric sphaerosiderite lines and their use for paleohydrology and paleoclimatology. *Geology*, 26: 1039-1042.
- MACEDO, J. and BRYANT, R. B., 1987. Morphology, mineralogy and genesis of a hydrosequence of Oxisols in Brazil: *Soil Science Society of America Journal*, 51: 690-698.
- , 1989. Preferential microbial reduction of hematite over goethite in a Brazilian Oxisol. *Soil Science Society of America Journal*, 53: 1114-1118.
- MANCINI, E. A., MINK, R. M., PAYTON, J. W. and BEARDEN, B. L., 1987. Environments of deposition and petroleum geology of Tuscaloosa Group (Upper Cretaceous) South Carlton and Pollard Fields, southwestern Alabama. *American Association of Petroleum Geologists Bulletin*, 71: 1128-1142.
- MCCARTHY, P. J. and PLINT, A. G., 1998. Recognition of interfluvial sequence boundaries: Integrating paleopedology and sequence stratigraphy. *Geology*, 26: 387-390.
- , 1999. Floodplain paleosols of the Cenomanian Dunvegan Formation, Alberta and British Columbia, Canada: Micromorphology, pedogenic processes and paleoenvironmental implications. In: Marriot, S.B. and Alexander, J., Eds., *Floodplains: Interdisciplinary approaches*, 289-310. Geological Society of America Special Paper 163.
- MCCARTHY, P. J., FACCINI, U. and PLINT, A. G., 1999b. Evolution of an ancient coastal plain: paleosols, interfluvial and alluvial architecture in a sequence stratigraphic framework, Cenomanian Dunvegan Formation, NE British Columbia, Canada. *Sedimentology*, 46: 861-892.
- MCCARTHY, P.J., MARTINI, I.P. and LECKIE, D.A., 1998. Pedogenic and diagenetic influences on void coating formation in Lower Cretaceous paleosols of the Mill Creek Formation, southwestern Alberta, Canada. *Geoderma*, 87: 209-237.
- MCCARTHY, P. J., MARTINI, I. P. and PLINT, A. G., 1999a. Pedogenic and diagenetic influences on void coating formation in Lower Cretaceous paleosols of the Mill Creek Formation, southwestern Alberta, Canada. *Geoderma*, 87: 209-237.
- MIALL, A. D., 1981. Facies models for meandering rivers. *American Association of Petroleum Geologists Special Volume A148*, 32-38. Tulsa: American Association of Petroleum Geologists.
- , 1992. Alluvial deposits. In: Walker, R.G. and Noel, J.P., Eds., *Facies Models: response to sea level change*, 119-142. St. Johns, NL: Geological Association of Canada.
- , 1977. A review of the braided river depositional environment. *Earth Science Review*, 13:1-62.
- MEYLAN, M. A., CAMERON, C. P., PATRICK, D. M. and KEITH, C. D., 1990. *Authigenic clay mineral distribution Lower Tuscaloosa Formation, Southwest Mississippi: Impact on sandstone reservoir quality, north Hustler Field area*. Final Report, MMRI Grant No. 90-2F, Bureau of Mines Grant No. G1184128, Mississippi Mineral Research Institute, The University of Southern Mississippi.
- NIGGEMANN, S., MANGINI, A., RICHTER, D.K. and WURTH, G., 2003a. A paleoclimate record of the last 17,600 years in stalagmites from the B7 cave, Sauerland, Germany: *Quaternary Science Review*, 22: 555-567.
- NIGGEMANN, S., MANGINI, A., MUDELSEE, M., RICHTER, D. K. and WURTH, G., 2003b. Sub-Milankovitch climatic cycles in Holocene stalagmites from Sauerland, Germany. *Earth and Planetary Science Letters* 216: 539-547.
- NORRIS, G., 1967. Spores and pollen from the lower Colorado Group (Albian-Cenomanian) of central Alberta. *Palaeontographica B*, 120: 73-115.
- ONAC, B. P., CONSTANTIN, S., LUNDBERG, J. and LAURITZEN, S.-E., 2002. Isotopic climate record in a Holocene stalagmite from Ursilor Cave (Romania). *Journal of Quaternary Science* 17: 319-327.
- PARRISH, J. T. and SPICER, R. A., 1989. Flora of the Dunvegan Formation (Cenomanian, British Columbia) and comparison with the flora of the Niakogon tongue of the Chandler Formation (Cenomanian, Alaska). *Geological Society of America, Abstracts and Program*, 21: A147.
- PESSAGNO, E. A., Jr., 1967. Upper Cretaceous planktonic Foraminifera from the western Gulf Coastal Plain. *Paleontographica Americana*, 5: 245-445.

- PHILLIPS, P. P. and FELIX, C. J., 1972. A study of lower and middle Cretaceous spores and pollen from the southeastern United States, I. Spores. *Pollen and Spores*, 13: 279-348.
- PLAYFORD, G., 1971. Palynology of Lower Cretaceous (Swan River) strata of Saskatchewan and Manitoba. *Palaeontology*, 14: 533-565.
- PLINT, A. G., 1996. Marine and nonmarine systems tracts in fourth-order sequences in the Early-Middle Cenomanian, Dunvegan Alloformation, northeastern British Columbia, Canada. In: Howell, J. A. and Aitken, J. F., Eds., *High resolution sequence stratigraphy: innovations and applications*, 159-191. Geological Society of London Special Publication 104.
- RAVN, R. L. 1995. Miospores from the Muddy Sandstone (upper Albian), Wind River Basin, Wyoming, U.S.A. *Palaeontographica B.*, 234:41-91.
- REINSON, G. E., 1992. Transgressive barrier island and estuarine systems. In: Walker, R. G. and Noel, J. P., Eds., *Facies Models: response to sea level change*, 179-194. Geological Association of Canada.
- RICHARDSON, J. L. and HOLE, F. D., 1979. Mottling and Iron distribution in a Glossoburalf-Haplaquill hydrosequence on a glacial moraine in northwestern Wisconsin. *Soil Science Society of America Journal*, 14: 552-558.
- SCHWETERMANN, U. and FANNING, D.S., 1976. Iron Manganese concretions in hydrosequence of soils in loess in Bavaria. *Soil Science Society of America Journal* 40: 731-738.
- SCOTESE, C. R., 2005. *Cretaceous paleogeography*. www.scotese.com
- SCULL, B. J., FELIX, C. J., MCCALED, S. B. and SHAW, W. G., 1966. The interdisciplinary approach to paleoenvironmental interpretations. *Transactions, Gulf Coast Association of Geological Societies* 16: 81-117.
- SIMONSON, G. H. and BOERSMA, L., 1972. Soil geomorphology and water table relations II: correlations between annual water table fluctuations and profile features. *Soil Science Society of America Proceedings* 36: 649-655.
- SINGH, C., 1971. Lower Cretaceous microfloras of the Peace River area, northwestern Alberta. *Research Council of Alberta Bulletin* 28: 1-542.
- SLOAN, L. C. and BARRON, E. J., 1990. "Equable" climate during Earth history? *Geology*, 18: 489-492.
- SMITH, D.G. and PUTNAM, P.E., 1980. Anastomosed River Deposits: modern and ancient examples in Alberta, Canada: *Canadian Journal of Earth Science*, 17: 1396-1406.
- SPICER, R. A and CORFIELD, R. M., 1992. A review of terrestrial and marine climates in the Cretaceous with implications for modeling the "Greenhouse Earth". *Geological Magazine*, 129: 169-180.
- SPICER, R.A. and PARRISH, J.T., 1990. Late Cretaceous-early Tertiary palaeoclimates of northern high latitudes: a quantitative review: *Geological Society of London Journal*, 147: 329-341.
- SRIVASTAVA, S. K. 1977. Microspores from the Fredericksburg Group (Albian) of the southern United States. *Paléobiologie Contributions*, 6: 1-119.
- STOLT, M. H., OGG, C. M. and BAKER, J. C., 1994. Strongly contrasting redoximorphic patterns in Virginia valley and ridge paleosols. *Soil Society of America Journal* 58: 477-484.
- TREBLE, P. C., CHAPPELL, J., GAGAN, M. K., MCKEEGAN, K. D. and HARRISON, T. M., 2005. In situ measurement of seasonal  $\delta^{18}\text{O}$  variations and analysis of isotopic trends in a modern speleothem from southwest Australia. *Earth and Planetary Science Letters*, 233: 17-32.
- UFNAR, D. F., GONZALEZ, L. A., LUDVIGSON, G. A., BRENNER, R. L., WITZKE, B. J., 2004a. High latitude meteoric  $\delta^{18}\text{O}$  compositions: Paleosol siderite in the middle Cretaceous Nanishuk Formation, North Slope, Alaska. *Geological Society of America Bulletin*, 116: 463-473.
- , 2004b. Diagenetic overprinting of the sphaerosiderite paleoclimate proxy: are records of pedogenic groundwater  $\delta^{18}\text{O}$  values preserved? *Sedimentology*, 51: 127-144.
- , 2004c. Evidence for increased heat transport during the Cretaceous (Albian) greenhouse warming. *Geology*, 32: 1049-1052.
- UFNAR, D. F., GONZALEZ, L. A., LUDVIGSON, G. A., BRENNER, R. L., WITZKE, B. J., 2002. The mid-Cretaceous water-bearer: Isotope mass balance quantification of the Albian hydrologic cycle. *Paleogeography Paleoclimatology Paleoecology*, 188:51-71.
- UFNAR, D. F., GONZALEZ, L. A., LUDVIGSON, G. A., BRENNER, R. L., WITZKE, B. J., 2001. Stratigraphic implications of meteoric sphaerosiderite  $\delta^{18}\text{O}$  compositions in paleosols of the Cretaceous (Albian) Boulder Creek Formation, NE British Columbia Foothills, Canada. *Journal of Sedimentary Research* 71:1017-1028.
- UPCHURCH, G. R. and WOLFE, J. A., 1993. Cretaceous vegetation of the Western Interior and adjacent regions of North America. In: Caldwell, W. G. E. and Kauffman, E. G., Eds., *Evolution of the Western Interior Basin*, 243-282. Geological Association of Canada. Special Paper 39.
- UPCHURCH, G. R. and WOLFE, J. A., 1987. Mid-Cretaceous to early Tertiary vegetation and climate: evidence from fossil leaves and woods. In: Friis, E. M., Chaloner, W. C. and Crane, P. R., Eds., *The origin of Angiosperms and their biological consequences*, 77-103. Cambridge: Cambridge University Press.
- VAN WAGONER, J. C., POSAMENTIER, H. W., MITCHUM, Jr., R. M., SARG, J. F., LOUTIT, T. S. and HARDENBOL, J., 1988. An overview of the fundamentals of sequence stratigraphy and key definitions. In: Wilgus, C. K., Hastings, B. S., Ross, C. A., Posamentier, H. W., Van Wagoner, J. C. and St. C. Kendall, C. G., Eds., *Sea-level changes: and integrated approach*, 39-45. SEPM Society for Sedimentary Geology Special Publication No. 42.
- VEPRASKAS, M. J., 1994. Redoximorphic features for identifying aquatic conditions. *North Carolina Agricultural Research Survey, Technical Bulletin* 30, 33 p.
- WANG, X., AULER, A. S., EDWARDS, R. L., CHENG, H., ITO, E. and SOLHEID, M., 2006. Interhemispheric anti-phasing of rainfall during the last glacial period. *Quaternary Science Reviews*, 25: 3391-3403.
- WARD, C. R., Editor, 1984. *Coal geology and coal technology*. Oxford: Blackwell, 345 p.
- WATKINS, H. V., Jr., 1962. "A subsurface study of the Lower Tuscaloosa Formation (Cretaceous) in southern Mississippi." Unpublished M.S. Thesis, University of Oklahoma, 58p.
- WHITE, T. S., WITZKE, B. J., LUDVIGSON, G. A., BRENNER, R. L., GONZALEZ, L. A., RAVN, R. L., 2000. The paleoclimatological significance of Albian (middle Cretaceous) sphaerosiderites from eastern Saskatchewan and western Manitoba:

- Summary of Investigations 2000, v. 1: *Saskatchewan Geological Survey Misc. Report* 2000-4. 1, 63-75.
- WHITE, T. S., WITZKE, B. J., LUDVIGSON, G. A. and POULSON, C., 2001. The mid-Cretaceous greenhouse hydrologic cycle of North America. *Geology*, 29: 363-366.
- WHITE, T. S., WITZKE, B. J., LUDVIGSON, G. A., BRENNER, R. L., 2005. Distinguishing base-level change and climate signals in a Cretaceous alluvial sequence. *Geology*, 33: 13-16.
- WILDING, L. P. and TESSIER, D., 1998. Genesis of vertisols: shrink-swell phenomena. In: Wilding, L. P. and Puente, R., Eds., *Vertisols: their distribution, properties, classification and management*, 205-225. College Station: Texas A&M, Technical Monographs 18.
- WILLIAMS, P. W., KING, D. N. T., ZHAO, J.-X. and COLLERSON, K. D., 2005. Late Pleistocene to Holocene composite speleothem  $^{18}\text{O}$  and  $^{13}\text{C}$  chronologies from South Island, New Zealand—did a global Younger Dryas really exist? *Earth and Planetary Science Letters*, 230:301-317.
- WINGATE, F. H. 1980. Plant microfossils from the Denton Shale Member of the Bokchito Formation (Lower Cretaceous, Albian) in southern Oklahoma. *Oklahoma Geological Survey Bulletin* 130: 1-93.
- WITZKE, B. J., 2003. Interpretations of North American Cretaceous dinosaur diversity trends. *Journal of Vertebrate Paleontology*, 23: 112A.
- WOLFE, J. A. and UPCHURCH, G. R., 1987. North American non-marine climates and vegetation during the Late Cretaceous: *Palaeogeography Palaeoclimatology Palaeoecology*, 61: 33-77.
- WRIGHT, V. P., TAYLOR, K. G. and BECK, V. H., 2000. The paleohydrology of Lower Cretaceous seasonal wetlands, Isle of Wight, southern England. *Journal of Sedimentary Research*, 70, 619-632.
- YUAN, D., CHENG, H., EDWARDS, R. L., DYKOSKI, C. A., KELLY, M. J., ZHANG, M., QING, J., LIN, Y., WANG, Y., WU, J., DORALE, J. A., AN, Z. and CAI, Y., 2004. Timing, duration and transitions of the Last Interglacial Asian Monsoon. *Science*, 304: 575-578.

Manuscript received August 22, 2006

Manuscript accepted March 5, 2007

# Conodont taxonomy and the recognition of the Frasnian/Famennian (Upper Devonian) Stage Boundary

Gilbert Klapper

1010 Eastwood Road, Glencoe, IL 60022

email: g-klapper@northwestern.edu

---

**ABSTRACT:** The boundary-stratotype for the base of the Famennian Stage at Coumiac in the Montagne Noire, southern France, was defined so as to coincide with the lower boundary of the Lower *triangularis* conodont zone. The definition of that biostratigraphic zone has to be modified in light of the present taxonomic distinction between *Palmatolepis triangularis* and a closely related species, *P. ultima*. As a result, *P. triangularis* no longer first occurs at the base of its nominal zone, but enters up within the zone. A revision of the lower boundary of the Lower *triangularis* Zone, defined by the flood occurrence of *P. ultima* immediately above the end-Frasnian conodont extinction event, is recommended and does not alter the boundary-stratotype (GSSP) in any way. The focus of the paper is the taxonomic distinction of two pairs of *Palmatolepis* species that have been widely confused in the literature and that affect the recognition of the Frasnian/Famennian boundary.

---

## INTRODUCTION

Two pairs of conodont species, *Palmatolepis ultima* - *P. triangularis* and *P. bogartensis* - *P. winchelli* have commonly been confused in much of the Devonian conodont literature. This is not only a taxonomic problem but also a consequential matter for biostratigraphy. Also, in the instance of the first pair it is ultimately a matter of concern for the chronostratigraphic definition of the Frasnian/Famennian Stage boundary. The purpose of this paper is to resolve the taxonomic differences between both pairs of species, which is necessary for a better understanding of the biostratigraphy and chronostratigraphy across this boundary. A third pair of species, *P. subperlobata* - *P. lobicornis*, has also been commonly confused in the past and their taxonomic distinction (Schülke 1995; 1999) is important for the biostratigraphy of the F/F boundary.

## BIOSTRATIGRAPHY AND CHRONOSTRATIGRAPHY OF THE FRASNIAN/FAMENNIAN STAGE BOUNDARY

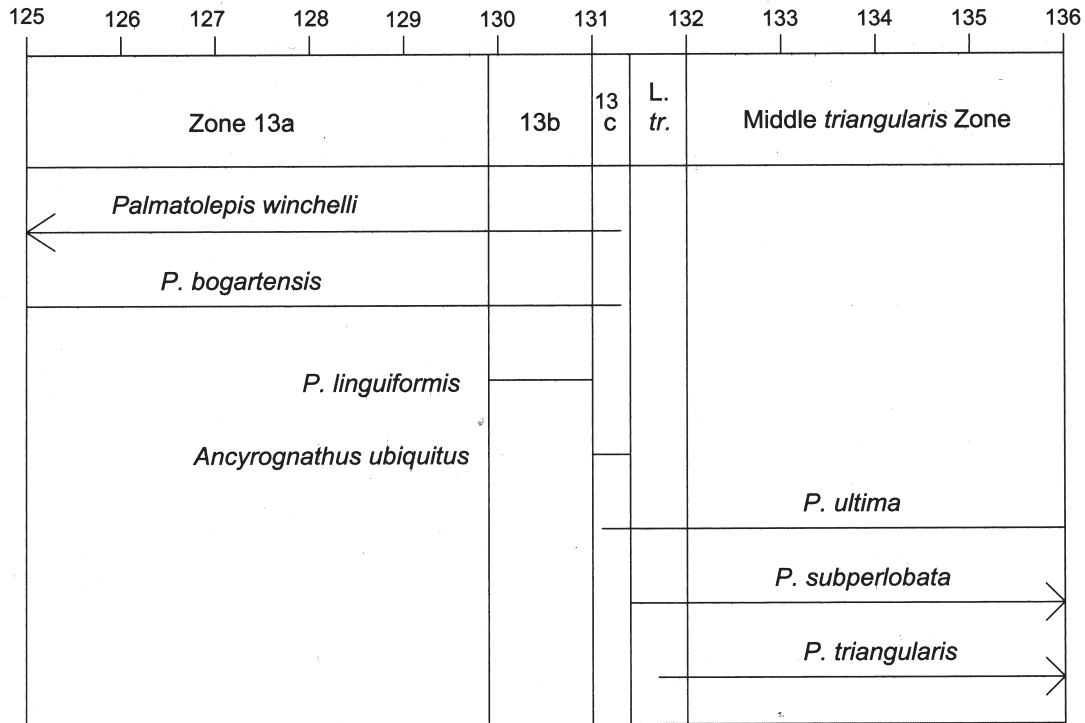
The formal chronostratigraphic definition of the Frasnian/Famennian Stage boundary was proposed by the Subcommittee on Devonian Stratigraphy in 1991 with the Global Stratigraphic Section and Point (GSSP) drawn at the base of Bed 32a in the Upper Devonian section at the Upper Coumiac Quarry in the Montagne Noire, southern France. The GSSP at Coumiac was chosen to coincide with the lower boundary of the Lower *triangularis* conodont Zone, as it was then understood. This was after agreement was reached on the biostratigraphic level of the boundary by the Subcommittee in 1989 (Klapper et al. 1994; House et al. 2000). Following these proposals, the recommended GSSP for the base of the Famennian Stage was ratified by the International Commission on Stratigraphy and the IUGS in 1993.

The lower boundary of the Lower *triangularis* Zone [common practice in Devonian conodont biostratigraphy has been to use only the species names for zones, as in the case of Jurassic ammonite zones] was originally defined on the first occurrence of *Palmatolepis triangularis* (Ziegler 1962; Ziegler and Sandberg 1990). This was predicated on an uncontroversial taxo-

nomic understanding of this species up to the time of the cited decisions on the GSSP. However, with the introduction of a closely related species, *Palmatolepis praetriangularis*, the taxonomy became complicated because some authors treated it as a separate species, while others regarded it as a junior synonym of *P. triangularis*. The present understanding of the taxonomy is discussed in detail by Klapper et al. (2004, p. 382-383) and in the Taxonomy section herein.

The importance for biostratigraphy and the chronostratigraphic definition of the GSSP is that *Palmatolepis ultima* [the senior synonym of *P. praetriangularis*] first occurs in the uppermost Frasnian Zone 13c (Girard et al. 2005), equivalent to the Upper *linguiformis* Zone as defined by Sandberg et al. (2002). *Palmatolepis ultima* ranges through the Frasnian/Famennian (F/F) conodont extinction event into the Lower *triangularis* Zone, where it occurs in flood abundance dominating a low-diversity conodont fauna immediately above the F/F boundary. Consequently *P. triangularis*, in the restricted sense required by the recognition of *P. ultima* as a separate species, does not first occur until up within the Lower *triangularis* Zone (text-fig. 1), rather than at the base of the zone (Girard et al. 2005, p. 190). A revision of the zone is required if one holds the view that the nominal species of a zone must by definition first occur at its base. Although many Upper Devonian conodont zones have been defined in this way, it is not obligatory.

Thus, a redefinition of the Lower *triangularis* Zone characterized by the flood occurrence of *P. ultima* immediately above the F/F conodont extinction event has been suggested by Klapper et al. (2004, p. 376-377; also earlier but with different nomenclature by Klapper et al. 1994, p. 436-437; Schülke 1999, p. 11) and is advocated herein. Using such an acme has been criticized on the grounds that it may be unreliable for correlation (Dzik 2002, p. 636) presumably because such an occurrence may only be a local ecologic effect. However, all F/F boundary sections published so far show the flood occurrence of *P. ultima* directly above the highest occurrence of the characteristic upper Frasnian species. The validity of using this acme for biostrati-



TEXT-FIGURE 1

Ranges of the six species of *Palmatolepis* discussed in this paper and *Ancyrognathus ubiquitous*, scaled against the Composite Standard (Klapper et al. 1995; Klapper 1997; updated herein). Only species discussed in the text are shown. The Frasnian/Famennian boundary is at the contact between Frasnian Zone 13c and the base of the Lower triangularis Zone. The latter horizon is defined by the flood occurrence of *P. ultima* directly above the Frasnian/Famennian boundary and is characterized by the first occurrence of *P. subperlobata*. The lowest occurrence of *P. triangularis* is up within the Lower triangularis Zone. Frasnian Zone 13 is subdivided into three units (Girard et al. 2005). Abbreviation L. tr. = Lower triangularis Zone. Arrows indicate range extensions.

graphic correlation, has been supported by graphic correlation. Additionally, the lowest occurrence of *P. subperlobata* Branson and Mehl 1934 characterizes the lower boundary of the Lower triangularis Zone, but the species is too rare to use as the defining criterion. In summary, the effect of the proposed revision does not change the GSSP in any way, as it still coincides with the base of the revised Lower triangularis Zone.

Biostratigraphic correlation beyond the GSSP at Coumiac and other Montagne Noire sections can use the revised definition of the Lower triangularis Zone effectively. For example, in all of the sections that cross the F/F boundary in the Canning Basin of Western Australia, the impoverished fauna dominated by *Palmatolepis ultima* and the first occurrence of *P. subperlobata* lies directly above the uppermost Frasnian conodont fauna of Zone 13c (Girard et al. 2005; Klapper 2007). *Palmatolepis subperlobata* has been overlooked previously in most conodont analyses of the F/F boundary, perhaps because the name of this early Famennian species has been incorrectly applied to a later and more often illustrated Famennian species, *P. lobicornis*. For the distinction between *P. subperlobata* and *P. lobicornis*, see Schülke (1999, p. 50-51) and Klapper et al. (2004, p. 382).

#### Uppermost Frasnian conodont zone

Directly below the impoverished fauna dominated by *Palmatolepis ultima*, marking the base of the Lower triangularis Zone (and the base of the Famennian), is another impoverished fauna in this case dominated by *P. bogartensis*. This latter fauna defines the uppermost Frasnian conodont zone, Zone 13c (Girard

et al. 2005, p. 190). In addition to the dominance of *P. bogartensis*, the lowest and generally rare occurrences of *P. ultima* and *Ancyrognathus ubiquitous* Sandberg, Ziegler, and Dreesen 1988a, characterize Zone 13c (text-fig. 1). The lowest occurrence of *Palmatolepis linguiformis* Müller 1956, defines the subjacent Zone 13b, but this species does not range into Zone 13c. Zone 13b is characterized by a diversity of other species of *Palmatolepis* and correlates with the Lower linguiformis Zone, whereas Zone 13c correlates with the Upper linguiformis Zone of Sandberg et al. (2002). It is the view here that many of the identifications of *P. winchelli* in Zone 13c result from misidentification and refer instead to one of the morphotypes of *P. bogartensis* (see discussion in Taxonomy and Table 1), although *P. winchelli* may occur rarely in some sections.

#### Criticism of the Frasnian/Famennian GSSP

The GSSP for the Frasnian/Famennian boundary at the Upper Coumiac Quarry in the Montagne Noire has been criticized on the grounds that "the F/F boundary stratotype at Coumiac is highly condensed and contains numerous hardgrounds, and the GSSP has been fixed surprisingly at the top of a hardground!" (Casier et al. 2006). Nevertheless, the hardgrounds within the Frasnian at Coumiac all prove to be intrazonal in terms of the conodont zonation (Klapper 1989) and the hardground at the GSSP (between beds 31g and 32a, House et al. 2000, fig. 4) does not appear to represent a significant amount of time lost in terms of the available geological resolution. This is because graphic correlation of the Upper Coumiac Quarry against a

TABLE 1  
Morphotypes of *Palmatolepis bogartensis*, as identified in the conodont literature.

Morphotype of <i>P. bogartensis</i>	Identification in literature	Reference
B	<i>Palmatolepis</i> sp. A	Klapper and Foster, 1986, pl. 1, fig. 4
B	<i>Palmatolepis bogartensis</i>	Klapper, 1989, pl. 2, fig. 7
C	<i>P. bogartensis</i>	Klapper, 1989, pl. 2, fig. 8
C	<i>Palmatolepis rotunda</i>	Ziegler and Sandberg, 1990, pl. 10, figs. 1, 3
B	<i>P. rotunda</i>	Ziegler and Sandberg, 1990, pl. 10, figs. 2, 4, 5
B	<i>Palmatolepis subrecta</i>	Ziegler and Sandberg, 1990, pl. 11, fig. 10
B	<i>P. subrecta</i>	Krejci, 1991, pl. 14, figs. 1, 2
B	<i>P. subrecta</i>	Luppold, 1991, pl. 8, fig. 12
B	<i>P. rotunda</i>	Matyja, 1993, pl. 22, fig. 1
A	<i>P. bogartensis</i>	Klapper and Foster, 1993, fig. 13.4, 13.15
B	<i>P. bogartensis</i>	Klapper and Foster, 1993, fig. 13.5-13.7, 13.11, 13.12, 13.14, 13.16
C	<i>P. bogartensis</i>	Klapper and Foster, 1993, fig. 13.8-13.10, 13.13
C	<i>P. rotunda</i>	Matyja and Narkiewicz, 1995, pl. 1, fig. 6
B	<i>P. subrecta</i>	Matyja and Narkiewicz, 1995, pl. 2, fig. 3
A?	<i>P. bogartensis</i>	Klapper, Kuz'min, and Ovnatanova, 1996, fig. 8.6
B	<i>P. bogartensis</i>	Schülke, 1997, pl. 3, figs. 1-4
B	<i>P. bogartensis</i>	Over, 1997, fig. 6.14, 6.15
A	<i>P. subrecta</i>	Schindler, Schülke, and Ziegler, 1998, pl. 5, figs. 27-29
B	<i>Palmatolepis hassi</i>	Schindler, Schülke, and Ziegler, 1998, pl. 4, fig. 23, pl. 5, fig. 31
A	<i>P. rotunda</i>	Bultynck, Helsen, and Hayduckiewich, 1998, pl. 4, figs. 5, 7, 8
B	<i>P. rotunda</i>	Bultynck, Helsen, and Hayduckiewich, 1998, pl. 4, figs. 4, 6, 9
C	<i>P. rotunda</i>	Bultynck, Helsen, and Hayduckiewich, 1998, pl. 4, figs. 1-3, 11?
A?	<i>P. rotunda</i>	Lazreq, 1999, pl. 9, figs. 7-9
B?	<i>P. rotunda</i>	Lazreq, 1999, pl. 9, fig. 5
B	<i>P. hassi</i>	Lazreq, 1999, pl. 8, figs. 1, 2
B	<i>P. bogartensis</i>	Schülke, 1999, pl. 3, figs. 1, 2, text-fig. 16 (Pa)
A	<i>Palmatolepis winchelli</i>	Schülke, 1999, pl. 9, figs. 2-4
B	<i>P. bogartensis</i>	Over and Rhodes, 2000, fig. 4.4, 4.5
C	<i>P. rotunda</i>	Morrow, 2000, pl. 2, fig. 1
A	<i>P. rotunda</i>	Gouwy and Bultynck, 2000, pl. 2, fig. 11
C	<i>P. rotunda</i>	Gouwy and Bultynck, 2000, pl. 2, figs. 10? (juv.), 12
B	<i>Lagovilepis bogartensis</i>	Dzik, 2002, figs. 41c, d, f, k, 42c, d
B	<i>P. bogartensis</i>	Klapper, Uyeno, Armstrong, and Telford, 2004, fig. 6.14
B	<i>P. bogartensis</i>	Klapper, 2007, fig. 1.1
C	<i>P. bogartensis</i>	Klapper, 2007, fig. 1.2

Frasnian Composite Standard (Klapper et al. 1995, p. 180-181, fig. 5; Klapper 1997, p. 114-115, fig. 2) demonstrates that there is no faunal break in the conodont sequence across the F/F boundary stratotype.

The conodont zonation at Coumiac is as complete as the section that competed for the GSSP, Steinbruch Schmidt in the Kellerwald of the Rhenish Slate Mountains, Germany (Sandberg et al. 1988b, fig. 7). At Steinbruch Schmidt there is also a sedimentological break at the F/F boundary: at the contact between Bed 16, which has a conodont fauna of Frasnian Zone 13c (= Upper *linguiformis* Zone), and Bed A (Sandberg et al. 1988b, fig. 7 and table 1) of the Lower *triangularis* Zone. It is likely that all preserved marine sections have a sedimentological break at the F/F boundary, as this was a time of a significant global eustatic sea-level fall (Johnson et al. 1985; Sandberg et al. 2002, p. 474-475).

### Evolutionary relationships

In the interpretation advocated herein, *Palmatolepis ultima* appeared abruptly in the higher part of Frasnian Zone 13c as a result of punctuated evolution. This follows from the observation that there does not seem to be an obvious ancestral species in Frasnian Zone 13, although this has been claimed in the literature.

Ziegler and Sandberg (1990, p. 42, figs. 2, 10) interpreted *P. praetriangularis* (a junior synonym of *P. ultima*) as having evolved from a "field of transition" including *P. subrecta* and

*P. rotunda* (junior synonyms of *P. winchelli* and *P. bogartensis*, respectively). However, these authors considered only Pa (or P1) elements in their analysis. In terms of multielement taxonomy, it seems highly unlikely that *P. ultima* could have been derived from *P. winchelli*. Although many of the elements are somewhat similar, a key element, the M element is substantially different in the two species (see reconstructions in Schülke 1999, as well as earlier reconstructions for *P. winchelli* and the first reconstruction for *P. ultima* in Schülke 1999, fig. 31, and that of Dzik 2002). *Palmatolepis bogartensis* is also an unlikely ancestor because of specific level differences in all the non-Pa elements (compare fig. 16 with fig. 31 of Schülke 1999, as well as earlier reconstructions of *P. bogartensis* in Klapper and Foster 1993, and Schülke 1997).

Schülke (1999, p. 54) proposed that there are morphologically transitional Pa elements between *P. winchelli* and *P. ultima* (*P. triangularis* in the nomenclature of his 1999 paper). But the Pa elements he illustrated as transitional (Schülke 1999, pl. 9, figs. 3, 4) are identical with morphotype A of *P. bogartensis* (Table 1). And, as indicated previously, all the non-Pa elements of the latter species are specifically different from those of *P. ultima*. Dzik (2002, p. 622) rejected the derivation of *P. ultima* from *P. winchelli*, also primarily on the basis of the M element. If *P. ultima* was derived from either *P. winchelli* or *P. bogartensis*, there remains a considerable morphological difference in terms of multielement taxonomy, especially in the differences between the M elements of *P. ultima* and *P. winchelli*.

In the cladistic analysis of phylogenetic relationships among the *Palmatolepis* species whose multielement apparatuses have been reconstructed (Donoghue 2001), *P. winchelli* and *P. bogartensis* are closely linked in all of the cladograms. Yet these species have very different M elements. However, the analysis considered the reconstructions of only 15 species, mostly Famennian, that were available at the time of preparation of the paper. The reconstructions (Schülke 1999) of *P. ultima* and *P. triangularis* were not included, and thus the question of the origin of *P. ultima* remains open.

None of this discussion affects the Frasnian numbered zonation (Klapper 1989, 1997, Girard et al. 2005) as that is grounded entirely on empirical analysis of stratigraphic ranges, rather than phylogenetic concepts (contra Dzik 2002, p. 568).

## TAXONOMY

Illustrated conodont specimens are in the fossil repository of The University of Iowa, Iowa City, under the SUI designation. The synonymy lists, while extensive, are not intended to be comprehensive.

### *Palmatolepis bogartensis* (Stauffer 1938)

Plate 1, figures 1-13

*Nothognathella bogartensis* STAUFFER 1938, p. 436, pl. 48, fig. 30 [=holotype].

*Palmatolepis* sp. A of KLAPPER and FOSTER 1986, p. 1216, pl. 1, fig. 1-4.

*Palmatolepis bogartensis* (Stauffer). — KLAPPER 1989, p. 458, pl. 2, fig. 7, 8. — KLAPPER and FOSTER 1993, p. 17-18, fig. 13.4-13.16, 19.1-19.5, 20.1-20.11 [synonymy]. — KLAPPER, KUZ'MIN and OVNATANOVA, 1996, p. 140, 143, fig. 8.6. — SCHÜLKE 1997, p. 44-45, pl. 3, fig. 1-20. — OVER 1997, p. 168, fig. 6.14, 6.15. — SCHÜLKE 1999, p. 30-31, pl. 3, fig. 1-13, text-fig. 16. — OVER and RHODES 2000, p. 103, fig. 4.1-4.5. — KLAPPER, UYENO, ARMSTRONG and TELFORD 2004, p. 386, fig. 6.14. — KLAPPER 2007, fig. 1.1, 1.2.

*Palmatolepis rotunda* ZIEGLER and SANDBERG 1990, p. 62, pl. 10, fig. 1-5. — MATYJA 1993, pl. 22, fig. 1. — MATYJA and NARKIEWICZ 1995, pl. 1, fig. 6. — BULTYNCK, HELSEN and HAYDUCKIEWICH 1998, p. 60, pl. 4, fig. 1-9, 11 [not fig. 10=?]. — LAZREQ 1999, p. 73-74, pl. 9, fig. 5, 7-9. — MORROW 2000, p. 50, pl. 2, fig. 1. — GOUWY and BULTYNCK 2000, p. 43, pl. 2, fig. 10-12.

*Palmatolepis subrecta* Miller and Youngquist. — ZIEGLER and SANDBERG 1990, p. 60-61, pl. 11, fig. 10 [only]. — KREJCI 1991,

pl. 14, fig. 1, 2. — LUPPOLD, 1991, p. 54, pl. 8, fig. 12. — MATYJA and NARKIEWICZ 1995, pl. 2, fig. 3. — SCHINDLER, SCHÜLKE and ZIEGLER 1998, p. 260, pl. 5, fig. 27-29.

*Palmatolepis hassi* Müller and Müller. — SCHINDLER, SCHÜLKE and ZIEGLER 1998, p. 260, pl. 4, fig. 23, pl. 5, fig. 31. — LAZREQ 1999, p. 69, pl. 8, fig. 1, 2 [only].

*Palmatolepis winchelli* (Stauffer). — SCHÜLKE 1999, p. 56-58, pl. 9, fig. 2-4 [only].

*Lagovilepis bogartensis* (Stauffer). — DZIK 2002, p. 596, fig. 41 C, D, F-K, M-O [not fig. A, B, E, I = *P. sp. indet. juvenile*], 42A-D, G-N [not fig. 42E = *P. winchelli*, nor 42F = *P. sp. indet. juvenile*], fig. 43.

**Diagnosis.** Pa element: Outline of platform almost semicircular, except for outer anterior sinus. Outer lobe narrow to wide, midline of lobe slightly anterior of central node, directed laterally or slightly to the anterior. Sinus anterior of lobe shallow to deep; small sinus just posterior of lobe. Margin posterior of the latter strongly convex in a continuous curve to tip. Blade-carina sigmoidal; blade and anterior carina distinctly curved. Blade anterior of platform short. Uniform fine nodes.

**Discussion.** In addition to the platform outline there are a number of other differences between the Pa elements of *Palmatolepis bogartensis* (= *P. rotunda*) and *P. winchelli* (= *P. subrecta*; compare respective diagnoses). Yet these two species have been widely confused in the literature, as can be seen in the synonymy list. Not only are the Pa elements different, but all the other elements of the apparatus are conspicuously different, except perhaps for the Sb element as noted by Klapper and Foster (1993, p. 18). However, the differences in the elements of the two apparatuses are considered here to be of specific, rather than generic rank.

Three informal morphotypes can be recognized within the variable Pa element of *P. bogartensis*. Morphotype A is illustrated on Pl. 1, figs. 1-4, morphotype B = Pl. 1, figs. 9-13, and morphotype C = Pl. 1, figs. 5-8. They are distinguished on the basis of the platform outline: morphotype A has a wider outer lateral lobe, morphotype B a narrower platform, and morphotype C a more nearly circular outline. There are transitional specimens between the morphotypes; e.g. the specimen on Pl. 1, fig. 9 is intermediate between B and C. Table 1 gives the morphotype identification for all the specimens listed in the synonymy. All differ from the Pa element of *P. winchelli* as outlined above. Because of the gradation among the morphotypes, they are not treated as distinct species.

## PLATE 1

All approximately  $\times 40$ . All are illustrations of Pa (P1) elements. Further locality and stratigraphic information is in the Appendix.

1-13. *Palmatolepis bogartensis* (Stauffer 1938).

1-4, 8, 12 SUI 103101-103106, Causses-et-Veyran South, CVS-29A, Frasnian Zone 13c;

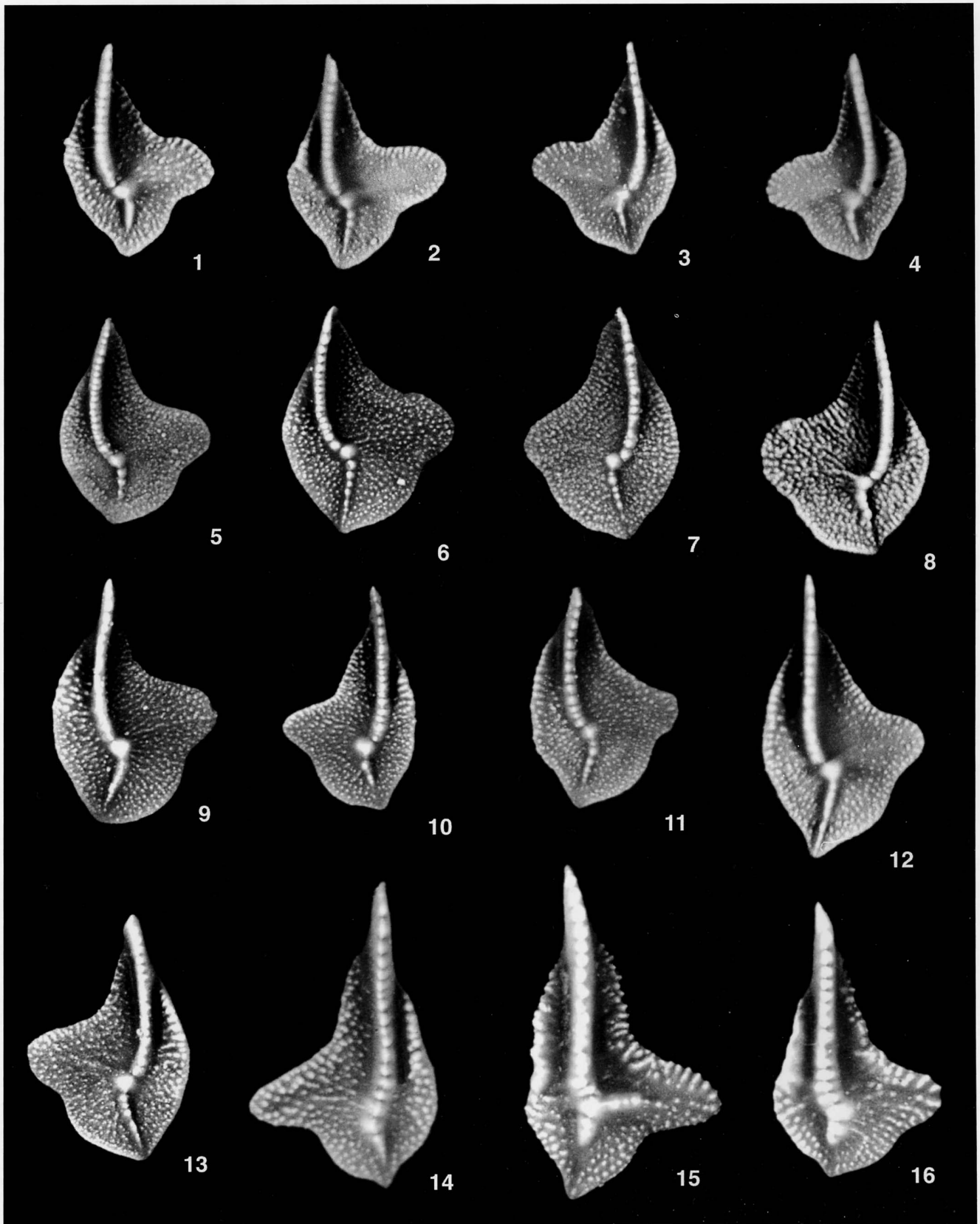
5-7, 10 SUI 53261, 53262, 53265, 53264, Upper Coumiac Quarry, UC-29A, Zone 13a (previously illustrated in Klapper and Foster, 1993, fig. 13.8-13.10, 13.7);

9 SUI 53260, Upper Coumiac Quarry, UC-29, Zone 13a (previously illustrated in Klapper and Foster, 1993, fig. 13.16);

11 SUI 53244, Upper Coumiac Quarry, UC-26, Zone 13a (previously illustrated in Klapper and Foster, 1993, fig. 13.12);

13 SUI 53271, Upper Coumiac Quarry, UC-30A, Zone 13a (previously illustrated in Klapper and Foster, 1993, fig. 13.11).

14-16 *Palmatolepis winchelli* (Stauffer 1938). SUI 52140, 81424, 53308, Sweetland Creek, TSC-7, Zone 13a (previously illustrated in Klapper and Foster, 1993, fig. 13.6, 13.10, 13.4).



***Palmatolepis winchelli*** (Stauffer 1938)

Plate 1, figures 14-16

*Bryantodus winchelli* STAUFFER 1938, p. 423, pl. 48, fig. 33.

*Palmatolepis subrecta* MILLER and YOUNGQUIST 1947, p. 513-514, pl. 75, fig. 7-11 [fig. 8 = lectotype selected by MÜLLER and MÜLLER 1957, p. 1104]. — ZIEGLER and SANDBERG 1990, p. 60-61, pl. 11, fig. 3, 7-9, 11, 12 [only; fig. 3 = reillustration of lectotype, not fig. 10 = *P. bogartensis*].

*Palmatolepis gigas* MILLER and YOUNGQUIST 1947, p. 512-513, pl. 75, fig. 1 [=holotype]. — KLAPPER and FOSTER 1993, p. 31-32, fig. 18.9 [reillustration of holotype].

*Palmatolepis gigas gigas* Miller and Youngquist. — ZIEGLER and SANDBERG 1990, p. 54, pl. 7, fig. 1, 2, 5, 6 [fig. 1, 2 = reillustration of holotype, not fig. 3, 4 = ?, nor pl. 8, fig. 5-7 = *P. paragigas* ZIEGLER and SANDBERG 1990].

*Palmatolepis winchelli* (Stauffer). — KLAPPER and FOSTER 1993, p. 24, 26, 31, fig. 13.1, 13.2, 18.1-18.8, 18.10, 18.11, 19.6-19.12 [fig. 19.12 = reillustration of holotype], 20.12-20.24 [synonymy]. — OVER 1997, p. 172, fig. 6.6-6.9. — SCHÜLKE 1999, p. 56-58, pl. 9, fig. 1, 5-12 [not fig. 2-4 = *P. bogartensis*]. — KLAPPER 2007, fig. 1.9-1.11.

*Manticolepis winchelli* (Stauffer). — DZIK 2002, p. 595-596, fig. 39A-Q.

*Manticolepis gigas* (Miller and Youngquist). — DZIK 2002, p. 594, fig. 38A-H [only].

*Lagovilepis bogartensis* (Stauffer). — DZIK 2002, p. 613, fig. 42E [only].

**Diagnosis.** Pa element: Outline of platform roughly triangular. Outer lobe wide, midline of lobe slightly anterior of, or aligned with central node, directed laterally or slightly to the posterior. Commonly deep sinus anterior of lobe, shallow to deep sinus posterior of lobe. Margin posterior of the latter convex. Margins commonly built up with concentration of strong nodes, in contrast with far fewer nodes in area around central node. Blade-carina sigmoidal, straight anteriorly except just before central node. Blade of moderate length anterior of platform.

**Discussion.** Although the margin posterior of the posterior sinus is also convex in the Pa element of *Palmatolepis bogartensis*, it has a different shape than in *P. winchelli*, in which there may be a small sinus just anterior of the tip. For further discussion of these two species, see Klapper (2007), in which the reason for including the holotype of *P. gigas* in synonymy under *P. winchelli* is also given.

***Palmatolepis triangularis*** Sannemann 1955

Plate 2, figures 13-19

*Palmatolepis triangularis* SANNEMANN 1955, p. 327-328, pl. 24, fig. 3 [=holotype]. — ZIEGLER 1962, p. 83-85, pl. 1, fig. 1-5, 7-10, 13, 14. — BOUCKAERT and ZIEGLER 1965, pl. 1, fig. 1-4 [only]. — ZIEGLER and SANDBERG 1990, p. 64-65, pl. 14, fig. 4, 5 [only; fig. 3 = ?]. — KLAPPER, UYENO, ARMSTRONG and TELFORD 2004, p. 382, fig. 6.12, 6.13. — KLAPPER, 2007, fig. 1.13-1.17. — SAVAGE, SARSDUD and BUGGISCH, 2006, p. 181, fig. 7D-I, S-U [only].

*Palmatolepis triangularis* Sannemann form a of BULTYNCK and MARTIN 1995, p. 18, pl. 5, fig. 6 [only].

*Palmatolepis triangularis* Sannemann form b of BULTYNCK and MARTIN 1995, p. 18, pl. 5, fig. 8, 9, pl. 6, fig. 3-5.

*Palmatolepis quadrantinodosalobata praeterita* SCHÜLKE 1995, p. 46-47, pl. 5, fig. 1-19.

*Palmatolepis praetriangularis* Ziegler and Sandberg. — HÜNEKE 1995, pl. 3, fig. 15.

*Palmatolepis abnormis abnormis* Branson and Mehl [sic]. — SCHÜLKE 1999, p. 25-26, pl. 1, fig. 1-11, text-fig. 12.

**Diagnosis.** Pa element: Outline of platform roughly triangular. Outer lobe relatively narrow, midline of lobe slightly anterior of central node, directed variably: slightly to the anterior, laterally, or slightly to the posterior. Moderate sinuses anterior and posterior of lobe. Blade-carina sigmoidal. Coarse nodes throughout platform, somewhat larger on anterior inner platform. Blade anterior of platform relatively short.

**PLATE 2**

All approximately ×40. All are illustrations of Pa (P1) elements. Further locality and stratigraphic information is in the Appendix.

1,9 *Palmatolepis subperlobata* Branson and Mehl 1934. 1, SUI 103107, Causses-et-Veyran South, CVS-30, Lower *triangularis* Zone; 9, SUI 103108, Upper Coumiac Quarry, UC-32A1, Lower *triangularis* Zone, 0-2 cm above base of 32A.

2-8,10,11 *Palmatolepis ultima* Ziegler 1958. 2-4, SUI 103109-103111, Upper Coumiac Quarry, UC-32A1, Lower *triangularis* Zone, 0-2 cm above base of 32A; 5, SUI 103112, Causses-et-Veyran South, CVS-32, Lower *triangularis* Zone; 6-8, 10, SUI 103113-103116, Causses-et-Veyran South, CVS-30, Lower *triangularis* Zone; 11, SUI 103117, Steinbruch Schmidt, Bed A, Lower *triangularis* Zone.

12 Specimen transitional between *P. ultima* and *P. triangularis*. SUI 103118, Causses-et-Veyran South, CVS-33, Middle *triangularis* Zone. Specimen has the platform outline of the former but the platform ornament of the latter.

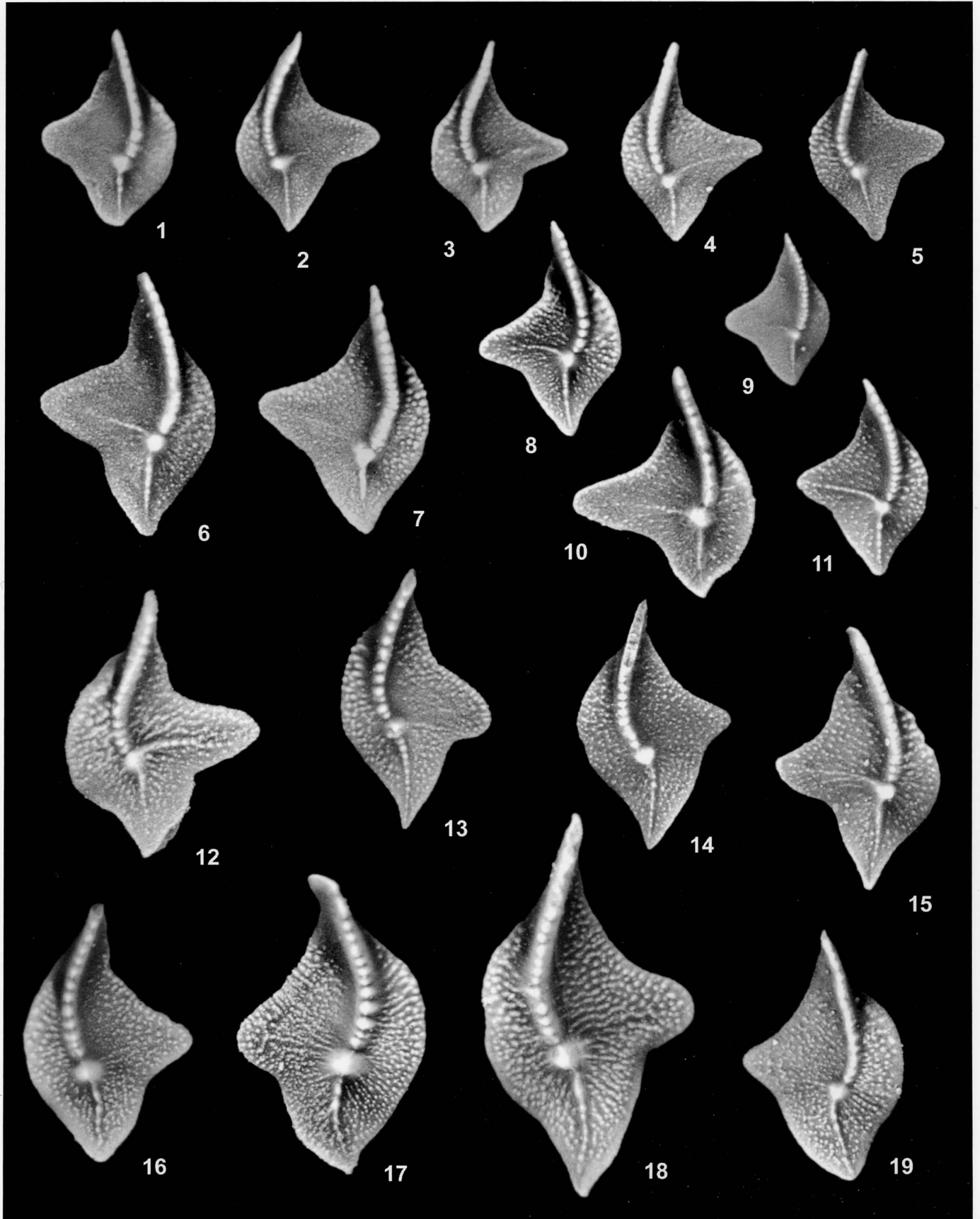
13-19 *Palmatolepis triangularis* Sannemann 1955.

13,16,17 SUI 103119-103121, Causses-et-Veyran South, CVS-33, Middle *triangularis* Zone;

14 SUI 103122, Upper Coumiac Quarry, UC32C, Middle *triangularis* Zone; 15, SUI 103123, Steinbruch Schmidt, Bed B, Lower *triangularis* Zone, 17-31 cm above top of Upper Kellwasser Limestone and base of Famennian;

18 SUI 103124, Steinbruch Schmidt, Bed D, Middle *triangularis* Zone, 47-57 cm above top of Upper Kellwasser Limestone and base of Famennian;

19 SUI 103125, Steinbruch Schmidt, Bed C, Middle *triangularis* Zone, 33-46 cm above top of Upper Kellwasser Limestone and base of Famennian.



**Discussion.** Treatment of *Palmatolepis triangularis* and *P. ultima* has a complex history, as can be seen in the synonymy lists and as discussed in detail by Klapper et al. (2004, p. 382-383). They have been treated as synonyms and as separate species by different authors. The platform outline of the Pa elements of these two species, though similar are distinguishable especially on the wider lobe in *P. ultima*. Furthermore, the platform is more extensive along the anterior-posterior axis in *P. triangularis*. The platform in *P. triangularis* is more robust, the upper surface is covered with coarser nodes, and the central node is somewhat larger. Although the posterior part of the platform of the Pa element of *P. triangularis* is commonly more strongly upturned than in *P. ultima*, this feature cannot provide the sole distinction between the species because it is gradational (Klapper et al. 2004, p. 382 for further discussion).

As reconstructed by Schülke (1999), the multielement apparatuses of the two species are closely similar if not identical.

Most of the Pa elements identified by Savage and Yudina (1999) as *P. triangularis* are juvenile specimens and thus are difficult to identify. At that size (e.g., their pl. 2, fig. 4, 6; pl. 3, fig. 10, 12) it is difficult to distinguish *P. triangularis* from *P. subperlobata*.

*Palmatolepis ultima* Ziegler 1958  
Plate 2, figures 2-8, 10, 11

*Palmatolepis ultima* ZIEGLER 1958, p. 67, pl. 9, fig. 2, 6, 10 [fig. 2 = holotype]. — KLAPPER, UYENO, ARMSTRONG and TELFORD, 2004, p. 382-383. — KLAPPER 2007, fig. 1.18-1.21.

*Palmatolepis (Manticolepis) triangularis* Sannemann. — BOOGAARD and KUHRy 1979, p. 34-35, fig. 5.

*Palmatolepis praetriangularis* ZIEGLER and SANDBERG 1988, p. 298-299, pl. 1, fig. 1-4. — BULTYNCK and MARTIN 1995, p. 17, pl. 4, fig. 1-9. — LEVMAN and VON BITTER 2002, pl. 1, p. 1802, fig. 17, 18 [not fig. 15, 16 = small Pa element of *P. winchelli* (Stauffer 1938); nor fig. 19 = indeterminate Pb element].

*Palmatolepis triangularis* Sannemann. — ZIEGLER and SANDBERG 1990, p. 64-65, pl. 14, fig. 1, 2 [only]. — SANDBERG, HASENMUELLER and REXROAD 1994, p. 252, pl. 2, fig. 7. — SCHÜLKE 1995, p. 55-57, pl. 11, fig. 1-3, 5, 6, 9, 10, 14, 15. — SCHÜLKE 1999, p. 52-54, pl. 8, fig. 2-14 [not fig. 1 = ?], text-fig. 31. — LEVMAN and VON BITTER 2002, p. 1804, pl. 2, fig. 13, 14. — SAVAGE, SARSDUD and BUGGISCH 2006, p. 181, fig. 7A-C [only].

*Palmatolepis triangularis* Sannemann form a of BULTYNCK and MARTIN 1995, p. 18, pl. 4, fig. 10, 11, pl. 5, fig. 1-5, 7 [not fig. 6 = *P. triangularis*], pl. 6, fig. 1, 6, 7.

*Palmatolepis triangularis triangularis* Sannemann. — OVER and RHODES 2000, p. 104-105, fig. 5.1-5.5.

*Klapperilepis praetriangularis* (Ziegler and Sandberg). — DZIK 2002, p. 607, fig. 44-46.

**Diagnosis.** Pa element: Outline of platform roughly triangular. Outer lobe wide, midline of lobe slightly anterior of central node, directed slightly to the anterior. Moderate sinuses anterior and posterior of lobe. Blade-carina sigmoidal. Uniform small nodes throughout platform, except on anterior inner platform where they are distinctly larger. Blade anterior of platform relatively short.

**Discussion.** Pa elements of *Palmatolepis ultima* and *P. subperlobata* Branson and Mehl 1934 have closely similar platform outlines, but differ in platform ornament. *P. subperlobata* (Pl. 2, fig. 1, 9) has an essentially smooth platform resembling the shagreen upper surface of many Famennian species. Nodes may be present on and near the anterior inner margin (Klapper et al. 2004, p. 382). In contrast, the platform of mature speci-

mens of *P. ultima* has distinct nodes covering the entire upper surface.

#### ACKNOWLEDGMENTS

Raimund Feist provided valuable and essential stratigraphic expertise for all my field work in the Montagne Noire, which occurred mainly in the 1980s and early 1990s. The late Michael House, William Kirchgasser, and Thomas Becker accompanied me in the field there on several occasions. The distinctness of *Palmatolepis bogartensis* and *P. winchelli* has been fully supported by shape analysis of the Pa elements (Catherine Girard and GK, unpublished). Over the years, Michael A. Murphy shared with me his critical understanding of the philosophical problems of biostratigraphy versus chronostratigraphy. Jonathan Adrain helped immensely with the digital photography. Peter Sadler, Michael Murphy, and Philip Donoghue reviewed an earlier draft of the manuscript. I would like to dedicate this paper to Michael House, who was and still is a constant source of inspiration.

#### REFERENCES

- BECKER, R. T., FEIST, R., FLAJS, G., HOUSE, M. R. and KLAPPER, G., 1989. Frasnian-Famennian extinction events in the Devonian at Coumiac, southern France. *Comptes Rendus de l'Académie des Sciences, Paris, Série II*, 309: 259-266.
- BOOGAARD, M. VAN DEN and KUHRy, B., 1979. Statistical reconstruction of the *Palmatolepis* apparatus (Late Devonian conodontophorids) at the generic, subgeneric, and specific level. *Scripta Geologica*, 49, 57 pp.
- BOUCKAERT, J. and ZIEGLER, W., 1965. Conodont stratigraphy of the Famennian Stage (Upper Devonian) in Belgium. *Mémoires pour servir à l'explication des Cartes géologiques et minières de la Belgique*, 5, 62 pp.
- BRANSON, E. B. and MEHL, M. G., 1934. Conodonts from the Grassy Creek Shale of Missouri. *University of Missouri Studies*, 8: 171-259. [Imprint 1933]
- BULTYNCK, P. and F. MARTIN., 1995. Assessment of an old stratotype: the Frasnian/Famennian boundary at Senzeilles, southern Belgium. *Bulletin Institut royal des Sciences naturelles de Belgique, Sciences de la Terre*, 65: 5-34.
- BULTYNCK, P., HELSEN, S. and HAYDUCKIEWICH, J., 1998. Conodont succession and biofacies in upper Frasnian formations (Devonian) from the southern and central parts of the Dinant Synclinorium (Belgium) – (Timing of facies shifting and correlation of late Frasnian events). *Bulletin Institut royal des Sciences naturelles de Belgique, Sciences de la Terre*, 68: 25-75.
- CASIER, J.-G., EL HASANI, A. and PRÉAT, A., 2006. Ostracods and rock facies of the Eifelian/Givetian and Givetian/Frasnian boundary stratotypes. *Geological Society of America, Abstracts with Programs*, 38(7): 552.
- DONOGHUE, P. C. J., 2001. Conodonts meet cladistics: recovering relationships and assessing the completeness of the conodont record. *Palaeontology*, 44: 65-93.
- DZIK, J., 2002. Emergence and collapse of the Frasnian conodont and ammonoid communities in the Holy Cross Mountains, Poland. *Acta Palaeontologica Polonica*, 47(4): 565-650.
- GIRARD, C., KLAPPER, G. and FEIST, R., 2005. Subdivision of the terminal Frasnian *linguiformis* conodont Zone, revision of the correlative interval of Montagne Noire Zone 13, and discussion of stratigraphically significant associated trilobites. In: Over, D. J., Mor-

- row, J. R. and Wignall, P. B., Eds., *Understanding Late Devonian and Permian-Triassic Biotic and Climatic Events: Towards an Integrated Approach*, 181-198. Developments in Palaeontology and Stratigraphy, 20, Elsevier, Amsterdam.
- GOUWY, S. and P. BULTYNCK., 2000. Graphic correlation of Frasnian sections (Upper Devonian) in the Ardennes, Belgium. *Bulletin Institut royal des Sciences naturelles de Belgique, Sciences de la Terre*, 70: 25-52.
- HOUSE, M. R., BECKER, R. T., FEIST, R., FLAJS, G., GIRARD, C. and KLAPPER, G., 2000. The Frasnian/Famennian boundary GSSP at Coumiac, southern France. *Courier Forschungsinstitut Senckenberg*, 225: 59-75.
- HÜNEKE, H., 1995. Early Devonian (Emsian) to Late Devonian (Famennian) stratigraphy and conodonts of the Antoinettenweg section in the Lower Harz Mountains (Germany). *Courier Forschungsinstitut Senckenberg*, 188: 99-131.
- JOHNSON, J. G. and KLAPPER, G., 1992. North American Mid-continent Devonian T-R cycles. In: Chaplin, J. R. and Barrick, J. E., Eds., *Special papers in paleontology and stratigraphy: A tribute to Thomas W. Amsden. Oklahoma Geological Survey Bulletin*, 145: 127-135.
- JOHNSON, J. G., KLAPPER, G. and SANDBERG, C. A., 1985. Devonian eustatic fluctuations in Euramerica: *Geological Society of America Bulletin*, 96: 567-587.
- KLAPPER, G., 1989. The Montagne Noire Frasnian (Upper Devonian) conodont succession. In: McMillan, N. J., Embry, A. F. and Glass, D. J. Eds., *Devonian of the World*, 449-468. Calgary, Canadian Society of Petroleum Geologists Memoir 14(III). [Imprint 1988]
- , 1997. Graphic correlation of Frasnian (Upper Devonian) sequences in Montagne Noire, France, and western Canada. In: Klapper, G., Murphy, M. A. and Talent, J. A., Eds., *Paleozoic sequence stratigraphy, biostratigraphy, and biogeography: Studies in Honor of J. Granville ("Jess") Johnson*, 113-129. Geological Society of America Special Paper, 321.
- , 2007. Frasnian (Upper Devonian) conodont succession at Horse Spring and correlative sections, Canning Basin, Western Australia. *Journal of Paleontology*, 81(3): 513-537.
- KLAPPER, G. and FOSTER, C. T., JR., 1986. Quantification of outlines in Frasnian (Upper Devonian) platform conodonts. *Canadian Journal of Earth Sciences*, 23: 1214-1222.
- , 1993. Shape analysis of Frasnian species of the Late Devonian conodont genus *Palmatolepis*. *Paleontological Society Memoir*, 32, 35 pp.
- KLAPPER, G., FEIST, R., BECKER, R. T. and HOUSE M. R., 1994. Definition of the Frasnian/Famennian Stage boundary. *Episodes*, 16(4): 433-441. [Imprint 1993]
- KLAPPER, G., KIRCHGASSER, W. T. and BAESEMANN, J. F., 1995. Graphic correlation of a Frasnian (Upper Devonian) composite standard. In: Mann, K. O. and Lane, H. R., Eds., *Graphic Correlation*, 177-184. SEPM Society for Sedimentary Geology Special Publication, 53.
- KLAPPER, G., KUZ'MIN, A. V. and OVNATANOVA, N. S., 1996. Upper Devonian conodonts from the Timan-Pechora region, Russia, and correlation with a Frasnian composite standard. *Journal of Paleontology*, 70: 131-152.
- KLAPPER, G., UYENO, T. T., ARMSTRONG, D. K. and TELFORD, P. G., 2004. Conodonts of the Williams Island and Long Rapids formations (Upper Devonian, Frasnian-Famennian) of the Onakawana B Drillhole, Moose River Basin, northern Ontario, with a revision of Lower Famennian species. *Journal of Paleontology*, 78: 371-387.
- KREJCI, Z., 1991. Conodonts. In: Hladil, J. et al., Carbonate ramp environment of Kellwasser time-interval (Lesní lom, Moravia, Czechoslovakia). *Bulletin de la Société belge de Géologie*, 100(1-2): 69-70.
- LAZREQ, N., 1999. Biostratigraphie des conodontes du Givétien au Famennien du Maroc central – Biofaciès et événement Kellwasser. *Courier Forschungsinstitut Senckenberg*, 214: 111 pp.
- LEVMAN, B. G. and VON BITTER, P. H., 2002. The Frasnian-Famennian (mid-Late Devonian) boundary in the type section of the Long Rapids Formation, James Bay Lowlands, northern Ontario, Canada. *Canadian Journal of Earth Sciences*, 39(12): 1795-1818.
- LUPPOLD, F. W., 1991. Conodontensystematik. In: Clausen, C. D., Korn, D. and Luppold, F. W., Litho- und Biofazies des mittel- bis oberdevonischen Karbonatprofils am Beringhäuser Tunnel (Messinghäuser Sattel, nördliches Rheinisches Schiefergebirge). *Geologie und Paläontologie in Westfalen*, 18: 19-31.
- MATYJA, H., 1993. Upper Devonian of Western Pomerania. *Acta Geologica Polonica*, 43(1-2): 27-94.
- MATYJA, H. and NARKIEWICZ, M., 1995. Conodont stratigraphy of the Upper Devonian in the Janczyce I borehole section, eastern Holy Cross Mts. *Geological Quarterly*, 39(2): 177-206.
- MILLER, A. K. and YOUNGQUIST, W., 1947. Conodonts from the type section of the Sweetland Creek Shale in Iowa. *Journal of Paleontology*, 21: 501-517.
- MORROW, J., 2000. Shelf-to-basin lithofacies and conodont paleoecology across Frasnian-Famennian (F-F, mid-Late Devonian) boundary, central Great Basin (western U.S.A.). *Courier Forschungsinstitut Senckenberg*, 219, 57 pp.
- MÜLLER, K. J., 1956. Zur Kenntnis der Conodonten-Fauna des europäischen Devons, 1. Die Gattung *Palmatolepis*. *Abhandlungen der Senckenbergischen Naturforschenden Gesellschaft*, 494, 70 pp.
- MÜLLER, K. J. and MÜLLER, E. M., 1957. Early Upper Devonian (Independence) conodonts from Iowa, part 1. *Journal of Paleontology*, 31: 1069-1108.
- OVER, D. J., 1997. Conodont biostratigraphy of the Java Formation (Upper Devonian) and the Frasnian-Famennian boundary in western New York State. In: Klapper, G., Murphy, M. A. and Talent, J. A., Eds., *Paleozoic sequence stratigraphy, biostratigraphy, and biogeography: Studies in Honor of J. Granville ("Jess") Johnson*, 161-177. Geological Society of America, Special Paper 321.
- OVER, D. J. and RHODES, M. K., 2000. Conodonts from the upper Olenitangy Shale (Upper Devonian, central Ohio) and stratigraphy across the Frasnian-Famennian boundary. *Journal of Paleontology*, 74: 101-112.
- SANDBERG, C. A., HASENMUELLER, N. R. and REXROAD, C. B., 1994. Conodont biochronology, biostratigraphy, and biofacies of Upper Devonian part of New Albany Shale, Indiana. In: Königshof, P. and Werner, R., Eds., *Willi Ziegler-Festschrift I. Courier Forschungsinstitut Senckenberg*, 168: 227-253.
- SANDBERG, C. A., MORROW, J. R. and ZIEGLER, W., 2002. Late Devonian sea-level changes, catastrophic events, and mass extinctions. In: Koeberl, C. and MacLeod, K. G., Eds., *Catastrophic Events and Mass Extinctions: Impacts and Beyond. Geological Society of America Special Paper 356*: 473-487.
- SANDBERG, C. A., ZIEGLER, W. and DREESEN, R., 1988a. *Ancyrognathus ubiquitous* n. sp. In: Sandberg, C. A., Ziegler, W., Dreesen, R.

- and Butler, J. L., 1988b. Late Frasnian mass extinction: Conodont event stratigraphy, global changes, and possible causes. *Courier Forschungsinstitut Senckenberg*, 102(3): 297-298.
- SANDBERG, C. A., ZIEGLER, W., DREESEN, R. and BUTLER, J. L., 1988b. Late Frasnian mass extinction: Conodont event stratigraphy, global changes, and possible causes. *Courier Forschungsinstitut Senckenberg*, 102(3): 263-307.
- SANNEMANN, D., 1955. Beitrag zur Untergliederung des Oberdevons nach Conodonten. *Neues Jahrbuch für Geologie und Paläontologie, Abhandlungen*, 100: 324-331.
- SAVAGE, N. M. and YUDINA, A. B., 1999. Late Devonian Syv'yu River section, Timan-Pechora Basin, northwestern Russia. In: Serpagli, E. and Coradini, C., Eds., *Studies on conodonts: Proceedings of the Seventh European Conodont Symposium, Bologna-Modena 23-25 June, 1998*, 361-373. *Bollettino della Società Paleontologica Italiana*, 37(2-3).
- SAVAGE, N. M., SARDSUD, A. and BUGGISCH, W., 2006. Late Devonian conodonts and the global Frasnian-Famennian extinction event, Thong Pha Phum, western Thailand. *Palaeoworld* 15: 171-184.
- SCHINDLER, E., 1990. Die Kellwasser-Krise (höhe Frasn-Stufe, Ober-Devon). *Göttinger Arbeiten zur Geologie und Paläontologie*, 46: 115 pp.
- SCHINDLER, E., SCHÜLKE, I. ZIEGLER, W., 1998. The Frasnian/Famennian boundary at the Sessacker Trench section near Oberscheld (Dill Syncline, Rheinisches Schiefergebirge, Germany). *Senckenbergiana lethaea* 77(1/2): 243-261.
- SCHÜLKE, I., 1995. Evolutive Prozesse bei *Palmatolepis* in der frühen Famenne-Stufe (Conodonta, Ober-Devon). *Göttinger Arbeiten zur Geologie und Paläontologie*, 67: 108 pp.
- , 1997. Conodont clusters and multielement reconstructions from the Upper Kellwasser horizon at La Serre (Late Frasnian, Montagne Noire, southern France). *Geologica et Palaeontologica*, 31: 37-66.
- , 1999. Conodont multielement reconstructions from the early Famennian (Late Devonian) of the Montagne Noire (southern France). *Geologica et Palaeontologica, Sonderband 3*: 123 pp.
- STAUFFER, C. R., 1938. Conodonts of the Olentangy Shale. *Journal of Paleontology*, 12: 411-433.
- ZIEGLER, W., 1958. Conodontenfeinstratigraphische Untersuchungen an der Grenze Mitteldevon/Oberdevon und in der Adorfstufe. *Notizblatt des Hessischen Landesamtes für Bodenforschung*, 87: 7-77.
- , 1962. Taxonomie und Phylogenie Oberdevonischer Conodonten und ihre stratigraphische Bedeutung. *Hessischen Landesamtes für Bodenforschung, Abhandlungen*, 38: 166 pp.
- ZIEGLER, W. and SANDBERG, C. A., 1988. *Palmatolepis praetriangularis* n. sp. In: Sandberg, C. A., Ziegler, W., Dreesen, R. and Butler, J. L., 1988b. Late Frasnian mass extinction: Conodont event stratigraphy, global changes, and possible causes. *Courier Forschungsinstitut Senckenberg*, 102(3): 298-299.
- ZIEGLER, W. and SANDBERG, C. A., 1990. The Late Devonian standard conodont zonation. *Courier Forschungsinstitut Senckenberg*, 121: 115 pp.

Manscript received January 30, 2007

Manscript accepted April 9, 2007

#### APPENDIX OF LOCALITIES

All samples collected by GK unless noted otherwise.

Causses-et-Veyran South (CVS), natural outcrop about 0.6 km west-northwest of main road in village of Causses-et-Veyran, Murviel-lès-Béziers 1:25000 sheet (2544 east), x = 660.05, y = 131.3, Montagne Noire, southern France. Bed 29A = lower 8cm of 20cm-thick Upper Kellwasser Limestone at top of Frasnian section, Zone 13c. Bed 30 = 0-14 cm above top of Upper Kellwasser Limestone (top of bed 29B) and coincident base of Famennian, Lower *triangularis* Zone. Bed 32 = 34-49 cm above base of Famennian, Lower *triangularis* Zone. Bed 33 = 49-63 cm above base of Famennian, Middle *triangularis* Zone.

Steinbruch Schmidt, near Bad Wildungen, Kellerwald, Rhenish Slate Mountains, Germany. Location map in Schindler (1990, p. 34). Bed A = 0-0.17m above top of Upper Kellwasser Limestone and base of Famennian (illustrated in Sandberg et al. 1988b, fig. 7; = Bed 100 in Schindler 1990, fig. 8), Lower *triangularis* Zone.

Bed B = 0.17-0.31m above same datum (= Bed 101 in Schindler 1990, fig. 8), Lower *triangularis* Zone. Bed C = 0.33-0.46 m above same datum (= Bed 102 in Schindler 1990), Middle *triangularis* Zone. Bed D = 0.47-0.57m above same datum (= Beds 103, 104 in Schindler 1990), Middle *triangularis* Zone. Collected with Willi Ziegler in 1984.

Sweetland Creek (TSC), type section of Sweetland Creek Shale, N1/2SW1/4 sec. 27, T77N, R1W, Illinois City quadrangle, Muscatine County, Iowa (Johnson and Klapper 1992, p. 131-132, fig. 2). Sample 7 = 2.70-2.90 m above base of section, Zone 13a.

Upper Coumiac Quarry (UC), abandoned marble quarry north of the road from Cessenon to Causses-et-Veyran, opposite the abandoned farm house, "Coumiac," and about 300m west of the farm house, "les Granges," Murviel-lès-Béziers 1:25000 sheet (2544 east), x = 658.53, y = 130.38, Montagne Noire. GK no. 26 = 19.05-19.23m (= Bed 26a in Becker et al. 1989, fig. 3 and House et al., 2000, fig. 4). GK no. 29 = 20.30-20.52m (= Bed 29a in Becker et al. 1989, fig. 3). GK no. 29A = 20.62-20.74m (= lower 12cm of Bed 30a in Becker et al. 1989). GK no. 30A = 21.02-21.19m (= Bed 31a, 31b in Becker et al. 1989) [GK nos. 26-30A are all in Frasnian Zone 13a]. Sample 32a1 = 0-2cm above base of Bed 32a, which is at 21.82m and coincides with the GSSP, Lower *triangularis* Zone. Bed 32c = 22.17-22.34m, Middle *triangularis* Zone. All measurements are above base of section (Klapper 1989, fig. 4). Sample from Beds 32a1 and 32c collected by Raimund Feist.

# Sedimentary cycles and stratigraphy

Walther Schwarzacher

School of Geography, Queen's University, Belfast BT7 1NN, Northern Ireland, U. K.  
email: w.schwarzacher@qub.ac.uk

---

**ABSTRACT:** Sedimentary cycles are repeated sequences in a stratigraphic section. This paper uses "stratigraphic cycles" to describe observed sequences of sediments in sections and "process cycle" to describe processes that generated the cycles. Repetition of cycles is never completely identical and statistical methods of time series analysis are used to describe cyclicity. The study of process cycles requires the knowledge of a time scale and therefore relies heavily on the interpretation of the sedimentary record.

---

## INTRODUCTION

Sedimentary cycles are traditionally defined as short sequences that are regularly repeated (Duff et al. 1967). Consider a section that contains only three lithologies, for example A, B, and C; then ABC is a cycle if it is followed by A. Indeed, any recurrence of A will define a cycle. However, the important feature of cyclic sections is that similar cycles are repeated. Thus the sequence ABCA is a cycle but it becomes more interesting if it is repeated in a section as: ABCABCABCA ... The regularity of repetition suggests a special mechanism that produced such sections. It is obvious that a precise repetition of sequences cannot be expected and the questions arise as to how much latitude of variation should be allowed and how often a cycle has to be repeated before the section can be described as cyclic. Cycles therefore are not precisely defined and without a more detailed description of the repetition pattern the cycle concept remains ambiguous.

The word "cycle" refers not only to repeated sequences of rocks, but also to the processes that generated it. In the following, cycles that are directly derived from the section will be called the "stratigraphic cycles" and the processes of cycle formation will be called the (environmental) "process cycle". The stratigraphic cycle is determined by the order of the different sediments and their positions, which are typically given in units of length, usually as distances from the base of a section. The environmental process cycle consists of a sequence of events within some time scale.

## STRATIGRAPHIC CYCLES

The record of stratigraphic sections contains two basic elements, an observation (that may be a rock type, a fossil content, or any other property of the sediment), and its position. The position is either given as a measured distance from a fixed point in a section, or given relatively in sequential order. However, it is doubtful whether sequential observations without any scale, are useful. Some scale must be at least implied by the specification of the data, for example, rock types or units like beds.

Stratigraphic data consist of observations that are sequentially ordered and therefore can be treated as a time series. The methods of time-series analysis are particularly well suited to clarifying stratigraphic cyclicity, as they can deal with data that either resulted from random processes (stochastic processes) or

at least, have been randomly disturbed. To visualize such a stochastic model of stratigraphic sections, one assumes that each consecutive observation is associated with a probability. The probability determines the event of a particular observation being made and the stratigraphic data are therefore the realization of the process. The word event is invariably used for the realization of a random process in probability theory and in statistics. The events in event stratification of Seilacher (1982), refer to episodic or rare events in what the authors call "cyclic" sections and there is therefore no conflict of terminology

The stochastic model gives a very realistic representation of stratigraphic sections and their fluctuations and cycles that are not rigidly repeated, can be described. Using such models one can show that there are four different patterns of repetition in sedimentary sections (Schwarzacher 1969).

A) Sediment changes that are completely at random and distributed as one would expect in data that have been perfectly shuffled and it is therefore impossible to predict any successive step.

B) Successive steps are not independent and a limited prediction is possible. However, predictability decreases exponentially. No distinct groups of steps are obvious.

C) Repetitions come in groups but the groups may not be all identical and precisely repeated.

D) Repetitions are in perfect order and correspond to the mathematical definition of periodicity.

Clearly, cases C and D correspond to the concept of sedimentary cycles. Because the definition of cycles relies very much on the position of the observation, any method to describe them must involve the correlation structure of the series. Analyses based on simple statistics like average cycle thickness or standard deviations, are not sufficient. The method most commonly used is power spectral analysis (e.g. Weedon 2003). In this analysis one calculates the variance that each frequency of the oscillations contributes to the series

The four types of repetition give the following spectra.

A) Independent random sequences produce a flat spectrum that is constant over the whole frequency range. Such spectra are known as white noise spectra.

B) Correlated random processes produce relatively smooth spectra and frequently rise towards the lower frequencies, indicating so-called red noise.

C) Sections containing one or more preferred frequencies, have distinct maxima at such frequencies.

D) Periodic sequences have sharp, spike-shaped maxima at the precise frequencies of the period.

The two extremes of A and D, randomness and perfect order, are never found in actual stratigraphic sections. Complete randomness would imply that there is no correlation between successive steps, but since changing environments control the sedimentation, transitions follow a logical pattern that generates specific sediment associations. Perfect cyclicality on the other hand, is just as unlikely as complete randomness, and there are many reasons why perfectly predictable sections never occur. Repetition type D clearly corresponds accurately to the definition of sedimentary cycles as given in the introduction but as indicated, D is not a realistic model.

Sequences with repetition patterns B and C, are frequently observed in stratigraphic sections. If one allows for the repeated groups not being completely identical, then spectra of type C can be objectively identified as cyclic.

#### ENVIRONMENTAL PROCESS CYCLES

The environment is a dynamic system that develops in both space and time. Process cycles describe the formation of sediments, resulting from movements and forces in this environment. To understand the formation of cycles one needs the dimension of time.

Most bedded sediments provide good evidence for regular repetitions and the analysis of such sections indicate one or more frequency maxima of recurring lithologies. However, if the stratigraphic position of the observed lithology is replaced by the actual time of its formation very different results could be obtained. The repetition pattern of the time history can again range from completely random to near periodic cyclicality. For example the time history of successive turbidites may be quite unpredictable but the history of varve formation approaches mathematical periodicity. The two processes are quite different and they can only be distinguished if the time history is known.

Systems that produce regularly but not necessarily periodically recurring states, are known as oscillating. Oscillations produce spectra with distinct frequency maxima and they are therefore equivalent to the geological definition of cycles.

Most real systems incorporate friction and persistent cycles can only be maintained by adding energy. If the energy supply remains in phase with the cycles, the system is self-oscillating (self cycling) and it can produce periodic and quasi-periodic cycles from a constant source of energy. The latter are cycles, the frequency of which is constant over considerable intervals of time. Practical examples of self-oscillating systems in daily life are clocks, steam engines or internal combustion engines. Self-oscillating systems are potentially unstable, and some instability can lead to chaotic behavior. Self-oscillating, as used in the theory of oscillators, should not be confused with "autocyclicity", which will be discussed later.

The sedimentary environment is a very complex system, in which different components such as climate, tectonism and de-

velopments in the biosphere, can give rise to many interactions and feedback processes that are potential oscillators. Therefore, there are many possible systems that could lead to cyclic sedimentation with periods representing hours to millions of years. However, apart from celestial mechanics, we know relatively little about systems that can generate oscillations with periods of thousands to millions of years. This is because the time spans involved are considerably longer than any available records of direct observation. Therefore, any explanation of such cycles must be based on hypotheses and theories. Climatologists have formulated theories that were originally developed to explain the repeated occurrence of ice ages involving oscillations caused by feedback between general temperature, land ice masses, and the albedo of the earth. Similar slow oscillations can also arise from the interaction of sea-ice cover and heat loss of the oceans.

Some cycles may result directly from sedimentation processes. Ginsburg (1971) suggested that an advancing tidal flat could cover the area of sediment production and that sedimentation would cease, until further subsidence takes place. Burgess and Wright (2003) considered a model in which a series of islands or shoals regulated the sediment flux, leading to a sequence that recorded alternating shallow and deeper water sedimentation. Ginsburg's model was never elaborated and does not explain oscillating behaviour. In theory, the Burgess and Wright model is capable of oscillation, but the authors assumed that it is driven by random sediment supply and it is consequently, not a self-oscillating system.

A large number of environmental cycles are connected with the daily, monthly, annual, or considerably slower orbital variations of the earth that are determined by celestial mechanics. The theory of such astronomic cycles is relatively well known and their frequencies are relatively constant. Most astronomical cycles are quasi-periodic, meaning that their frequencies are constant over considerable intervals of time, and they are therefore well-suited as stratigraphic time markers. Environmental processes are often more easily understood, if they are thought of as consisting of several subsystems that are causally related to each other. Different subsystems may be responsible for different properties of the environment, or they may interact to produce a specific cycle. For example, solar radiation may be an important component of an environment, but this reacts with the atmosphere and hydrosphere to determine the climate, which in turn, has an effect on some biological activity that could be responsible for cyclic sedimentation. Because different systems interfere with each other, and because random elements can be introduced at various stages, many environmental cycles will have the nature of random (stochastic) processes. The resulting power spectra could be quite complex and a wide variety of frequencies can be generated in this way.

#### THE DOMAIN OF PROCESS CYCLES AND AUTOCYCLICITY

The physical boundaries of an environment depend very much on how it is defined by the geologist. It can be a sedimentary basin, or some part of it like a tidal flat, or a carbonate platform. The physical area of a cycle generating system, defines its domain (Schwarzacher 2000). Domains can be quite limited or they can be world-wide; they can even, as in the case of astronomical cycles, include the solar system. Knowing the scale of the domain would clearly help to identify the mechanism of cycle formation. Unfortunately, the distribution of stratigraphic cycles that can be correlated, does not necessarily coincide with

the limits of domains. Domains, like the limits of environments that provide the evidence of a studied cycle, are often ill defined and arbitrary. In many cases, the domain can be identified, only if the origin of the cycles is also known.

A cycle is called an induced cycle if its domain is larger than the extent of a cycle-producing environment (for example a particular basin). A cycle is called an autonomous cycle if its domain is contained within the environment limits (Brinkman 1932). Beerbower (1961) developed a very similar classification and called the autonomous cycles “autocycles” and the induced cycles “allocycles”. Beerbower’s terminology is more commonly used, although it postdates Brinkman’s terminology. Clearly, unless the domain and the extent of environments are specified or known, the terms autocycle and allocycle should not be applied.

The word autocycle seems to suggest that such cycles are self-generated. However, autocyclicality or allocyclicality do not generate cycles. It is the oscillating systems that have to be understood to explain the origin of cycles. A cycle’s origin is not explained, as has been frequently done, by simply calling it autocyclic.

#### **THE SPACE-TIME RELATIONSHIP**

Connecting the process cycle to the grouping of rock types, involves the difficult and often unknown relationship between stratigraphic position and time. The interpretation of sediments, in terms of physical processes therefore, is largely determined by how well, accumulated sediments can be translated into time. This depends mainly on three properties: resolution, completeness, and continuity of sedimentation. The resolution of a sediment section is the shortest time between two recognizable events. The completeness is the degree with which the stratigraphic record is filled by such events and the continuity is determined by the consistency with which events of a given resolution occur.

Every sedimentary sequence contains intervals that, at a given scale, can be regarded as being instantaneous and such intervals have at this scale, no time or stratigraphic significance. Rare event deposits of Seilacher (1982) are typical examples of such intervals, as they can only be used as instant time markers and cannot measure time at the scale they recorded. Clearly, rarity depends on the length of time under consideration. Conversely, intervals of non-deposition (hiatuses) do not contribute recognizable time. Only intervals that are long enough to have a meaningful average rate of sedimentation provide stratigraphic divisions that can be used for stratigraphic dating and correlation.

The time-space relationship plays a very important role in connecting stratigraphic cyclicality with process cyclicality. If accumulation rates were constant throughout a section, then cycles of equal thickness would represent equal time intervals. However, we know that sedimentation is frequently interrupted and rarely remains constant. Unequal thickness cycles therefore, do not necessarily indicate unequal time cycles, but equal thickness cycles are very probably the result of equal time cycles. This rule was first given by Sander (1936) and it implies that time cyclicality can be deduced from the stratigraphic section but non-cyclicality of time cannot be proved from the sedimentary record.

All arguments concerning cyclicality have to be combined with detailed sedimentological examinations and two basic questions have to be decided. Are lithological boundaries primary sediment surfaces? Has sedimentation been steady and continuous?

#### **CYCLOSTRATIGRAPHY**

The second report of the Cyclostratigraphy Working Group recommended that the term “sedimentary cycle” be restricted to repetitive changes in the stratigraphic record that have, or are inferred to have, time significance (Hilgen et al, 2003). It would indeed be peculiar if cycles used in stratigraphy were not time related. In practice, only astronomical cycles with periods from days to millions of years, millions of years, are used in cyclostratigraphy.

The study of cyclic sedimentation has led to the development of an astronomical time-scale that extends from the present to the Miocene (Gradstein et al. 2004). It is based on the calculated changes of solar radiation due to variations in the earth’s orbit. Orbital cycles have been recognized as far back as the Cambrian, but time scales derived from such cycles are not tied to the present. As floating time scales, they can only be used for relative dating or for stratigraphic correlation. The challenge is to recognize sedimentary sections that can be used to expand and refine the astronomical time scale.

For orbital cycles to be recorded and to be recognized, a number of conditions are necessary. To interpret time as accumulated sediment thickness, it is important that the continuity of sedimentation is commensurate with the scale of the cycles. Obviously, the sediment must be capable of recording the cyclic variables of the environment through one or more of its properties, bio-content, or composition. Needless to say, the sedimentation has to be sensitive to the astronomic variation that will be responsible for variable solar radiation. Support for the assumption that observed cycles are indeed of astronomic origin, can be obtained by at least approximate radio-isotopic dating and by observing the expected ratios of frequencies.

#### **CONCLUSIONS AND SUMMARY**

The definition of sedimentary cycles as representing repeated groups like A,B,C,A,B,C... leads to a problem. Repetitions of stratigraphic events are never exact and some variability has to be allowed for. However, if variation of cycles is considered possible, then every sedimentary sequence could ultimately be regarded as cyclic and the term loses its meaning. The change from complete randomness to perfect order of periodicity is continuous and without any natural boundaries. Spectral analysis can indicate maxima in the recurrence pattern, but it is the investigator who has to decide their significance.

A better understanding of cycles is gained by considering the processes that produce cycles. Repetition of similar sediments can either be due to unpredictable random events, or due to events that are correlated in time. The latter is the case for most natural processes. A repetition of process cycles is generated by feedback of interacting events at different moments of time, in the development of the process. Recurring states in dynamic systems due to feedback are known as oscillations. “Repetitions created by oscillating systems”, could well serve as a definition of sedimentary cycles, as it covers what most geologists mean by the term cycle, even if they do not express it explicitly. Obviously, in order to recognize oscillations or cycles and to differentiate them from random fluctuations, the time history of the cycle formation has to be known. Therefore, recognizing

cyclicality always depends on geological and sedimentological judgement, and cannot be deduced exclusively from quantitative analysis.

#### ACKNOWLEDGMENTS

I thank F.P. Agterberg for his pre-review of this paper and F. J. Rodriguez-Tovar for his helpful suggestions. P. Enos spent considerable time in reviewing the paper and drew my attention to points that had not been clear. I am very grateful to all reviewers.

#### REFERENCES

- BEERBOWER, J.R., 1964. Cyclothems and alluvial plain sedimentation. *Kansas State Geological Survey Bulletin*, 169(1): 31-42.
- BRINKMAN, R., 1932. Über Schichtung und ihre Bedingungen. *Fortschritte der Geologie und Paleontologie*, 11:187-202
- BURGESS, P. M., and WRIGHT, V. P., 2003. Numerical forward modelling of carbonate platform dynamics: an evaluation of complexity and completeness in carbonate strata. *Journal of Sedimentary Research*, 73: 637-652.
- DUFF, P.McL.D., HALLAM, A. and WALTON, E.K., 1967. *Cyclic sedimentation: Developments in Sedimentology 10*. Amsterdam: Elsevier, 280 pp.
- GINSBURG, R. N., 1971. Landward movement of carbonate mud. New model for regressive cycles in carbonates. *American Association of Petroleum Geologists Bulletin*, 55: 340.
- GRADSTEIN, F.M., OGG, J.G., and SMITH, A.G., 2004. *A geologic time scale 2004*. Cambridge: Cambridge University Press: 589pp.
- HILGEN, F., SCHWARZACHER, W., and STRASSER, A., 2004. *Concept and definitions in Cyclostratigraphy. (Second report of the Cyclostratigraphy working group)*, 303-305. S E P M Special Publication 81.
- SANDER, B., 1936. Beiträge zur Kenntnis der Ablagerungs Gefüge. *Mineralogische Petrographische Mitteilungen* 48: 27-139.
- SCHWARZACHER, W., 1969. The use of Markov chains in the study of Sedimentary cycles. *Mathematical Geology*, 1: 7 – 39.
- , 2000. Repetitions and cycles in stratigraphy. *Earth Science Reviews*, 50 (2000): 5 1-75
- SEILACHER, A., 1982. General remarks about event deposits. In: Einsele, G., Seilacher, A., Eds., *Cyclic and event stratification*, 161. Berlin, Heidelberg, New York: Springer.
- WEEDON, G. P., 2003. *Time-Series Analysis and Cyclostratigraphy*: Cambridge: Cambridge University Press: 259pp.

Manuscript received September 15, 2006

Manuscript accepted April 6, 2007